

Received 8 June 2023, accepted 12 July 2023, date of publication 24 July 2023, date of current version 11 August 2023.

Digital Object Identifier 10.1109/ACCESS.2023.3298105

RESEARCH ARTICLE

The Deep Sleep Optimizer: A Human-Based Metaheuristic Approach

SUNDAY O. OLADEJO¹, STEPHEN O. EKWE², LATEEF A. AKINYEMI³,
AND SEYEDALI A. MIRJALILI^{4,5}, (Senior Member, IEEE)

¹School for Data Science and Computational Thinking, University of Stellenbosch, Stellenbosch 7600, South Africa

²Department of Electrical, Electronic and Computer Engineering, Cape Peninsula University of Technology, Cape Town 7535, South Africa

³Department of Electronic and Computer Engineering, Faculty of Engineering, Lagos State University, Epe Campus, Lagos 102101, Nigeria

⁴Centre for Artificial Intelligence Research and Optimisation, Torrens University, Brisbane, QLD 4006, Australia

⁵University Research and Innovation Center, Obuda University, 1034 Budapest, Hungary

Corresponding author: Sunday O. Oladejo (sunday@sun.ac.za)

This work was supported in part by the Division for Research Development, Stellenbosch University, South Africa.

ABSTRACT Owing to the no free lunch theorem, no single optimisation algorithm can solve all optimisation problems accurately, so new optimisation techniques are required. In this paper, a novel metaheuristic called the deep sleep optimiser (DSO) is proposed. The deep sleep optimiser mimics the sleeping patterns of humans to solve optimisation problems. The DSO is modelled on the rise and fall of homeostatic pressure during the human sleep process. Human sleep is often modelled on the four sleep stages and the deep sleep stage is employed in this work. The mathematical model of sleep homeostatic pressure is employed to simulate and determine the deep sleep state. The performance of DSO is demonstrated by employing 23 traditional functions (i.e., unimodal, multimodal, and fixed multi-modal functions), six composite functions, three engineering design problems, two knapsack problems, and six widely known travelling salesman's problems. Additionally, the performance is evaluated in terms of accuracy, computational running time, the Wilcoxon rank sum, and the Friedman test. Lastly, the DSO is compared with 11 other metaheuristics, including GA, PSO, TLBO, and GWO. The DSO fares comparably well and, in most instances, it outperforms other metaheuristics.

INDEX TERMS Optimisation, metaheuristics, deep sleep, REM, non-REM.

I. INTRODUCTION

Recently, metaheuristic optimisation techniques have garnered high levels of interest in academia and industry thanks to their ability to avoid local optima and finding near optimal or optimal solutions in reasonable time; flexibility and robustness; simplicity and ease of implementation; and mathematical derivation-free solutions (i.e., they do not require gradient-based information) [1], [2], [3], [4]. Their ability to avoid locally optima entrapment is due to the integration of controlled randomisation techniques. Consequently, metaheuristic algorithms have been employed in several fields as shown in Fig. 1, such as wireless communications [5], [6], [7], [8], [9]. Metaheuristics are characteristically stochastic and not deterministic. Stochastic optimisation techniques are dependent on the randomness of the modelling operators.

The associate editor coordinating the review of this manuscript and approving it for publication was Yilun Shang.

They escape the entrapment of local optima better than conventional optimisation algorithms [10]. They usually generate different solutions on each simulation run. Whereas, deterministic optimisation gives the same solutions for all simulation runs.

Metaheuristics can be classified in several ways, such as the population (i.e., solutions) size, the source of inspiration of the metaheuristics, the solution or search strategy, and the search experience [4], [11], [12], [13], [14]. According to the solution size, metaheuristics can be broadly classified into: (i) single-solution based (otherwise known as trajectory based [10], [15]) metaheuristics and (ii) population-based metaheuristics. As the name implies, a single-solution based metaheuristic generates only one solution which is based on the iterative application of a generation and replacement stage. In the generation stage, a single solution develops a set of candidate solutions bound by local transformations of the single solution. To this end, the replacement stage begins.



FIGURE 1. Some areas of application of metaheuristic algorithms.

In the replacement stage, a new single solution is selected from the candidate set of solutions generated in the first stage (i.e., generated stage). An iterative process takes place between the two stages until the maximum iteration number is reached or a stopping criterion is met. Popular examples of single-solution based metaheuristics are Simulated Annealing (SA) [16], Iterative Local Search (ILS) [17], [18], Tabu Search (TS) [10], [19], and Greedy Randomized Adaptive Search Procedures (GRASP) [20].

Population-based metaheuristics are broadly inspired by different aspects of nature [21], [22]. In population-based metaheuristics, an initial set (i.e., population) of solutions is generated. This set of solutions is then replaced with a new set of solutions which is an improvement on the old set of solutions. This process iteratively continues until a stopping criterion is met or a predefined maximum iteration is reached. The novel metaheuristic proposed in this work is population-based. Examples of widely-known population-based metaheuristics are the Genetic Algorithm (GA) [23], [24], Particle Swarm Optimisation (PSO) [25], Differential Evolution (DE) [26], Ant-Colony Optimisation (ACO) [27], [28], Grey Wolf Optimisation (GWO) [1], Artificial Bee Colony (ABC) [29], [30], Harris Hawk Optimisation (HHO) [31], and the Whale Optimisation Algorithm (WOA) [2].

Additionally, metaheuristics are categorised based on their source of inspiration: (i) evolutionary-based, (ii) swarm-based, (iii) physics-based, and (iv) human-based techniques. Evolution-based metaheuristics are inspired by biological evolution. Natural evolution relies on changes in attributes or characteristics of species over many generations that influence the process of natural selection. These changes in characteristics may be advantageous to the individual over other individuals and can then be passed to future generations (i.e., offspring). This strategy is exploited by evolution-based metaheuristics in reaching global optima. Popular evolutionary-based metaheuristics [15] are GA [23], [24], DE [26], Genetic Programming (GP) [32], Biogeography-based Optimiser (BBO) [33], Evolutionary

Strategy (ES) [34], Evolutionary Programming (EP) [35], [36], [37], Covariance Matrix Adaptation Evolution Strategy (CMAES) [38], and the Quantum-Inspired Evolutionary Algorithm [39].

Swarms such as termites, bees, spiders, ants, fish, and birds have inspired many metaheuristics due to swarm emergence, which is the collective (i.e., social) cooperation of these swarms [40], [41] for finding their location and food foraging. Examples of swarm-based metaheuristics are PSO, ACO, ABC, Firefly Algorithm (FFA) [42], Bat Algorithm (BA) [43], Grasshopper Optimisation Algorithm (GOA) [44], GWO, Cuckoo Search (CS) [45], Dolphin Echolocation (DEL) [46], [47], Salp Swarm Algorithm (SSA) [3], and Ant Lion Optimiser (ALO) [48].

Physics-based metaheuristics are inspired by the physical laws of the universe such as gravity, annealing, relativity, explosions, Brownian motion of gases, and Boltzmann distribution of thermic equilibrium [49]. Widely-known examples of physics-based metaheuristics are SA, Sine Cosine Algorithm [50], Big-Bang Big-Crunch (BBBC) [51], Gravitational Search Algorithm (GSA) [52], Central Force Optimisation (CFO) [53], the Solar System Algorithm (SoSA) [54], and the Crystal Structure Algorithm (CSA) [55].

Human-based metaheuristics are based on animal/human-social behaviour, otherwise referred to as ‘life-style based’ metaheuristics. Examples of human-inspired metaheuristics are TS, Group Search Optimiser (GSO) [56], [57], Teaching Learning Based Optimisation (TLBO) [58], [59], Social Network Search (SNS) for Global Optimisation [60], Harmony Search (HS) [61], and the Firework Algorithm (FA) [62].

Furthermore, metaheuristics can be categorised according to memory usage [12], [13], [14] into (i) memory-usage and (ii) memory-less methods. Classification is based on whether the search experience of agents can influence future search direction in the search landscape [4], [12], [13], [14]. Memory-usage inspired metaheuristics are TS, GA, ACO, ABC, PSO, BA, GWO, and the Firefly Algorithm (FFA) [63], [64]. Memory-less based metaheuristics employ only the current state search information (i.e., a Markov-like process). Examples of memory-less based metaheuristics are LS, GRASP, and SA. Figure 2 illustrates the different ways metaheuristics can be classified.

Additionally, metaheuristics can also be categorised based on their solution or search strategies as [13] and [11]: (i) constructive, (ii) local search-based, and (iii) population-based. The authors in [11] and [13] posit that metaheuristics can belong to more than one group. Constructive metaheuristics start the solution-finding process with an empty set of solutions. A solution is found from their constituted element (which may differ based on the problem, e.g., for the travelling salesman’s problem the elements are the cities) during each iteration, i.e., a move [65], [66]. In other words, constructive metaheuristics do not solve the optimisation problem at once but by dividing the optimisation problem into sub-problems, and each is solved one at a time, i.e.,

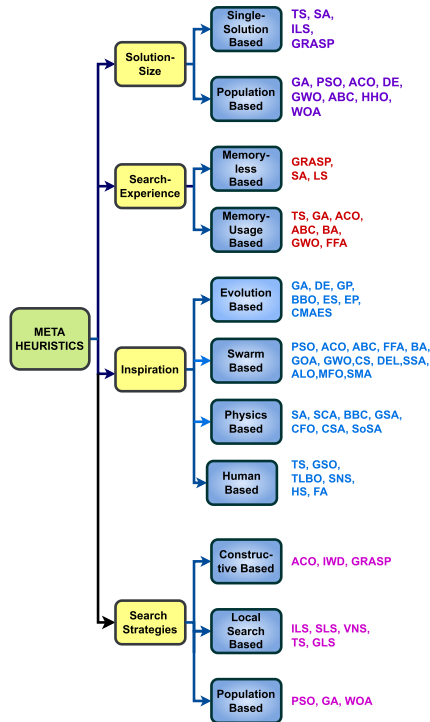


FIGURE 2. An illustration of the primary classification types of metaheuristics algorithms in the literature and popular examples of the categorisations.

incrementally. The solutions to the sub-problems are combined to obtain the complete solution [67]. Constructive metaheuristics found their roots in greedy algorithms, and hence they often generate suboptimal solutions [11]. In recent times there have been several approaches such as randomisation [68], memorisation [69], look-ahead strategy [70] to overcome this drawback. Examples of constructive metaheuristics are ACO, Intelligent Water Drops [71] (employed in [72], and GRASP. Unlike constructive metaheuristics that build solutions incrementally, thereby creating a set of partial solutions [67], local search-based metaheuristics generate a set of solutions (known as the neighbourhood of the solution) for each iteration or move. Each group of iterations produces solutions from the incumbent solutions [73] that become closer to the optimal solution. Hence, local search-based metaheuristics are known as a trajectory or neighborhood search methods [11]. Examples of local search-based metaheuristics are ILS [17], [73], stochastic local search (SLS) [74], Variable Neighborhood Search (VNS) [75], TS, and the Guided Local Search (GLS) [76].

Several metaheuristics have been proposed in the last couple of years. This is primarily attributed to the No Free Lunch (NFL) theorem [77]. The NFL theorem opines that no single algorithm is better than other algorithms for all optimisation problems. In other words, there is no universal metaheuristic that can efficiently solve all problem types. Similar to other works, this is premised on the NFL theorem in proposing the Deep Sleep Optimiser, a novel metaheuristic.

It is important to state that other than metaheuristics, classical solutions [78], [79], [80], learning methods [81], [82], [83], and algorithms have been employed in the literature to find global solutions or optima solutions for some real-world in fields such as social networks [84], [85], [86], [87], [88], wireless networks [89], and machine learning problems [90], [91], [92]. However, the focus of this work is on applying metaheuristics in the search for an optimum or near-optima solutions.

The outline of this paper is as follows. In Section II, a brief background of this work is presented. Section III describes DSO, its mathematical foundation, and computational complexity. Furthermore, we give a detailed description of the performance evaluation of the DSO and comparisons with other metaheuristics in Section IV. Section V presents the application of DSO to some engineering case studies. In Section VI, the ability of DSO to solve NP-Hard problems, specifically, the travelling salesman's problem and the knapsack problem is demonstrated. Section VII discusses the generalizability, challenges, and applications of DSO. We conclude this paper in Section VIII.

II. BACKGROUND

Sleep is a coordinated sequence of alterations in the brain affecting muscle and eye movement, heart rate, and respiratory rhythm [93], [94]. It is a critical function that greatly affects the mental and physical health of humans. Insomnia (i.e., sleep-disorder) affects the cognitive abilities, energy levels, and immune systems of humans [95], [96]. Understanding the brain is crucial to understanding the process of sleep [97], [98]. Structures in the brain that participate in the sleep process are the hypothalamus, suprachiasmatic nucleus (SCN), amygdala, basal forebrain, brain stem, pineal gland, and thalamus.

In birds and mammals, sleep can broadly be categorised into Rapid Eye Movement (REM) and non-REM stages. In REM sleep, dreaming occurs, muscles are relaxed (i.e., temporarily paralysed) and the activity of the brain increases (i.e., brain waves are faster). In non-REM sleep, body temperature reduces and the transition from wakefulness to sleep begins. Eye movement reduces, brain activity slows, and muscles relax, with random twitches/spasms. Non-REM sleep is associated with deep sleep. It is important to state that the sleep cycle starts with the non-REM sleep stage and then REM sleep. The REM-nonREM cycle occurs several times and the average time for a cycle is between 90mins and 120mins. In a typical night, humans may experience 4 – 6 sleep cycles [99], [100], [101], [102].

Recently, the American Academy of Sleep Medicine (AASM) classified the stages of sleep: (1) non-REM stage 1 (N1), (ii) non-REM stage 2 (N2), (iii) non-REM stage 3 (N3), and (iv) REM. N1 is the early transition from wakefulness to sleep and lasts a few minutes (i.e., between 5 – 10). In this phase, the eye muscles and movement slow down. The heart beat and breathing rhythm lower and the brain waves slow

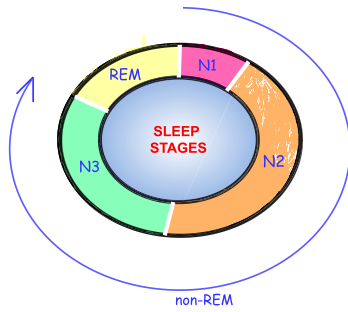


FIGURE 3. The four stages of sleep.

TABLE 1. List of notations.

Symbol	Description
$\mathcal{N}, \mathcal{N} $	Set of Agents and Number of agents
I	Number of maximum function evaluations
\mathcal{T}	Maximum duration of sleep
x_s	Sleep power index
x_w	Wake power index
t	Time (hour)
$\vec{H}(t)$	Homeostatic pressure value
$H(t)^{max}$	Maximum homeostatic pressure threshold
$H(t)^{min}$	Minimum homeostatic pressure threshold
H_o	Initial homeostatic pressure value
\vec{H}_o	Initial homeostatic pressure value
H_o^+	Maximum initial homeostatic pressure threshold
H_o^-	Minimum initial homeostatic pressure threshold
a	Circadian cost per unit function
$C(t)$	Circadian periodic function
$\mu(t)$	Agent switch asymptote
\vec{X}_{best}	Best candidate solution of the agents in deep sleep
\vec{X}_{mean}	Mean homeostatic pressure of agents in deep sleep
$\vec{\gamma}$	Initial solution of the agent

down. In some instances, people feel a sense of “falling”, which is referred to as hypnic myoclonic. The N2 stage entails further relaxation of the eye muscles and movement. The body temperature drops further and likewise the brain wave activity. The N3 stage is the deep sleep stage, during which the person does not respond to environmental stimuli. It is, therefore, difficult to wake a person in N3 sleep stage. This is as a result of the pressure release during sleep. Additionally, there is no eye or muscle movement and the brain waves are very slow. The last stage is the REM stage. The REM sleep stage has been explained in the preceding paragraph. Figure 3 illustrates the stages of sleep by the AASM.

III. DEEP SLEEP OPTIMISATION

In this section, we first describe the inspiration of the proposed DSO. The mathematical model is then discussed. Table 1 shows the main notations to be used in the following sections.

A. INSPIRATION OF THE DSO

Modern medicine contends that humans who are sleep deprived are less active and alert. Furthermore, sleep deprivation affects human cognitive ability [103], [104]. An agent

(i.e., an individual) that experiences adequate sleep will be much more physically active, alert, and cognitively fit compared to a sleep deprived agent.

At the beginning of the sleep process, agents feel a gradual sense of unconsciousness which is akin to a gradual descent into a hole; and pleasure, thanks to a reduction in levels of cortisone (i.e., the stress hormone). Moreover, it is generally said that people fall asleep. Figure 4 illustrates the “fall into a hole” concept of sleep, with the descent experienced just after the peaks. The depth of the “sleep hole” reached by an individual depends on the sleep stages attained during the sleep process.

To this end, the deeper a person sleeps, the further agent falls into the hole. The deep sleep state is synonymous with reaching the bottom of the hole. Consequently, in this work, we mimic the sleeping patterns of agents, especially the descent into a hole as a pressure release. The process of a gradual descent into the “sleep hole” is quite similar to finding the global optimum in Optimisation Theory. The global minima are akin to the bottom of the “sleep hole”.

Since sleep is associated with a “fall into a hole”, we will leverage this into finding a global minimum of an optimisation problem. This is as a result of the pressure release during sleep. Furthermore, a careful examination of the sleep process/cycle indicates that to avoid a local optimal in the search space, an agent is encouraged to experience deep sleep stage (i.e., N3). The main inspiration of the DSO stems from the sleeping pattern of a group of agents, which is explored such that the individual that attains the longest duration of the deep sleep stage determines the near-optimal or global-optimal solution to an optimisation problem. From the categorisation and classification of metaheuristics in Section, we see that DSO is not a constructive metaheuristic, but rather a population-based metaheuristic. Additionally, DSO mimics the human patterns of sleep activity in finding the optimal or near-optimal solutions to an optimisation problem. Therefore, we may also categorise DSO as a Human-based metaheuristic.

B. MATHEMATICAL MODEL OF THE DSO

The DSO mathematical model is based on the two-process sleep regulation model [105], [106], otherwise known as the Two-Process Model (TPM). The two-process sleep regulation model is based on the sleep-wake cycle and is dependent on two processes: (1) Homeostatic processes, in which, as the wakeful period increases, so does the need for sleep. In other words, the homeostatic processes increase exponentially while we are awake and exponentially decline during sleep. (2) Circadian processes determine the rhythmic changes between sleep to wake and also wake-sleep. For emphasis, the circadian process determines the onset and termination of a sleep episode [105], [107], [108], [109]. The sleep-wake cycle in a two-process sleep regulation is illustrated in Fig. 4.

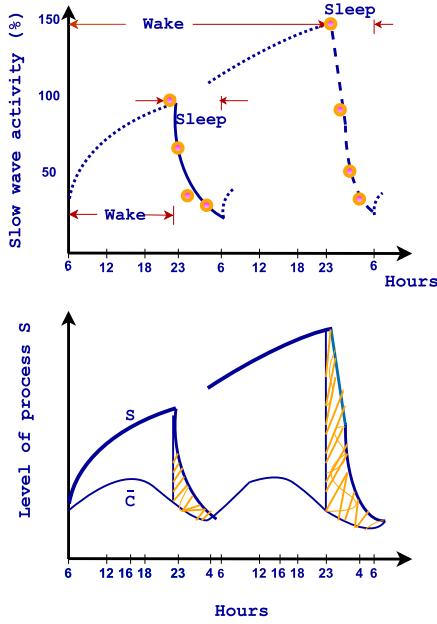


FIGURE 4. Illustration of the two-process sleep regulation showing the homeostatic pressure (S) [105].

In the two-process sleep regulation, an agent can either be in a sleep or wake state. The homeostatic pressure $\vec{H}(t)$ of an agent at a given time t is given as [110]

$$\vec{H}(t) = \begin{cases} \vec{H}_o(t) \cdot e^{(t_o-t)/x_s}, & \text{sleep state} \\ \mu(t) + (\vec{H}_o(t) - \mu(t)) \cdot e^{(t_o-t)/x_w}, & \text{wake state} \end{cases} \quad (1)$$

where x_s and x_w are the sleep power index and wake power index, respectively. $\vec{H}_o(t)$ denotes the initial homeostatic value. $\mu(t)$ denotes the threshold of wake or vice versa. $\mu(t)$ is the ‘‘upper asymptote’’ if agent is awake and with $\mu(t) = 1$. However, $\mu(t) = 0$ (i.e., lower asymptote) if agent is in sleep state. $\vec{H}(t)$ must lie within a maximum threshold, $\vec{H}(t)^{max}$, and a minimum threshold $\vec{H}(t)^{min}$, respectively, which are given as

$$\vec{H}(t)^{max} = \vec{H}_o^+ + a \times \mathcal{C}(t), \quad (2)$$

and

$$\vec{H}(t)^{min} = \vec{H}_o^- + a \times \mathcal{C}(t), \quad (3)$$

where a and $\mathcal{C}(t)$ denote the circadian cost per unit function and $\mathcal{C}(t)$ is the circadian periodic function. Besides, \vec{H}_o^+ and \vec{H}_o^- represent the maximum and minimum initial homeostatic values, respectively. The circadian periodic function $\mathcal{C}(t)$ of 24hrs is given as

$$\mathcal{C}(t) = \sin\left(\frac{2\pi}{T}(t - \alpha)\right), \quad (4)$$

α is circadian time shift variable which specifies the shift from the circadian maximum. α is a uniform distribution

```

Initialize searchAgentMax
nAgent=0;
while nAgent < searchAgentMax
    Obtain initial solution
    Randomly select and bound violating asymptote
    Compute new candidate solution based on Sleep-Wake cycle
    Evaluate new candidate solution
    Apply greedy selection strategy
    Update fitness value and position
    nAgent ++
end while
return best fitness value and position of Agent
    
```

FIGURE 5. Illustration of the DSO pseudo code.

random variable that lies between 0 and 1. Moreover, the initial homeostatic value $\vec{H}_o(t)$ in (1) is given as

$$\vec{H}_o(t) = \vec{\gamma} + \vec{r} \cdot (\vec{X}_{best} - \mu(t) \cdot \vec{X}_{mean}), \quad (5)$$

where \vec{X}_{mean} is the mean homeostatic value of the agents. \vec{X}_{best} is the best candidate solution of the agents in deep sleep. \vec{r} is a uniformly distributed random vector in $[0, 1]$. In addition, $\vec{\gamma}$ is the initial population of the agents. It is important to state that the initial homeostatic value updates the sleeping state of the agent.

As stated earlier, $\mu(t)$ denotes threshold of sleep or vice versa which lies between 0 and 1. Moreover, $\mu(t)$ helps to tune the exploratory and exploitation capability of DSO. As $\mu(t)$ tends towards 1, the exploration capability of the optimiser increases and accordingly, so does the avoidance of local optima. Whereas as $\mu(t)$ tends towards 0, the exploitation ability of DSO takes precedence over its exploratory abilities. DSO is designed to escape from a local optimum by ensuring the flexible movements of agents in the search space. In DSO, each candidate solution exists within a sleep-wake cycle based on the homeostatic pressure of its search agent. The homeostatic pressure decreases during the deep sleep phase or increases during the wake phase, allowing each agent to explore or exploit the search space within the confines of feasibility. It selects a new candidate solution by temporally restricting the evaluation of the previous solutions using a greedy selection strategy.

C. THE DSO ALGORITHM

The DSO optimiser is a global optimisation algorithm that explores and exploits a search space while leveraging the natural sleep-wake cycle modelled in humans. In the algorithm, an agent exploits the search space by mimicking a fall in a hole concept, which decreases the homeostatic pressure, inducing sleep. Where the quality of sleep is directly proportional to the depth and pressure achieved.

In exploration, the agent’s homeostatic pressure increases, mimicking the wake-phase of the cycle. With each sleep-wake cycle, the agent shares its fitness and position, which becomes the initial guide for the next agent mimicking the sleep-wake cycle. These actions allow for cognitive and social learning, less energy consumption, and quick convergence at the global minimum (NREM or near-NREM regions).

Algorithm 1 The DSO Algorithm

Input: $\mathcal{N}, \mathcal{I}, \mathcal{T}, a, x_s, x_w, \mathcal{H}_o^+, \mathcal{H}_o^-, UB, LB$

- 1: $\mathcal{F} \leftarrow$ Preallocate vector for the fitness of agents
- 2: $\mathcal{F}_{sol} \leftarrow$ Preallocate vector for best fitness solution of the each iteration
- 3: Compute the circadian periodic func. using (4)
- 4: Set the upper and lower homeostatic thresholds using (2) and (3)
- 5: $\vec{\gamma} \leftarrow$ Initialise position of the agents randomly
- 6: **for** $n \leftarrow 1$ to $|\mathcal{N}|$ **do**
- 7: $\mathcal{F}(n) \leftarrow$ Evaluate the fitness of agent n
- 8: **end for**
- 9: $\mathcal{F}_{sol}(1) \leftarrow$ Initial best fitness solution of the agents
- 10: **for** $i \leftarrow 1$ to \mathcal{I} **do**
- 11: **for** $n \leftarrow 1$ to $|\mathcal{N}|$ **do**
- 12: $\mathcal{F}(n) \leftarrow$ Evaluate the fitness of agent n
- 13: $k \leftarrow$ Determine the position of agent with best fitness
- 14: $\vec{X}_{best} \leftarrow$ Determine the best fitness solution
- 15: $\mu \leftarrow$ Randomly generate the upper asymptote
- 16: $\mathcal{H} \leftarrow$ Bound μ within \mathcal{H}^{min} & \mathcal{H}^{max}
- 17: Compute the initial homeostatic value using (5)
- 18: Determine if agent is asleep or awake using μ
- 19: $\mathcal{F}_n \leftarrow$ Evaluate the new fitness of the agent updated state
- 20: **if** $\mathcal{F}_n \leq \mathcal{F}(n)$ **then**
- 21: $\gamma(n, :) \leftarrow \vec{\mathcal{H}}$
- 22: $\mathcal{F}(n) \leftarrow \mathcal{F}_n$
- 23: **end if**
- 24: **end for**
- 25: $\mathcal{F}_{sol}(i+1) \leftarrow \min(\mathcal{F})$
- 26: **end for**
- 27: $\mathcal{F}_{sol}^* \leftarrow \operatorname{argmin}(\mathcal{F}_{sol})$
- 28: **return**

The pseudo code of DSO is presented in Fig. 5, while a detailed DSO-TPM algorithm as implemented in this study is expressed in Alg. 1. Consequently, with each iteration, an initial solution is first obtained from an agent then a new candidate solution is computed based on a randomly chosen asymptote value that is confined within reasonable bounds. The new solution is evaluated and a greedy selection strategy is applied. The fitness value and position of the new solution are repeatedly updated to ensure that global best values are achieved.

D. COMPUTATIONAL COMPLEXITY

In this subsection, we describe the computational complexity of the DSO. The computational complexity depicts the worst-case scenario running performance of an algorithm and DSO in this case. Moreover, we employ the big Omicron (big- \mathcal{O}) in characterising the DSO. The big- \mathcal{O} portrays the

TABLE 2. Unimodal benchmark functions.

Function	Var.	Range	f_{min}
$F_1(\mathcal{X}) = \sum_{i=1}^n \mathcal{X}_i^2$	30	[-100,100]	0
$F_2(\mathcal{X}) = \sum_{i=1}^n \mathcal{X}_i + \prod_{i=1}^n \mathcal{X}_i $	30	[-10,10]	0
$F_3(\mathcal{X}) = \sum_{i=1}^n (\sum_{j=1}^i \mathcal{X}_j)^2$	30	[-100,100]	0
$F_4(\mathcal{X}) = \max_i \{ \mathcal{X}_i , 1 \leq i \leq n\}$	30	[-100,100]	0
$F_5(\mathcal{X}) = \sum_{i=1}^{n-1} [100(\mathcal{X}_{i+1} - \mathcal{X}_i^2) + (\mathcal{X}_i - 1)^2]$	30	[-30, 30]	0
$F_6(\mathcal{X}) = \sum_{i=1}^n (\mathcal{X}_i + 0.5)^2$	30	[-100,100]	0
$F_7(\mathcal{X}) = \sum_{i=1}^n i\mathcal{X}_i^4 + \operatorname{random}[0, 1)$	30	[-1.28,1.28]	0

theoretical worst-case growth rate of the computational memory or execution time [111], [112].

From Alg. 1, we see that the big- \mathcal{O} of notation of the computational complexity of the DSO is given as $\mathcal{O}(\max(|\mathcal{N}|, |\mathcal{N}| * \mathcal{I}))$. This can be approximated to $\mathcal{O}(|\mathcal{N}| * \mathcal{I})$, where $|\mathcal{N}|$ denotes the cardinality of the set of agents \mathcal{N} and \mathcal{I} represents the maximum number of function evaluations.

IV. RESULTS AND DISCUSSIONS

In this section, the performance of the DSO is evaluated via extensive Monte Carlo simulations in a MATLAB environment. The DSO's MATLAB codes are in <https://github.com/DayoSun/Deep-Sleep-Optimiser>. The DSO's performance is premised on the widely accepted 23 traditional benchmark test functions, six composite functions, and selected engineering problems. Moreover, the DSO is compared with 11 state-of-the-art metaheuristics in the literature. First, in Tables 2-4, we describe the traditional benchmark test functions. Additionally, we give the control parameters of the 11 metaheuristics and DSO employed in the performance evaluation simulation in Table 5.

These benchmark functions [113], [114], [115], [116] are primarily grouped into three classes: (i) unimodal, (ii) multimodal, and (iii) fixed-dimension multimodal benchmark functions. The unimodal functions in Table 2 are characterised by convergence, leading to a single global solution, whereas the multimodal functions given in Table 3 are often associated with a harsh search landscape with several local optima and single global optima. However, the number of variables of fixed-dimension multimodal functions given in Table 4 cannot be adjusted. An in-depth description of these benchmark functions can be found in [113], [114], [115], and [116]. To ensure fairness, each metaheuristic ran recursively for 30 individual runs and terminated at 200 iterations per run.

A. TRADITIONAL BENCHMARK TEST FUNCTIONS**1) ACCURACY TEST COMPARISON**

In Tables 6-10, we investigate the performance of the DSO for variables ranging from 30, 100, 250, and 500 dimensions, considering the functions described in Tables 2-4. Moreover, the DSO's accuracy, taking into consideration the mean and

TABLE 3. Multimodal benchmark functions.

Function	Var.	Range	f_{min}
$F_8(\mathcal{X}) = \sum_{i=1}^n -\mathcal{X}_i \sin(\mathcal{X}_i ^{0.5})$	30	[-500, 500]	-418.9829
$F_9(\mathcal{X}) = 10n + \sum_{i=1}^n [\mathcal{X}_i^2 - 10 \cos(2\pi\mathcal{X}_i)]$	30	[-5.12, 5.12]	0
$F_{10}(\mathcal{X}) = -20e^{-0.2(\frac{1}{n} \sum_{i=1}^n \mathcal{X}_i^2)^{0.5}} - e^{[\frac{1}{n} \sum_{i=1}^n \cos(2\pi\mathcal{X}_i)]} + 20 + e$	30	[-32, 32]	0
$F_{11}(\mathcal{X}) = \frac{1}{4000} \sum_{i=1}^n \mathcal{X}_i^2 - \prod_{i=1}^n \cos(\frac{\mathcal{X}_i}{\sqrt{i}}) + 1$	30	[-600, 600]	0
$F_{12}(\mathcal{X}) = \frac{\pi}{n} [10 \sin(\pi y_1) + \sum_{i=1}^{n-1} (y_i - 1)^2 [1 + 10 \sin^2(\pi y_{i+1})]] + \sum_{i=1}^n u(\mathcal{X}_i, 10, 100, 4)$	30	[-50,50]	0
$y_i = 1 + \frac{\mathcal{X}_i + 1}{4}, u(\mathcal{X}_i, a, k, m) = \begin{cases} k(\mathcal{X}_i - a)^m, & \mathcal{X}_i > a \\ 0, & -a < \mathcal{X}_i < a \\ k(-\mathcal{X}_i - a)^m, & \mathcal{X}_i < -a \end{cases}$			
$F_{13}(\mathcal{X}) = 0.1 \left[\sin^2(3\pi\mathcal{X}_1) + \sum_{i=1}^n (\mathcal{X}_i - 1)^2 [1 + \sin^2(3\pi\mathcal{X}_i + 1)] + (\mathcal{X}_n - 1)^2 [1 + \sin^2(2\pi\mathcal{X}_n)] \right] + \sum_{i=1}^n u(\mathcal{X}_i, 5, 100, 4)$	30	[-50,50]	0

TABLE 4. Fixed-dimension multimodal benchmark functions.

Function	Var.	Range	f_{min}
$F_{14}(x) = (\frac{1}{500} \sum_{j=1}^{25} \frac{1}{j + \sum_{i=1}^2 (x_i - a_{ij})^6})^{-1}$	2	[-65, 65]	1
$F_{15}(x) = \sum_{i=1}^{11} [a_i - \frac{x_1(b_i^2 + b_i x_2)}{b_i^2 + b_i x_3 + x_4}]^2$	4	[-5, 5]	0.00030
$F_{16}(x) = 4x_1^2 - 2.1x_1^4 + \frac{1}{3}x_1^6 + x_1x_2 - 4x_2^2 + 4x_2^4$	2	[-5, 5]	-1.0316
$F_{17}(x) = (x_2 - \frac{5.1}{4\pi^2}x_1^2 + \frac{5}{\pi}x_1 - 6)^2 + 10(1 - \frac{1}{8\pi}) \cos x_1 + 10$	2	[-5, 5]	0.398
$F_{18}(x) = [1 + (x_1 + x_2 + 1)^2(19 - 14x_1 + 3x_1^2 - 14x_2 + 6x_1x_2 + 3x_2^2)] \times [30 + (2x_1 - 3x_2)^2 \times (18 - 32x_1 + 12x_1^2 + 48x_2 - 36x_1x_2 + 27x_2^2)]$	2	[-2,2]	3
$F_{19}(x) = -\sum_{i=1}^4 C_i e^{(-\sum_{j=1}^3 a_{ij}(x_j - P_{ij})^2)}$	3	[1, 3]	-3.86
$F_{20}(x) = -\sum_{i=1}^4 C_i e^{(-\sum_{j=1}^6 a_{ij}(x_j - P_{ij})^2)}$	6	[0, 1]	-3.32
$F_{21}(x) = -\sum_{i=1}^5 [(x - a_i)(x - a_i)^T + C_i]^{-1}$	4	[0, 10]	-10.1532
$F_{22}(x) = -\sum_{i=1}^7 [(x - a_i)(x - a_i)^T + C_i]^{-1}$	4	[0, 10]	-10.4028
$F_{23}(x) = -\sum_{i=1}^{10} [(x - a_i)(x - a_i)^T + C_i]^{-1}$	4	[0, 10]	-10.5363

standard deviation as performance metrics, is compared with 11 metaheuristics including the TLBO, GA, DE, PSO, ABC, GWO, SCA, BBO, ACO, RCSA, and HS. Hence, the average values in Tables 6-10 are compared with the expected values in Tables 2-4 (i.e., f_{min} column). We see that the DSO outperforms the other algorithms as the variable dimension increases. This is due to its exploitation ability. It is worth mentioning that even with the harsh terrains of the fixed multi-modal function landscape of functions F14-F23, the DSO was able to obtain the global optimum for functions F16 and F17, and fared quite well with other multimodal functions.

2) SEARCH AND CONVERGENCE ANALYSIS

In addition, the search and convergence performance of the DSO is investigated. Figs. 6-13 show the search and convergence analysis of the DSO.

Owing to the paucity of space in this paper, we only show the convergence of functions F1, F4, F7, F9, F10, F13, F14, and F16. The search history plot shows the position of agents in the search landscape. The homeostatic pressure plot shows

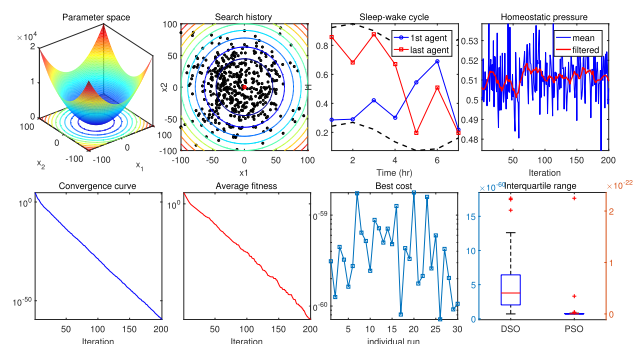


FIGURE 6. Illustration of the DSO search and convergence analysis for F1.

the rise and fall of the homeostatic pressure given (1) for different iterations. The convergence curve shows the convergence of an agent over the course (i.e., iterations) of the search space of a respective function. Owing to space, we compare the interquartile ranges of the DSO and PSO, rather than all the 11 metaheuristics. In Figs. 6-13, we observe that the DSO is able to benefit from its exploration and exploitation ability

TABLE 5. The control parameters of the respective metaheuristics.

Metaheuristic	Control Param.	Values
DSO	Minimum initial homeostatic	0.17
	Maximum initial homeostatic	0.85
	Sleep power index	4.2
	Wake power index	18.2
	Maximum sleep duration	24
TLBO	Teaching factor,	1.2
GA	Distribution index for crossover	20
	Distribution index for mutation	20
	Probability of crossover	0.8
	Probability of mutation	0.2
DE	Crossover probability	0.8
	Scaling factor	0.45
PSO	Inertia weight	0.45
	Personal learning coef.	1
	Global learning coef.	1
ABC	Percentage onlooker bee	50% of the colony
	Number of scout	1
GWO	Convergence parameter	Linear reduction 2 to 0
SCA	Convergence parameter	Linear reduction 2 to 0
BBO	Probability of modifying a habitat	1
ACO	Deviation-distance ratio	1
	Intensification Factor	0.5
	Sample size	40
	Convergence parameter	Linear reduction 2 to 0
RCSA	Initial Temp.	0.1
	Temp. reduction rate	0.99
	Mutation rate	0.5
	Mutation range	0.1(UB-LB)
	Max. no of sub-iterations	20
HS	Neighbors per individual	5
	No. of new harmonies	20
	Harmony memory consideration rate	0.9
	Pitch adjustment rate	0.1
	Fret width damp ratio	0.995

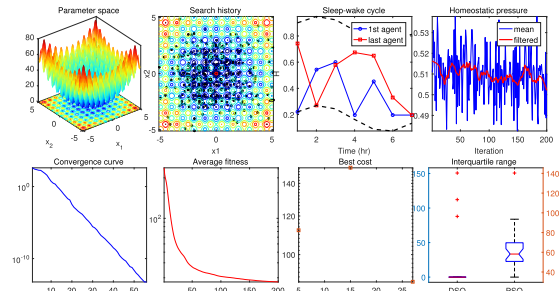


FIGURE 9. Illustration of the DSO search and convergence analysis for F9.

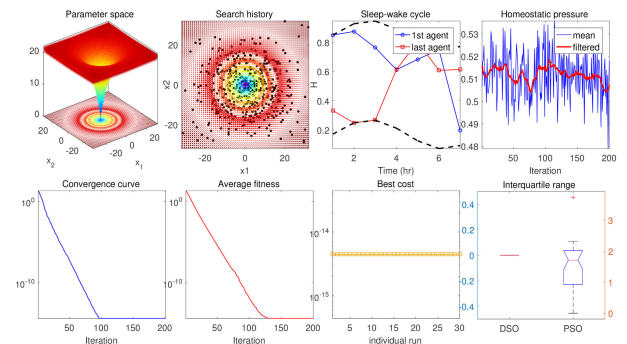


FIGURE 10. Illustration of the DSO search and convergence analysis for F10.

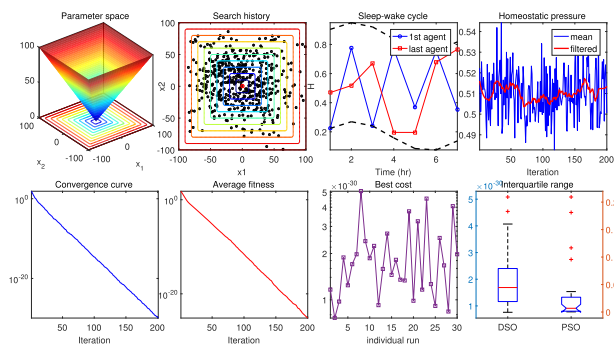


FIGURE 7. Illustration of the DSO search and convergence analysis for F4.

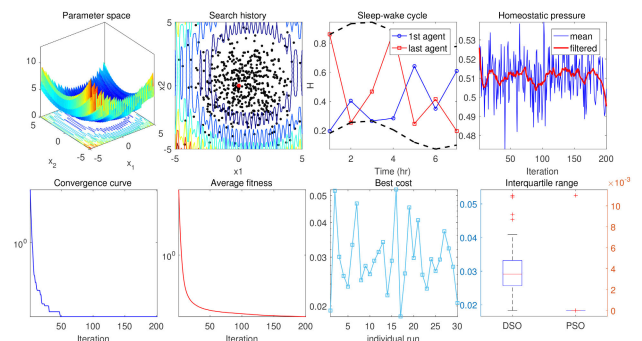


FIGURE 11. Illustration of the DSO search and convergence analysis for F13.

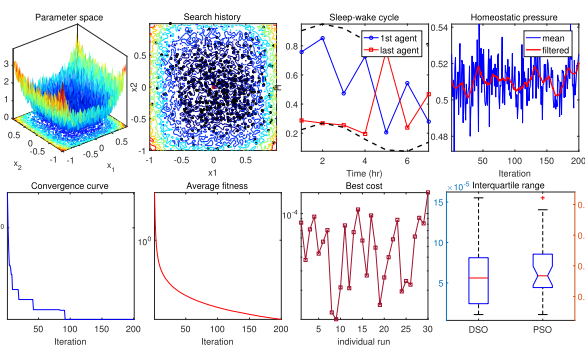


FIGURE 8. Illustration of the DSO search and convergence analysis for F7.

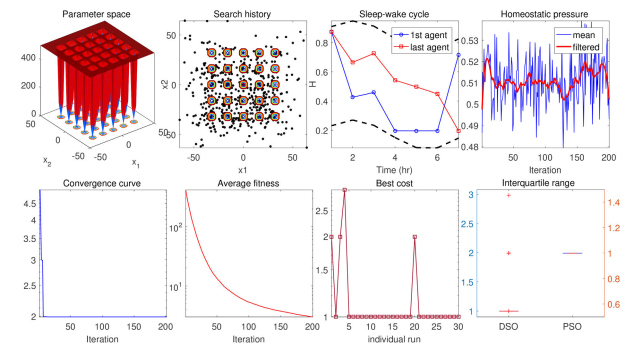


FIGURE 12. Illustration of the DSO search and convergence analysis for F14.

to find the global optima for the traditional test functions. As per the convergence, the DSO's performance is impressive even in the face of several local optima in the landscape of

the multimodal functions F14 and F16 in Figs. 12 and 13. Furthermore, we investigate the sleep-wake cycle patterns of the agents in Figs. 6-13. We observe that sleep-wake patterns

TABLE 6. Results of benchmark functions with 30 dimensions.

Func.	Metric	DSO	TLBO	GA	DE	PSO	ABC	GWO	SCA	BBO	ACO	RCSA	HS
1	AVG	1.8105E-113	6.1805E-86	4.4169E+04	1.5123E+02	1.4081E+03	3.8010E+03	3.2188E-01	2.4293E+01	4.0403E+00	6.1540E+00	7.3589E-06	2.1429E+02
	STD	4.3998E-113	1.1398E-85	6.1499E+03	2.2156E+02	1.0926E+03	2.1354E+03	3.0880E-01	3.8962E+01	9.5070E-01	3.5752E+00	1.0796E-06	7.6459E+01
2	AVG	6.1609E-58	1.8252E-43	6.5864E+03	4.8424E-01	4.8844E+01	1.7595E+01	4.9248E-02	4.3297E-02	6.4002E-01	5.2285E-01	1.1411E-03	2.5807E+00
	STD	1.3459E-57	2.6806E-43	2.7532E+04	1.3965E+00	1.6958E+01	4.3012E+00	5.5593E-02	9.0305E-02	6.9257E-02	3.0744E-01	9.1755E-05	6.4914E+01
3	AVG	3.0197E-108	7.7693E-20	6.8815E+04	2.2340E+03	1.3941E+04	3.9206E+04	2.0140E+03	1.2738E+04	7.8708E+02	4.6451E+04	3.2530E-05	1.6797E+04
	STD	7.1364E-108	2.8051E-19	1.5833E+04	1.2758E+03	6.3997E+03	4.3247E+03	1.2904E+03	7.7288E+03	2.3681E+02	7.0623E+03	7.4802E-06	3.8737E+03
4	AVG	5.6696E-57	5.4204E-36	7.2428E+01	3.1957E+01	3.3031E+01	7.0970E+01	1.1710E+01	4.2963E+01	2.5128E+00	8.6415E+01	1.1868E-03	2.0931E+01
	STD	1.1719E-56	7.2883E-36	4.3213E+00	7.2931E+00	6.4000E+00	3.4699E+00	7.2161E+00	1.3185E+01	1.2127E+00	5.1717E+00	1.3634E-04	2.6509E+00
5	AVG	2.8813E+01	2.5892E+01	1.0831E+08	2.0116E+05	1.3242E+05	1.4373E+06	9.4606E+01	1.4993E+05	2.0429E+02	2.0133E+04	1.5967E+01	1.5230E+04
	STD	3.8628E-02	4.4840E-01	2.9643E+07	4.5443E+05	1.3308E+05	1.2775E+06	1.0310E+02	3.1914E+05	2.2318E+02	3.0240E+04	1.6491E+01	8.4078E+03
6	AVG	7.3730E+00	6.4521E-04	4.3298E+04	1.2062E+02	1.3264E+03	4.5524E+03	6.1551E+00	4.9065E+01	3.5766E+00	5.5533E+00	7.4732E-06	2.3879E+02
	STD	2.3039E-01	9.9460E-04	6.1171E+03	1.6477E+02	8.7720E+02	1.8617E+03	3.4447E-01	7.2557E+01	8.3720E-01	2.8234E+00	1.0664E-06	7.1177E+01
7	AVG	3.1145E-04	1.0942E-03	5.3731E+01	1.6118E-01	3.7776E+00	7.6136E+00	5.8775E-01	1.6822E-01	2.6785E-02	1.9606E-01	7.7341E-03	2.0048E-01
	STD	1.9713E-04	4.3750E-04	1.1706E+01	1.4023E-01	1.4392E+00	3.4796E+00	3.1714E-01	2.5038E-01	9.2472E-03	8.3129E-02	3.0451E-03	6.2526E-02
8	AVG	-5.0142E+03	-7.5484E+03	-5.0630E+03	-7.8595E+03	-6.6655E+03	-7.2381E+03	-5.6348E+03	-3.5514E+03	-7.6129E+03	-4.5429E+03	-1.1360E+04	-1.2422E+04
	STD	6.7112E+02	9.0285E+02	5.7891E+02	1.0511E+03	6.7513E+02	3.5895E+02	8.9416E+02	2.8695E+02	8.7357E+02	3.4796E+02	3.5346E+02	6.8042E+01
9	AVG	5.0859E+01	1.6242E+01	2.8881E+02	1.2143E+02	1.1727E+02	1.4990E+02	1.7714E+02	3.4803E+02	7.1422E+01	2.6784E+02	4.2251E-01	1.8642E+01
	STD	7.9501E+01	1.0224E+01	3.0708E+01	3.7714E+01	2.7472E+01	2.2610E+01	3.1288E+01	3.0152E+01	1.6020E+01	1.4684E+01	9.7649E+00	2.9925E+00
10	AVG	4.4409E-15	2.2612E-01	1.9587E+01	3.1425E+00	1.5357E+01	2.0854E+01	1.3377E+01	7.7697E-01	1.4325E+01	6.3567E+01	1.3567E+02	4.9440E+00
	STD	0.0000E+00	0.0000E+00	2.3270E-01	1.6066E+00	1.6494E+00	1.0404E+01	1.6835E-01	8.9014E+00	1.6419E-01	8.5704E+00	5.1765E-05	4.7486E-01
11	AVG	1.2388E-03	0.0000E+00	4.0360E+02	1.8891E+00	2.1902E+01	4.2566E+01	3.5465E-01	1.2542E+00	1.0204E+00	1.0445E+00	1.0936E+02	9.2946E+00
	STD	4.8731E-03	0.0000E+00	6.5058E+01	2.2182E+00	2.5618E+01	1.5277E+01	2.5085E-01	6.7883E-01	2.4756E-02	4.6791E-02	1.0208E-02	6.1035E-01
12	AVG	1.1419E+00	2.8123E-04	1.9800E+08	1.7891E+05	1.1663E+02	8.9739E+05	3.5554E+00	5.5000E+04	3.0035E-02	6.6439E+03	3.4556E-03	5.5059E+01
	STD	3.7090E-01	1.5300E-03	9.2854E+07	4.4038E+05	3.1123E+02	1.1961E+06	1.7956E+00	1.8246E+05	5.5424E-02	1.1090E+04	1.8927E-02	2.2526E+00
13	AVG	5.9659E-02	2.3370E-01	4.3280E+08	3.8578E+05	2.2878E+04	7.1467E+06	3.2760E+00	2.6746E+05	1.8063E-01	7.7928E+04	7.3273E-04	8.6518E+01
	STD	1.6898E-02	2.2513E-01	9.6947E+07	8.6325E+05	6.4965E+04	9.5681E+06	1.2670E+00	5.1810E+05	5.0867E-02	1.6628E+05	2.7877E-03	9.2590E+01

TABLE 7. Results of benchmark functions with 100 dimensions.

Func.	Metric	DSO	TLBO	GA	DE	PSO	ABC	GWO	SCA	BBO	ACO	RCSA	HS
1	AVG	1.5464E-113	6.1873E-79	2.2698E+05	8.0840E+03	5.5659E+04	1.1256E+05	5.2790E+02	9.5369E+03	2.9493E+02	1.7520E+05	1.4978E-04	2.9211E+04
	STD	3.1065E-113	1.0010E-78	1.7200E+04	2.4240E+03	1.4345E+04	1.7964E+04	3.6378E+02	5.8030E+03	2.4410E+01	1.0756E+04	1.3619E-05	2.6394E+03
2	AVG	2.7748E-57	2.6558E-40	2.3312E+34	4.1849E+01	3.0116E+02	6.6561E+02	1.3704E+00	1.0266E+01	1.3439E+01	2.5646E+33	1.0966E-02	8.1658E+01
	STD	3.2228E-57	2.0792E-40	1.1681E+35	1.2713E+01	2.4336E+02	2.6593E+03	1.0749E+00	8.9188E+00	1.7839E+00	1.3545E+34	6.0303E-04	5.9300E+00
3	AVG	8.2932E-104	6.8958E-09	6.8358E+05	1.4912E+05	1.6139E+05	4.0484E+05	1.6612E+05	2.4147E+05	5.8839E+04	6.7082E+05	2.2751E-02	4.0075E+05
	STD	2.3627E-103	1.5696E-08	1.4052E+05	3.2479E+04	4.5151E+04	6.1078E+04	3.6983E+04	5.7558E+04	9.7224E+03	7.3348E+04	2.7452E-03	5.9645E+04
4	AVG	7.2927E-57	6.7468E-33	8.9516E+01	9.6522E+01	5.3016E+01	9.2474E+01	9.1907E+01	9.0236E+01	3.0715E+01	9.6830E+01	5.2988E-03	6.4946E+01
	STD	1.9602E-56	4.5052E-33	1.9763E+00	1.0580E+00	1.5852E+00	1.5781E+00	5.3846E+00	2.7722E+00	3.0148E+00	1.0780E+00	2.4019E-04	1.3027E+00
5	AVG	9.3483E+01	9.7238E+01	8.3337E+08	1.1578E+07	6.6459E+07	3.1400E+08	4.2737E+05	1.3440E+08	7.2636E+03	1.1925E+09	1.1671E+02	4.7122E+07
	STD	1.1205E-01	7.0405E-01	1.4129E+08	6.1102E+06	3.3249E+07	9.4369E+07	4.0323E+05	6.5901E+07	1.6063E+03	9.8382E+03	7.0073E+01	6.6565E+06
6	AVG	2.4863E+01	4.5894E+00	2.2867E+05	7.6385E+03	6.0772E+04	1.1127E+05	5.3309E+02	9.4744E+03	2.9331E+02	1.7676E+05	1.4920E-04	2.9176E+04
	STD	2.9140E-01	6.7576E-01	1.7238E+04	2.9580E+03	1.2226E+04	2.0289E+04	3.1022E+02	7.3879E+03	3.1174E+01	1.0696E+04	1.4236E-05	2.5646E+03
7	AVG	2.8930E-04	1.4655E-03	1.3423E+03	1.5637E+01	1.6288E+02	6.8109E+02	1.6613E+00	1.5910E+02	2.2663E-01	1.2696E+03	8.6267E-02	6.5736E+01
	STD	1.9041E-04	5.8867E-04	1.9416E+02	5.2389E+00	6.2524E+01	1.5227E+02	8.6850E-01	7.2705E+01	4.4702E-02	1.7358E+02	1.5957E-02	8.8175E+00
8	AVG	-1.0733E+04	-1.8636E+04	-9.8784E+03	-1.4596E+04	-1.6282E+04	-1.7964E+04	-9.4453E+03	-6.7438E+03	-2.2077E+04	-8.2825E+03	-3.1284E+04	-3.3584E+04
	STD	1.1051E+03	2.8277E+03	1.0641E+03	3.7682E+03	1.4434E+03	1.0602E+03	1.0268E+03	6.2496E+02	1.1337E+03	5.2018E+02	9.6306E+02	5.9746E+02
9	AVG	0.0000E+00	5.6932E+00	1.3534E+03	4.9445E+02	7.4019E+02	9.7411E+02	8.3425E+02	3.1186E+02	4.1039E+02	1.4454E+03	2.5259E+02	3.5557E+02
	STD	0.0000E+00	3.1183E+01	5.4938E+01	1.7311E+02	8.6661E+01	5.5084E+01	8.6260E+01	1.5315E+02	4.2597E+01	3.2250E+01	3.4241E+01	2.3641E+01
10	AVG	4.4409E-15	3.1732E-01	2.0536E+01	1.1458E+01	1.8415E+01	1.9743E+01	2.0879E+01	1.6942E+01	3.6860E+00	2.0714E+01	1.5829E-03	1.4932E+01
	STD	0.0000E+00	1.7381E+00	9.2811E-02	1.1871E+00	4.8831E-01	1.9057E-01	1.2070E-01	5.2679E+00	1.3511E-01	3.5794E-02	7.1983E-05	3.3187E-01
11	AVG	0.0000E+00	0.0000E+00	2.0174E+03	8.0200E+01	4.8831E+02	9.6115E+02	5.5762E+00	1.2696E+02	3.6815E+00	1.5822E+03	1.0274E-03	2.6591E+02
	STD	0.0000E+00	0.0000E+00	5.1819E+02	3.0660E+01	1.0395E+02	1.4619E+02	3.2927E+00	8.2749E+01	2.8035E-01	9.6870E+01	2.7941E-03	2.3917E+01
12	AVG	1.2874E+00	4.9309E-02	1.8002E+09	1.1285E+07	4.9881E+07	7.0486E+08	8.4625E+04	3.2572E+08	8.0527E+00	2.9001E+09	1.1403E-02	4.2087E+01
	STD	6.1045E-02	1.1996E-02	3.5926E+08	1.2300E+07	6.6804E+07	1.7282E+08	2.1612E+05	1.5696E+08	3.1236E+00	2.6523E+08	2.6444E-02	8.9680E+06
13	AVG	3.2568E-01	6.9547E+00	3.4895E+09	2.7272E+07	1.8627E+08	1.4423E+09	2.5235E+05	5.2352E+08	1.6483E+01	5.5485E+09	2.2028E-03	1.3407E+08
	STD	5.8328E-02	1.0221E+00	5.1593E+08	1.1025E+07	1.5594E+08	4.0951E+08	4.6501E+05	2.9241E+08	2.6076E+00	4.9357E+08	4.4721E-03	1.5944E+07

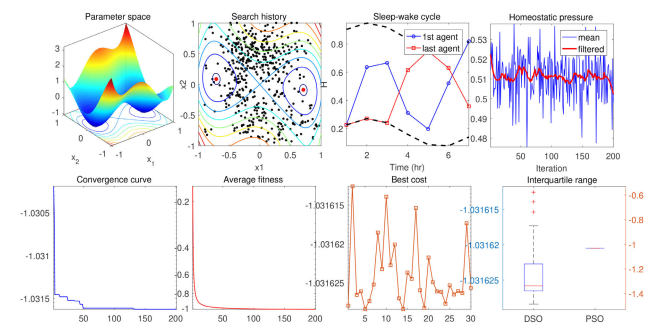


FIGURE 13. Illustration of the DSO search and convergence analysis for F16.

of the agents follow the trend illustrated in Fig. 4. To this end, we demonstrate the sleep-wake cycle of the first and last agent for the respective functions.

Furthermore, we discuss the convergence capabilities of DSO for the functions illustrated in Figs. 8 – 13 that primarily

represent unimodal, multimodal, and fixed-dimensional multimodal functions. In Fig. 8, we observe that DSO converges before the 100th iteration. This is fair for a high dimensional quartic function with Gaussian noise. Similar to the convergence in Fig. 8, in Fig. 10, we observe that the DSO converges at about the 100th iteration for the multimodal Ackley function (i.e., F10). With careful fine-tuning of DSO's parameters, the convergence could be accelerated. However, for a less rugged search landscape in Fig. 11, we see that the DSO converges at about the 50th iteration. It shows that the terrain of the search landscape plays a role in the convergence of the proposed metaheuristic. Additionally, for the fixed-dimensional multimodal functions (F14 and F16) in Figs. 12 and 13 with a less harsh search landscape, we observe that the DSO converges less than or at about the 50th iteration.

3) SEARCH TRAJECTORY OF THE AGENTS

Figures 14-21 present the search trajectory of the agents. Figures 14-19 illustrate the search route of the agents in

TABLE 8. Results of benchmark functions with 250 dimensions.

Func.	Metric	DSO	TLBO	GA	DE	PSO	ABC	GWO	SCA	BBO	ACO	RCSA	HS
1	AVG	3.5418E-113	6.9204E-77	6.5418E+05	8.4816E+04	2.7709E+05	4.9767E+05	8.3389E+03	7.8684E+04	2.3600E+03	7.4354E+05	1.3977E-03	1.9258E+05
	STD	9.0074E-113	9.6287E-77	3.1431E+04	1.0109E+04	2.9345E+04	3.5484E+04	3.2962E+03	3.7458E+04	1.6328E+02	2.3694E+04	7.7488E-05	1.1910E+04
2	AVG	6.6096E-57	2.2393E-39	6.7723E+109	3.0848E+02	8.0663E+02	7.6371E+69	7.1056E+00	9.1740E+01	9.1740E+01	2.0502E+122	8.2060E+02	4.3182E+02
	STD	1.1980E-56	1.4657E-39	3.1348E+110	2.7058E+01	7.2667E+01	4.1830E+70	4.2474E+00	2.8144E+01	6.0283E+00	1.0659E+123	1.8719E+02	1.7694E+01
3	AVG	8.3790E-100	7.8574E-05	4.3974E+06	1.1849E+06	1.0192E+06	2.4346E+06	2.0290E+06	1.8111E+06	4.2336E+05	3.8869E+06	2.6485E+04	2.6979E+06
	STD	4.5653E-99	1.8220E-04	9.1904E+05	2.3561E+05	2.9106E+05	2.8308E+05	4.7440E+05	4.5465E+05	5.9926E+04	4.8071E+05	3.2084E+03	3.4093E+05
4	AVG	1.0140E-56	6.2853E-32	9.6683E+01	9.8479E+01	6.3637E+01	9.7104E+01	9.8945E+01	9.7698E+01	4.9640E+01	9.8612E+01	2.9793E+00	8.4754E+01
	STD	1.4804E-56	3.6394E-32	9.8607E-01	4.8535E-01	2.9210E+00	5.5100E-01	4.7956E-01	6.9634E-01	2.3231E+00	4.5284E-01	1.6597E+00	7.1041E-01
5	AVG	2.4740E+02	2.4750E+02	2.6158E+09	1.2641E+08	6.2310E+08	2.1001E+09	2.8635E+07	7.9543E+08	1.8300E+05	3.5123E+09	2.8511E+02	5.1124E+08
	STD	2.6727E-01	3.9845E-01	2.5106E+08	3.8570E+07	1.3767E+08	2.1745E+08	2.4272E+07	1.8493E+08	1.9885E+04	1.4497E+08	8.1625E+01	5.0804E+07
6	AVG	6.2433E+01	3.0621E+01	6.6469E+05	8.6424E+04	2.6450E+05	4.9331E+05	8.3772E+03	7.5551E+04	2.4907E+03	7.4619E+05	1.4057E-03	1.9480E+05
	STD	1.6743E-01	1.5983E+00	3.3495E+04	1.4179E+04	1.5435E+02	6.4907E+02	1.1154E+03	7.5340E+01	6.9372E+02	3.1773E-04	6.0574E+02	1.2255E+02
7	AVG	3.0690E-04	1.7217E-03	1.0838E+04	5.2082E+02	2.2114E+03	8.5432E+03	1.0392E+02	2.8663E+03	1.8300E+00	1.3913E+04	4.5190E-01	1.8765E+03
	STD	2.4503E-04	5.9209E-04	1.2595E+03	1.5435E+02	6.4907E+02	1.1154E+03	7.5340E+01	6.9372E+02	3.1773E-04	6.0574E+02	5.8893E-02	1.2255E+02
8	AVG	-2.0351E+04	-3.1596E+04	-1.5904E+04	-2.5453E+04	-2.8615E+04	-2.9464E+04	-1.5235E+04	-1.0471E+04	-4.8792E+04	-1.3142E+04	-7.0742E+04	-6.0645E+04
	STD	2.6322E+03	5.8982E+03	2.4371E+03	1.0319E+04	2.5692E+03	2.9352E+03	1.3188E+03	7.7229E+02	2.1583E+03	9.5636E+02	2.0593E+03	1.3129E+03
9	AVG	0.0000E+00	0.0000E+00	3.8475E+03	1.5591E+03	2.3547E+03	3.2828E+03	2.2490E+03	6.7477E+02	1.5239E+03	4.2430E+03	9.6690E+02	1.8243E+03
	STD	0.0000E+00	0.0000E+00	9.3624E+01	3.0602E+02	1.4918E+02	1.3832E+02	1.9708E+02	2.8968E+02	8.4061E+01	5.9753E+01	8.4122E+01	5.6468E+01
10	AVG	4.4409E-15	1.1912E+00	2.0821E+01	1.6608E+01	1.9513E+01	2.0479E+01	2.0909E+01	1.8847E+01	5.5818E+00	2.0897E+01	3.0594E-03	1.8332E+01
	STD	0.0000E+00	3.6543E+00	4.4644E-02	6.1798E-01	1.6185E-01	1.0346E-01	5.3137E-02	3.8906E+00	1.9083E-01	2.1383E-02	6.9613E-05	1.3139E-01
11	AVG	0.0000E+00	0.0000E+00	6.0726E+03	7.5674E+02	2.4421E+03	4.6850E+03	8.6601E+01	7.3668E+02	2.2956E+01	6.6809E+03	9.4481E-04	1.7421E+03
	STD	0.0000E+00	0.0000E+00	2.4373E+02	1.0955E+02	2.5935E+02	2.7602E+02	3.0762E+01	3.1311E+02	1.8523E+00	2.3774E+02	1.8102E-03	6.5853E+01
12	AVG	1.2238E+00	2.7930E-01	6.7568E+09	1.3868E+08	8.5653E+08	4.7600E+09	1.0031E+08	2.2467E+09	3.5876E+02	8.4445E+09	1.1281E+00	8.9971E+08
	STD	1.9824E-02	3.3967E-02	5.1097E+08	5.4770E+07	3.8953E+08	7.3411E+08	1.1021E+08	5.1329E+08	6.0353E+02	4.7952E+08	5.4201E-01	6.4707E+07
13	AVG	9.1548E-01	2.4857E+01	1.2438E+10	4.1233E+08	2.0886E+09	9.0664E+09	1.4327E+08	3.5751E+09	2.5711E+04	1.5463E+10	5.9089E-03	1.9577E+09
	STD	1.6791E-01	1.1505E-02	9.2088E+08	1.2605E+08	6.2395E+08	1.1607E+09	1.0642E+08	1.0244E+09	1.8669E+04	7.9818E+08	9.0112E-03	1.7867E+08

TABLE 9. Results of benchmark functions with 500 dimensions.

Func.	Metric	DSO	TLBO	GA	DE	PSO	ABC	GWO	SCA	BBO	ACO	RCSA	HS
1	AVG	8.5668E-112	1.6496E-75	1.4531E+06	3.0017E+05	6.7871E+05	1.2908E+06	4.3704E+04	2.0717E+05	1.3570E+04	1.5451E+06	7.7412E-03	6.2374E+05
	STD	3.4816E-111	2.9811E-75	3.1558E+04	2.8733E+04	7.4767E+04	4.6608E+04	9.6993E+03	6.4583E+04	1.1107E+03	3.1140E+04	3.3718E-04	2.1374E+04
2	AVG	1.9998E-56	9.4708E-39	3.1364E+246	9.9584E+02	1.4581E+80	3.0125E+201	2.5820E+01	1.1279E+02	6.0494E+02	1.7840E+265	1.6796E+99	1.3849E+03
	STD	4.8998E-56	6.2028E-39	Inf	5.3518E+01	7.9864E+80	Inf	5.5185E+00	5.4604E+01	2.4604E+02	Inf	9.1998E+99	3.3423E+01
3	AVG	2.7239E-103	4.7744E-03	1.7978E+07	5.4147E+06	3.8680E+06	9.6217E+06	9.4681E+06	7.0210E+06	1.7244E+06	1.6272E+07	2.9939E+05	1.1167E+07
	STD	8.5701E-103	1.2149E-02	4.6690E+06	9.8897E+05	8.9268E+05	1.3332E+06	1.6537E+06	1.5331E+06	2.3253E+05	1.9217E+06	1.7318E+04	1.2148E+06
4	AVG	1.4843E-56	3.0070E-31	9.8791E-01	9.9295E+01	6.9280E+01	9.8602E+01	9.9730E+01	9.9120E+01	6.2230E+01	9.9306E+01	4.8033E+01	2.2389E+01
	STD	1.9348E-56	1.8954E-31	2.8871E-01	2.2647E-01	3.4643E+00	1.2121E-01	2.2617E-01	2.8586E-01	1.9774E+00	2.4597E-01	2.3518E+00	4.2115E-01
5	AVG	4.9572E+02	4.9730E+02	6.4532E+09	3.7418E+09	1.9578E+09	5.4173E+09	2.6194E+08	1.9671E+09	3.2056E+06	7.2656E+09	6.8628E+02	1.9710E+09
	STD	5.6176E-01	2.3373E-01	3.0808E+08	3.3032E+09	2.9817E+08	3.9003E+08	1.2697E+08	4.9685E+08	5.2340E+05	2.3233E+08	3.4863E+02	8.2392E+07
6	AVG	1.2500E+02	8.4840E+01	1.4326E+06	3.0448E+05	6.9418E+05	1.2721E+06	4.6361E+04	1.8861E+05	1.3448E+04	1.5350E+06	7.8257E-03	6.1657E+05
	STD	1.7121E-02	2.3652E+00	5.6868E+04	2.8823E+04	6.2377E+04	7.0943E+04	1.2402E+04	7.8156E+04	1.1112E+03	2.7635E+04	2.4807E-04	1.5399E+04
7	AVG	2.8448E-04	1.6346E-03	5.0765E+04	4.3022E+03	1.5454E+04	4.4993E+04	1.9481E+03	1.6393E+04	2.8314E+01	5.8887E+04	1.3697E+00	1.4635E+04
	STD	2.5612E-04	6.1093E-04	2.8923E+03	9.7123E+02	3.1173E+03	3.3393E+03	8.6111E+02	4.3284E+03	5.5605E+00	4.3284E+03	1.1611E-01	7.3929E+02
8	AVG	-2.8728E+04	-4.1030E+04	-2.2033E+04	-3.1461E+04	-4.2428E+04	-4.2467E+04	-2.1913E+04	-1.5101E+04	-8.7685E+04	-1.8526E+04	-1.3137E+05	-8.8219E+04
	STD	3.4136E+03	1.1856E+04	2.5216E+03	1.0911E+04	5.2090E+03	4.9269E+03	1.7945E+03	1.2637E+03	4.1658E+03	1.1429E+03	2.5131E+03	2.0046E+03
9	AVG	0.0000E+00	0.0000E+00	8.0862E+03	3.7127E+03	5.4563E+03	7.3720E+03	4.2783E+03	1.1652E+03	3.8845E+03	8.8290E+03	2.4204E+03	5.0257E+03
	STD	0.0000E+00	0.0000E+00	1.5896E+02	2.8281E+02	2.6456E+02	2.2893E+02	7.7246E+02	4.8115E+02	1.3231E+02	1.0800E+02	1.3306E+02	8.3042E+01
10	AVG	4.4409E-15	1.0883E+00	2.0946E+01	1.8193E+01	1.9891E+01	2.0757E+01	2.0890E+01	1.9416E+01	1.0601E+01	2.0972E+01	1.4486E+00	1.9581E+01
	STD	0.0000E+00	3.3215E+00	3.6591E-02	3.3330E-01	2.1818E-01	5.9238E-02	3.9427E-02	3.1796E+00	1.1813E+00	1.4624E-02	1.2519E-01	8.1676E-02
11	AVG	0.0000E+00	0.0000E+00	1.2839E+04	2.7670E+03	6.2528E+03	1.1325E+04	4.2277E+02	1.8018E+03	1.2049E+02	1.3807E+04	2.7000E-03	5.5433E+03
	STD	0.0000E+00	0.0000E+00	5.8869E+02	2.7100E+02	5.0080E+02	4.7113E+02	1.5262E+02	6.2379E+02	8.1041E+00	3.6492E+02	1.3096E-03	1.5626E+02
12	AVG	1.2059E+00	5.4733E-01	1.5398E+10	1.5551E+10	3.4076E+09	1.3431E+10	1.5114E+09	6.0459E+09	3.6734E+05	1.7690E+10	5.4406E+00	3.8490E+09
	STD	4.3973E-03	2.6498E-02	7.9188E+08	5.9348E+09	1.1221E+09	1.1013E+09	8.9402E+08	1.2138E+09	1.5881E+05	4.5410E+08	5.3176E-01	2.1162E+08
13	AVG	2.0591E+00	4.9824E+01	2.8772E+10	2.3361E+10	7.6597E+09	2.5258E+10	1.5466E+09	9.9941E+09	3.1368E+06	3.2583E+10	9.0563E+00	8.0378E+09
	STD	2.4420E-01	1.1282E-02	1.4960E+09	1.4342E+10	1.4172E+09	9.5148E+08	7.9779E+08	2.1004E+09	7.7801E+05	1.0865E+09	1.3578E+09	3.9626E+08

unimodal and multimodal functions (i.e., F1, F4, F7, F9, F10, and F13 in Tables 2 and 3). Similarly, Figs. 20 and 21 show the search direction of the agents in fixed multi-multimodal functions (i.e., F14 and F16 in Table 4). We observe that, at the beginning of the search by the DSO agents, exploration of the search landscape takes precedence over exploitation. This gives the DSO the ability to avoid the local optima trap (i.e., for multimodal landscape) though this comes with a drawback of a longer convergence time. Moreover, as the iteration progresses, exploitation takes precedence to achieve convergence and an optimal solution. Consequently, we see that the search trajectory of the DSO agents for multi-modal

functions is unique owing to the difficult landscape of the functions. We observe that the DSO converges close to the optimal point if not at the optima.

4) COMPUTATIONAL TIME

Tables 11-15 present the computational running time of the DSO for 30, 100, 250, and 500 variable dimensions. We observe that the DSO performs better than the other metaheuristics as the number of dimensions increases. Specifically for 30 (i.e., F5, F8, F11), 100 (i.e., F2), 250 (i.e., F3-F7, F11, F12), and 500 (i.e., F5-F12) dimensions, the DSO converges fastest respectively. For lower dimensions such as 30, the

TABLE 10. Results of multimodal benchmark functions with fixed dimensions.

Func.	Metric	DSO	TLBO	GA	DE	PSO	ABC	GWO	SCA	BBO	ACO	RCSA	HS
14	AVG	8.5453E+00	9.9800E-01	1.2309E+00	2.2468E+00	6.6528E+00	9.9800E-01	1.6945E+01	2.7168E+00	9.9011E+00	1.0643E+00	9.9800E-01	9.9800E-01
	STD	4.4015E+00	1.4283E-16	4.9974E-01	2.2142E+00	5.3106E+00	4.8426E-07	3.5651E+00	2.3860E+00	5.6482E+00	2.5219E-01	1.7249E-16	9.5083E-12
15	AVG	3.7032E-04	1.1092E-03	8.4799E-03	1.7310E-03	4.4810E-03	1.1567E-03	6.5078E-04	9.2521E-04	8.2738E-03	4.8687E-03	2.5300E-03	5.3350E-03
	STD	1.4296E-04	3.6474E-03	1.2747E-02	3.5719E-03	1.1077E-02	2.9006E-04	9.4049E-05	3.8359E-04	9.0292E-03	7.9494E-03	6.0589E-03	8.2143E-03
16	AVG	-1.0296E+00	-1.0316E+00	-1.0154E+00	-1.0316E+00	-1.0316E+00	-1.0316E+00	-9.6125E-01	-1.0315E+00	-1.0044E+00	-1.0316E+00	-1.0316E+00	-1.0316E+00
	STD	6.1425E-03	6.6486E-16	3.2658E-02	6.7122E-16	6.5843E-16	2.4426E-06	2.0341E-01	9.5232E-05	1.4901E-01	6.7752E-16	5.6985E-16	1.6848E-07
17	AVG	3.9792E-01	3.9789E-01	4.5084E-01	3.9789E-01	3.9789E-01	3.9789E-01	3.9987E-01	4.0061E-01	3.9789E-01	3.9789E-01	3.9789E-01	3.9789E-01
	STD	2.9546E-05	0.0000E+00	9.9262E-02	0.0000E+00	0.0000E+00	1.4084E-06	2.5291E-03	2.6406E-03	1.6753E-11	0.0000E+00	6.1435E-16	7.6039E-08
18	AVG	3.9113E+00	3.0000E+00	3.5962E+00	3.0000E+00	6.6000E+00	3.0069E+00	4.1909E+01	3.0001E+00	1.4702E+01	3.0000E+00	3.0000E+00	3.9227E+00
	STD	4.9283E+00	1.0752E-15	1.6920E+00	1.7964E+00	1.5426E+01	1.0246E-02	4.0749E+01	1.4511E+04	2.2069E+01	6.8501E-16	2.4119E-14	4.9267E+00
19	AVG	-3.0048E-01	-3.0048E-01	-3.0048E-01	-2.9970E-01	-3.0048E-01	-3.0048E-01	-3.0048E-01	-3.0048E-01	-3.0048E-01	-3.0048E-01	-3.0048E-01	-3.0048E-01
	STD	2.2584E-16	2.2584E-16	2.2584E-16	4.2445E-03	2.2584E-16	2.2584E-16	2.2584E-16	2.2584E-16	2.2584E-16	2.2584E-16	2.2584E-16	2.2584E-16
20	AVG	-3.1942E+00	-3.2951E+00	-2.9468E+00	-3.2564E+00	-3.2079E+00	-3.196E+00	-3.2758E+00	-2.7468E+00	-3.2744E+00	-3.2903E+00	-3.2458E+00	-3.2824E+00
	STD	1.1695E-01	4.8310E-02	2.7124E-01	6.3202E-02	2.9265E-01	1.4980E-03	5.7133E-02	4.7593E-01	5.9241E-02	5.3475E-02	5.6210E-02	5.7005E-02
21	AVG	-9.6868E+00	-1.0153E+01	-3.5401E+00	-8.7015E+00	-5.4632E+00	-9.9766E+00	-4.5079E+00	-1.8071E+00	-4.6402E+00	-5.8254E+00	-7.5296E+00	-6.6493E+00
	STD	1.3413E+00	2.3573E-04	2.1042E+00	2.9006E+00	2.6014E+00	1.2941E-01	3.6085E-01	1.6572E+00	2.9615E+00	3.6430E+00	3.1484E+00	3.6325E+00
22	AVG	-9.9148E+00	-9.9573E+00	-4.1824E+00	-9.7428E+00	-5.0731E+00	-1.0221E+01	-4.4963E+00	-3.4820E+00	-6.3240E+00	-8.6670E+00	-9.2075E+00	-5.7565E+00
	STD	1.1841E+00	1.6943E+00	2.2454E+00	1.7964E+00	2.3770E+00	1.1412E-01	1.1870E+00	1.6504E+00	3.6772E+00	2.9430E+00	2.7473E+00	3.6225E+00
23	AVG	-9.6266E+00	-9.2104E+00	-4.0040E+00	-9.3513E+00	-4.1363E+00	-1.0367E+01	-4.3421E+00	-3.1950E+00	-4.6633E+00	-8.8332E+00	-9.2143E+00	-4.5365E+00
	STD	1.9767E+00	2.5840E+00	2.0787E+00	2.7246E+00	2.4529E+00	1.8474E-01	6.6813E-01	1.6052E+00	3.3522E+00	3.1590E+00	2.7453E+00	3.1136E+00

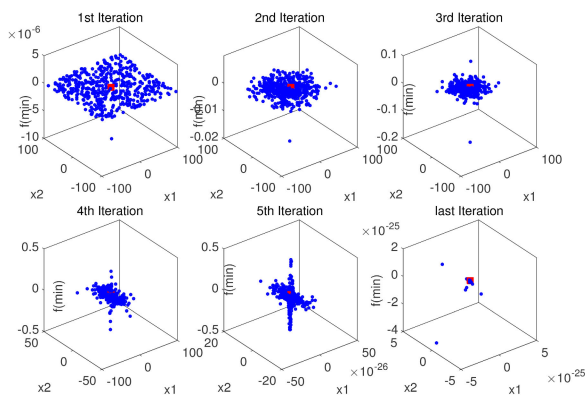


FIGURE 14. Illustration of the DSO search trajectory for F1.

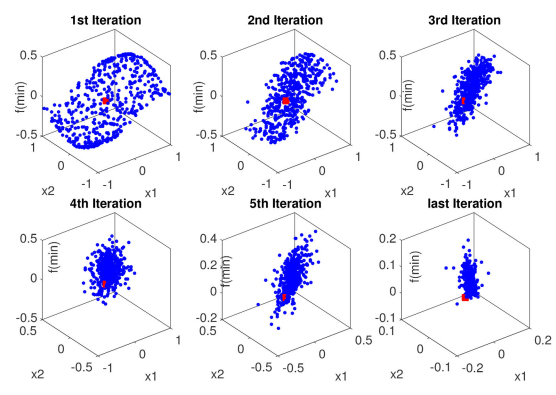


FIGURE 16. Illustration of the DSO search trajectory for F7.

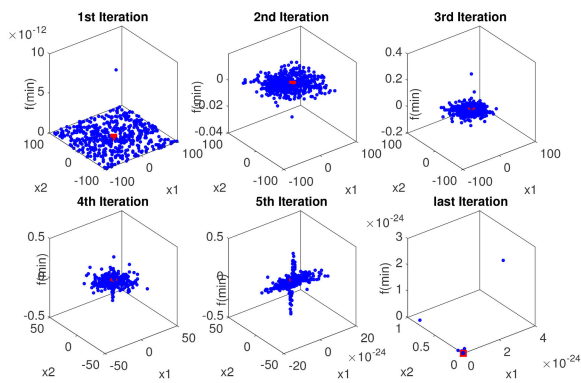


FIGURE 15. Illustration of the DSO search trajectory for F4.

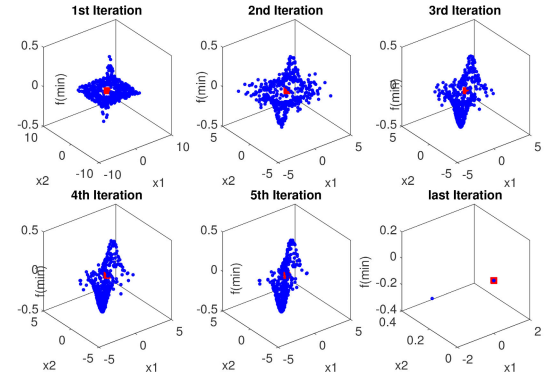


FIGURE 17. Illustration of the DSO search trajectory for F9.

computational time of the DSO remains on par with other metaheuristics.

5) WILCOXON RANK SUM TEST AND FRIEDMAN TEST

To demonstrate that the performance of the DSO is not a random occurrence, we employ the Wilcoxon rank sum test, which is a non-parametric test. With a statistical significance level of 5% [117], the probability values (p-value) of the DSO and other metaheuristics for the respective test functions with different dimensions are indicated in Tables 16-20.

We observe that the DSO’s p-values for all the test functions irrespective of the number of dimensions are far lower than 0.05. This clearly shows that the performance of the DSO is not a random occurrence. Consequently, the null hypothesis is rejected, and the alternative hypothesis is true (i.e., the superior performance of the DSO is statistically significant). We observe that, in most instances, the DSO p-value is less than the other metaheuristics.

Furthermore, we explore the Friedman test to give a per-spicious ranking of the metaheuristics. Friedman test allows

TABLE 11. Results of the computational running time of benchmark functions with 30 dimensions.

Func.	Metric	DSO	TLBO	GA	DE	PSO	ABC	GWO	SCA	BBO	ACO	RCSA	HS
1	AVG	1.0521E-01	2.9843E-01	6.1948E-01	1.7506E-01	6.1522E-02	2.1500E-01	8.1394E-02	1.5152E-01	1.3709E+00	1.9805E+00	1.7320E+01	1.4679E+00
	STD	5.9877E-02	1.5344E-01	2.8038E-01	1.0728E-01	4.0876E-02	1.2968E-01	5.7904E-02	9.2873E-02	2.6908E-01	1.9935E-01	4.9447E-01	2.7458E-01
2	AVG	8.4423E-02	2.3590E-01	4.8893E-01	1.3132E-01	4.8252E-02	1.6507E-01	4.9229E-02	1.0273E-01	1.2322E+00	1.8682E+00	1.7567E+01	1.3397E+00
	STD	1.0941E-02	4.0474E-02	6.8135E-02	2.8112E-02	1.0113E-02	9.7842E-03	1.2443E-03	2.0977E-02	4.1040E-02	5.4912E-02	2.8546E-01	5.0475E-02
3	AVG	2.1179E-01	4.7944E-01	1.0104E+00	2.3021E-01	1.6077E-01	4.0404E-01	1.6453E-01	2.1266E-01	1.3475E+00	2.0794E+00	2.8970E+01	1.4862E+00
	STD	4.7981E-02	4.9425E-02	5.9996E-02	9.4471E-03	9.7081E-03	4.4881E-02	3.8901E-02	1.8404E-02	4.2911E-02	4.1652E-02	1.1104E+00	2.5026E-01
4	AVG	7.9772E-02	2.3375E-01	4.7209E-01	1.2539E-01	4.5789E-02	1.5396E-01	4.8508E-02	9.7234E-02	1.2552E+00	1.8908E+00	1.7375E+01	1.4035E+00
	STD	1.1774E-02	4.2188E-02	4.7237E-02	1.6724E-02	7.1530E-03	2.1087E-02	4.0246E-03	1.1368E-02	1.0107E-01	1.1234E-01	7.2423E-01	2.7551E-01
5	AVG	1.0642E-01	2.7106E-01	5.4272E-01	1.4089E-01	6.5722E-02	2.0133E-01	6.5664E-02	1.1916E-01	1.2485E+00	1.8940E+00	1.9766E+01	1.3332E+00
	STD	2.2588E-02	7.6489E-03	2.2090E-02	1.4088E-02	2.1547E-03	4.9335E-03	6.9819E-03	1.3288E-02	3.3591E-02	3.9733E-02	3.0790E-01	4.6261E-02
6	AVG	7.9412E-02	2.1992E-01	4.5717E-01	1.2277E-01	4.5132E-02	1.5297E-01	4.7414E-02	9.4952E-02	1.2187E+00	1.8375E+00	1.6979E+01	1.3151E+00
	STD	1.6171E-02	3.8106E-03	1.3325E-02	1.0539E-02	2.0185E-03	3.0783E-03	1.4707E-03	3.7615E-03	3.8627E-02	3.1164E-02	2.1040E-01	5.1883E-02
7	AVG	1.3519E-01	3.3628E-01	7.2335E-01	1.7518E-01	1.0265E-01	2.7731E-01	1.0053E-01	1.5177E-01	1.2947E+00	1.9919E+00	2.2676E+01	1.3677E+00
	STD	1.2368E-02	6.4632E-03	2.9476E-02	1.1469E-02	9.0350E-03	2.0815E-02	5.3288E-03	6.3674E-03	4.3713E-02	7.1245E-02	3.2688E-01	4.0586E-02
8	AVG	1.0425E-01	2.6852E-01	5.5389E-01	1.4766E-01	6.5047E-02	2.0889E-01	7.0720E-02	1.2900E-01	1.2514E+00	1.9038E+00	2.0512E+01	1.3516E+00
	STD	1.4823E-02	8.5078E-03	5.0322E-02	2.4728E-02	5.4552E-03	1.6622E-02	1.2920E-02	3.8566E-02	3.9942E-02	3.6117E-02	2.4541E-01	4.8023E-02
9	AVG	8.5141E-02	2.4155E-01	5.0942E-01	1.3436E-01	5.4385E-02	1.7698E-01	5.5405E-02	1.0299E-01	1.2354E+00	1.8697E+00	1.8856E+01	1.3267E+00
	STD	1.0881E-02	1.0857E-02	2.5268E-02	1.7649E-02	1.4087E-03	6.5833E-03	1.0393E-03	2.2886E-03	3.8527E-02	3.7538E-02	3.1612E-01	4.2794E-02
10	AVG	8.7069E-02	2.3754E-01	5.1469E-01	1.2952E-01	5.8847E-01	1.8456E-01	5.6810E-02	1.0942E-01	1.2318E+00	1.8900E+00	1.8407E+01	1.3242E+00
	STD	1.3099E-02	8.0750E-03	9.0934E-03	2.6208E-03	6.5503E-03	6.8305E-03	1.1119E-03	3.8306E-03	3.2860E-02	2.8521E-02	3.2385E-01	3.6913E-02
11	AVG	1.0973E-01	2.7948E-01	6.0385E-01	1.4750E-01	7.4160E-02	2.3370E-01	7.4772E-02	1.2310E-01	1.2660E+00	1.9484E+00	2.0867E+01	1.3537E+00
	STD	1.8967E-02	6.3348E-03	1.8910E-02	2.0102E-03	2.3364E-03	2.9999E-03	1.8899E-03	2.2398E-03	4.1613E-02	7.9857E-02	2.3752E-01	3.9350E-02
12	AVG	2.9447E-01	6.2233E-01	1.3654E+00	3.0080E-01	2.2701E-01	5.6836E-01	2.2116E-01	2.7490E-01	1.4291E+00	2.2837E+00	3.7486E+01	1.5419E+00
	STD	6.2598E-02	1.3721E-02	4.9333E-02	8.8185E-03	3.4983E-03	1.0841E-02	3.1963E-03	3.6080E-02	4.1115E-02	5.8563E-02	4.1115E-01	5.4198E-02
13	AVG	2.7685E-01	6.2581E-01	1.3485E+00	3.0105E-01	2.3332E-01	5.6658E-01	2.2389E-01	2.7561E-01	1.4432E+00	2.2772E+00	3.7669E+01	1.5366E+00
	STD	2.9003E-02	2.4484E-02	2.1997E-02	5.2702E-03	1.8196E-02	1.3690E-02	8.7598E-03	5.8657E-03	5.7569E-02	5.2934E-02	3.8423E-01	3.7045E-02

TABLE 12. Results of the computational running time for benchmark functions with 100 dimensions.

Func.	Metric	DSO	TLBO	GA	DE	PSO	ABC	GWO	SCA	BBO	ACO	RCSA	HS
1	AVG	1.2945E-01	3.4384E-01	1.1444E+00	2.3467E-01	9.0365E-02	1.9715E-01	1.5822E-01	2.7802E-01	3.7673E+00	5.4972E+00	2.1396E+01	3.6540E+00
	STD	7.3404E-02	1.8085E-01	4.9669E-01	1.6997E-01	4.7374E-02	7.7935E-02	4.0699E-02	5.9965E-02	3.3261E-01	2.8087E-01	4.8943E-01	3.2664E-01
2	AVG	1.1258E-01	2.9441E-01	1.0131E+00	1.8787E-01	7.9638E-02	1.7943E-01	1.3751E-01	2.5085E-01	3.6184E+00	5.3882E+00	2.1936E+01	3.5645E+00
	STD	2.8407E-02	5.6994E-02	1.6009E-01	4.0499E-02	1.3430E-02	6.8805E-03	7.6726E-03	2.2545E-02	1.1605E-01	1.5780E-01	4.3870E-01	2.3629E-01
3	AVG	5.3646E-01	1.1403E+00	3.0347E+00	5.9763E-01	5.1188E-01	1.0355E+00	5.7567E-01	6.7068E-01	4.0546E+00	6.2450E+00	6.4416E+01	3.9757E+00
	STD	6.9038E-02	8.2145E-02	2.0163E-01	4.6102E-02	5.9230E-02	8.2793E-02	7.0482E-02	5.2209E-02	1.0878E-01	1.4851E-01	3.8227E+00	2.2135E-01
4	AVG	1.0072E-01	2.6704E-01	9.5105E-01	1.7401E-01	7.4428E-02	1.6323E-01	1.3372E-01	2.3981E-01	3.6282E+00	5.4334E+00	2.1374E+01	3.5463E+00
	STD	1.5928E-02	1.3352E-02	4.6803E-02	1.0353E-02	7.9498E-03	3.8896E-03	4.4382E-03	4.9779E-03	1.4603E-01	1.5759E-01	3.1916E-01	1.6421E-01
5	AVG	1.2820E-01	3.4037E-01	1.0666E+00	2.0236E-01	9.9621E-02	2.2530E-01	1.5660E-01	2.6323E-01	3.6358E+00	5.4059E+00	2.3824E+01	3.6074E+00
	STD	3.3617E-02	8.5074E-02	1.7338E-01	3.7712E-02	1.9707E-02	4.4720E-02	2.5804E-02	1.1898E-02	1.0912E-01	1.4281E-01	2.1815E-01	1.6143E-01
6	AVG	1.1814E-01	3.3941E-01	1.1261E+00	2.0899E-01	9.2158E-02	1.8773E-01	1.6281E-01	2.9884E-01	4.1773E+00	5.8337E+00	2.3983E+01	4.0543E+00
	STD	5.6851E-02	1.6777E-01	5.3746E-01	1.0125E-01	4.0167E-02	4.9821E-02	1.0398E-02	1.5204E-01	1.6769E+00	7.0478E-01	1.8958E+00	8.6641E-01
7	AVG	2.9585E-01	6.4468E-01	1.8039E+00	3.5831E-01	2.8120E-01	5.6658E-01	3.2155E-01	4.4716E-01	4.2350E+00	6.3911E+00	3.7999E+01	3.7598E+00
	STD	8.0489E-02	1.2837E-01	3.1327E-01	6.6581E-02	1.1949E-01	1.4732E-01	7.2176E-02	1.0649E-01	1.2617E+00	1.6558E+00	1.5767E+00	2.1501E-01
8	AVG	1.4707E-01	3.5879E-01	1.1421E+00	2.2529E-01	1.1406E-01	2.6581E-01	1.8082E-01	2.9727E-01	3.6548E+00	5.4962E+00	2.6958E+01	3.5946E+00
	STD	2.1517E-02	1.2611E-02	4.8240E-02	2.7645E-02	3.8115E-03	2.4599E-02	3.0626E-02	4.6924E-02	8.1737E-02	1.5988E-01	5.5092E-01	1.3263E-01
9	AVG	1.0920E-01	2.8979E-01	1.0857E+00	2.1067E-01	1.0164E-01	2.3351E-01	1.5971E-01	2.6532E-01	3.6471E+00	5.5277E+00	2.4916E+01	3.5748E+00
	STD	1.1116E-02	8.9377E-03	3.6971E-02	2.3790E-02	2.6303E-03	6.4221E-03	4.8461E-03	7.3177E-03	1.0306E-01	2.9206E-01	4.4259E-01	1.4673E-01
10	AVG	1.2019E-01	2.9455E-01	1.1151E+00	2.0962E-01	1.0933E-01	2.4668E-01	1.5958E-01	2.7906E-01	3.6604E+00	5.3081E+00	2.4448E+01	3.6471E+00
	STD	2.4370E-02	1.3404E-02	1.3770E-02	6.1885E-02	5.7120E-03	2.0852E-02	4.6766E-03	9.2509E-03	1.1698E-01	1.8148E-01	5.8376E-01	1.7814E-01
11	AVG	1.4743E-01	3.7201E-01	1.2887E+00	2.3994E-01	1.3239E-01	3.2178E-01	1.9185E-01	3.0731E-01	3.7293E+00	5.5600E+00	2.7049E+01	3.6379E+00
	STD	2.9467E-02	7.3296E-02	3.3707E-01	3.8721E-02	1.2495E-02	4.9391E-02	3.6353E-02	5.4153E-02	1.2635E-01	1.6876E-01	3.9297E-01	1.8490E-01
12	AVG	5.4455E-01	1.1451E+00	2.9917E+00	5.9447E-01	4.9223E-01	1.0529E+00	5.3876E-01	6.5261E-01	4.0849E+00	6.3156E+00	6.5093E+01	4.0284E+00
	STD	6.6507E-02	8.0462E-02	3.6353E-02	2.3902E-02	9.7956E-03	2.0390E-02	1.1621E-02	1.1445E-02	1.0881E-01	1.8424E-01	1.3824E+00	1.6444E-01
13	AVG	5.4418E-01	1.1307E+00	3.0023E+00	5.9625E-01	4.9362E-01	1.0826E+00	5.5679E-01	6.6865E-01	4.0756E+00	6.2852E+00	6.5121E+01	3.9994E+00
	STD	9.3773E-02	1.2592E-01	7.0388E-02	1.9671E-02	1.2993E-02	1.3206E-01	9.4915E-02	3.7774E-02	1.1452E-01	1.6492E-01	1.7720E+00	1.5162E-01

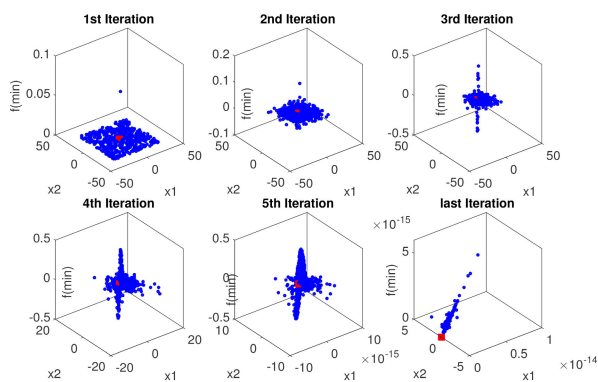


FIGURE 18. Illustration of the DSO search trajectory for F10.

us to compare more than two populations with a blocking variable without assuming the observations are normal distributions. Therefore, we use the ranks of the observed

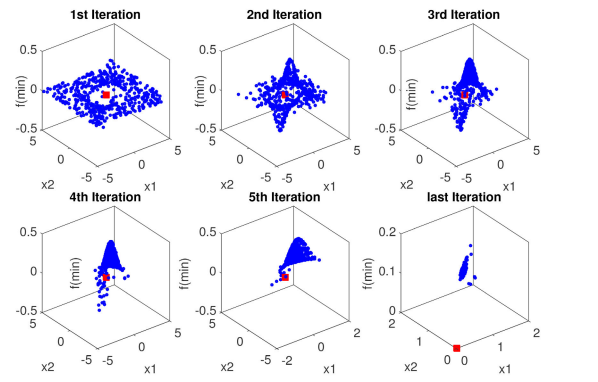


FIGURE 19. Illustration of the DSO search trajectory for F13.

values to determine the rankings of the metaheuristics. A brief mathematical basis of the Friedman test is described in Appendix B. In Tables 21 - 26, we present the ranking results

TABLE 13. Results of the computational running time for benchmark functions with 250 dimensions.

Func.	Metric	DSO	TLBO	GA	DE	PSO	ABC	GWO	SCA	BBO	ACO	RCSA	HS
1	AVG	1.4599E-01	3.7713E-01	2.0313E+00	2.8938E-01	1.4336E-01	1.8875E-01	3.1915E-01	5.6026E-01	8.8493E+00	1.2986E+01	2.9167E+01	8.3387E+00
	STD	3.5960E-02	5.6613E-02	1.2814E-01	1.5582E-01	3.5507E-03	5.3394E-03	5.9406E-03	1.5394E-02	2.2655E-01	4.3922E-01	5.0146E-01	3.3141E-01
2	AVG	1.5495E-01	4.0505E-01	2.0799E+00	2.9675E-01	1.5095E-01	2.1310E-01	3.3295E-01	5.8061E-01	9.1453E+00	1.2944E+01	3.0030E+01	8.4570E+00
	STD	3.3526E-02	7.7944E-02	6.9019E-02	1.2374E-02	2.0398E-02	9.2383E-03	1.8900E-02	4.4372E-02	6.8991E-01	3.8446E-01	6.2666E-01	3.5647E-01
3	AVG	1.4471E+00	3.0350E+00	8.5047E+00	1.5887E+00	1.4590E+00	2.8816E+00	1.6300E+00	1.8587E+00	1.0220E+01	1.5497E+01	1.6077E+02	9.6506E+00
	STD	1.0178E-01	1.9682E-01	5.5056E-01	1.0383E-01	1.0917E-01	2.1505E-01	1.3461E-01	1.0523E-01	3.9795E-01	2.6124E-01	1.0152E+01	5.2013E-01
4	AVG	1.4027E-01	3.6897E-01	1.9931E+00	2.8326E-01	1.4376E-01	1.8613E-01	3.1983E-01	5.5606E-01	8.8512E+00	1.2944E+01	2.9408E+01	8.3672E+00
	STD	3.2368E-02	7.4842E-02	6.0757E-02	7.9618E-03	3.9562E-03	1.1736E-02	6.1597E-03	8.9961E-03	2.1567E-01	3.7089E-01	4.5939E-01	3.4677E-01
5	AVG	1.5602E-01	4.1836E-01	2.0636E+00	3.1760E-01	1.7455E-01	2.4757E-01	3.4042E-01	5.7920E-01	8.9236E+00	1.2982E+01	3.2063E+01	8.3692E+00
	STD	6.5125E-03	1.3607E-02	3.7534E-02	2.9520E-02	1.9221E-02	7.4437E-03	7.0710E-03	1.2634E-02	2.3113E-01	4.1015E-01	4.8521E-01	3.2189E-01
6	AVG	1.3466E-01	3.6442E-01	2.0265E+00	2.9845E-01	1.4995E-01	1.9114E-01	3.1934E-01	5.5707E-01	8.9111E+00	1.2949E+01	2.9335E+01	8.3256E+00
	STD	1.5865E-02	2.0397E-02	6.6982E-02	5.6770E-02	2.0998E-02	1.0572E-02	6.9071E-03	1.0370E-02	1.5070E-01	3.7281E-01	4.7303E-01	3.3636E-01
7	AVG	5.0633E-01	1.1119E+00	3.8157E+00	6.6218E-01	5.1712E-01	9.6604E-01	6.9683E-01	9.4175E-01	9.4664E+00	1.4023E+01	6.6433E+01	8.7082E+00
	STD	2.3382E-02	3.1869E-02	8.0254E-02	2.2886E-02	1.4098E-02	5.1875E-02	3.9310E-02	3.6160E-02	7.2080E-01	1.2317E+00	9.2155E-01	3.4235E-01
8	AVG	2.3231E-01	5.5400E-01	2.4352E+00	3.7343E-01	2.2733E-01	3.8461E-01	4.0416E-01	6.4243E-01	8.9633E+00	1.3210E+01	3.9116E+01	8.4372E+00
	STD	2.4689E-02	4.1082E-02	6.4899E-02	8.6836E-03	5.1139E-03	1.2166E-02	1.0604E-02	8.4807E-03	2.2490E-01	5.6459E-01	6.0977E-01	3.3174E-01
9	AVG	1.6113E-01	4.1020E-01	2.3551E+00	3.5800E-01	2.1209E-01	3.4785E-01	3.8556E-01	6.0915E-01	8.9456E+00	1.3069E+01	3.6451E+01	8.3904E+00
	STD	4.9316E-03	1.3183E-02	4.2944E-02	9.3391E-03	6.0455E-03	6.0615E-03	1.5553E-02	1.3674E-02	2.2371E-01	3.6809E-01	4.800E-01	3.1116E-01
10	AVG	1.6405E-01	4.2176E-01	2.4180E+00	3.7536E-01	2.2586E-01	3.7289E-01	3.8298E-01	6.5146E-01	8.9420E+00	1.3125E+01	3.5571E+01	8.4712E+00
	STD	8.8004E-03	3.9793E-02	7.5863E-02	1.5217E-02	1.0282E-02	1.2747E-02	1.2104E-02	3.0025E-02	2.2484E-01	3.8721E-01	5.0203E-01	3.4951E-01
11	AVG	2.0070E-01	4.9279E-01	2.5572E+00	4.0419E-01	2.5420E-01	4.6156E-01	4.2506E-01	6.8167E-01	9.0118E+00	1.3227E+01	3.9209E+01	8.4837E+00
	STD	1.1102E-02	2.6829E-02	5.9539E-02	1.0384E-02	5.1886E-03	1.2914E-02	1.0498E-02	3.0300E-02	2.4795E-01	3.8974E-01	5.6150E-01	3.3745E-01
12	AVG	1.1031E+00	2.2145E+00	6.5849E+00	1.2194E+00	1.1256E+00	2.1964E+00	1.2652E+00	1.5352E+00	9.9616E+00	1.5115E+01	1.2269E+02	9.4444E+00
	STD	1.9535E-01	5.6914E-02	1.7417E-01	5.0282E-02	1.5279E-01	2.5777E-01	1.8275E-01	2.0129E-01	3.7464E-01	8.0479E-01	1.6806E+00	5.9052E-01
13	AVG	1.0824E+00	2.1230E+00	6.5745E+00	1.1958E+00	1.0706E+00	2.0798E+00	1.2112E+00	1.4735E+00	9.8071E+00	1.4821E+01	1.2247E+02	9.3043E+00
	STD	1.9366E-01	6.0389E-02	2.7551E-01	1.7013E-02	3.3529E-02	3.3545E-02	1.6309E-02	3.8684E-02	2.3084E-01	4.0335E-01	1.9159E+00	3.4716E-01

TABLE 14. Results of the computational running time of benchmark functions with 500 dimensions.

Func.	Metric	DSO	TLBO	GA	DE	PSO	ABC	GWO	SCA	BBO	ACO	RCSA	HS
1	AVG	2.1709E-01	5.3660E-01	3.7983E+00	5.0932E-01	2.7653E-01	2.1446E-01	6.2717E-01	1.0879E+00	1.7590E+01	2.5306E+01	4.2019E+01	1.6453E+01
	STD	5.8523E-02	1.3591E-01	1.6922E-01	1.1180E-01	5.1809E-02	4.0034E-02	1.8252E-02	2.2855E-02	3.8014E-01	7.8682E-01	6.9402E-01	7.5667E-01
2	AVG	2.2282E-01	5.4608E-01	3.8070E+00	4.9367E-01	2.6572E-01	2.3527E-01	6.3552E-01	1.0917E+00	1.7539E+01	2.5253E+01	4.2269E+01	1.6380E+01
	STD	4.9775E-02	1.0483E-01	1.1740E-01	2.2841E-02	5.5530E-03	5.2220E-03	1.3055E-02	1.7639E-02	4.3971E-01	7.3082E-01	5.5722E-01	7.5848E-01
3	AVG	3.7990E+00	7.6363E+00	2.1174E+01	3.9589E+00	3.7715E+00	7.2868E+00	4.0991E+00	4.5680E+00	2.1047E+01	3.2391E+01	3.9149E+02	2.0046E+01
	STD	3.8861E-01	5.0337E-01	1.0927E+00	2.0180E-01	2.1662E-01	4.2459E-01	2.1759E-01	2.1233E-01	5.2801E-01	6.5128E-01	2.0125E+01	1.3799E+00
4	AVG	2.1264E-01	5.1496E-01	3.7243E+00	4.7481E-01	2.6517E-01	1.9705E-01	6.3497E-01	1.0998E+00	1.7698E+01	2.5818E+01	4.1906E+01	1.6313E+01
	STD	5.3123E-02	9.7402E-02	1.2939E-01	1.3316E-02	7.1288E-03	6.3641E-03	5.0114E-02	5.5605E-02	6.0121E-01	9.1717E-01	6.4898E-01	6.4898E-01
5	AVG	2.2273E-01	5.8170E-01	3.8905E+00	5.2358E-01	3.0472E-01	2.7827E-01	6.5896E-01	1.1275E+00	1.7696E+01	2.5594E+01	4.5678E+01	1.6468E+01
	STD	8.1877E-03	3.3329E-02	1.3579E-01	5.6446E-02	1.5961E-02	6.6291E-03	2.9951E-02	3.3605E-02	5.0936E-01	1.1268E+00	9.1663E-01	7.3124E-01
6	AVG	1.9888E-01	5.3513E-01	3.8055E+00	4.8049E-01	2.6352E-01	2.0666E-01	6.2771E-01	1.0873E+00	1.7518E+01	2.5236E+01	4.1954E+01	1.6416E+01
	STD	3.7324E-02	1.3291E-01	2.6154E-01	1.6055E-02	3.6144E-03	3.1944E-03	2.0163E-02	1.9590E-02	4.2232E-01	7.3355E-01	5.3287E-01	7.8260E-01
7	AVG	9.5314E-01	1.9864E+00	7.3397E+00	1.2212E+00	9.9380E-01	1.6956E+00	1.3611E+00	1.8160E+00	1.8267E+01	2.6764E+01	1.1563E+02	1.6987E+01
	STD	1.2918E-01	9.9847E-02	1.0168E-01	4.1200E-02	1.6867E-02	4.2998E-02	4.0207E-02	3.2869E-02	4.9239E-01	7.2627E-01	1.4619E+00	6.8798E-01
8	AVG	3.6621E-01	8.3557E-01	4.5448E+00	6.4308E-01	4.2746E-01	5.6139E-01	7.7990E-01	1.2534E+00	1.7809E+01	2.5599E+01	5.9537E+01	1.6441E+01
	STD	8.9467E-03	1.1634E-02	1.0055E-01	1.7817E-02	7.2233E-03	1.1431E-02	1.3954E-02	2.8444E-02	4.9742E-01	7.0795E-01	1.0341E+00	6.4622E-01
9	AVG	2.6628E-01	6.1999E-01	4.4998E+00	6.2554E-01	4.0553E-01	5.2451E-01	7.6860E-01	1.1803E+00	1.7740E+01	2.5528E+01	5.9200E+01	1.6465E+01
	STD	5.6101E-02	1.1487E-01	1.0386E-01	1.5591E-02	1.5164E-02	1.9105E-02	1.0451E-01	2.7973E-02	4.2556E-01	6.8892E-01	7.2605E-01	7.1584E-01
10	AVG	2.6010E-01	6.4031E-01	4.5402E+00	6.5194E-01	4.1952E-01	5.4626E-01	7.4672E-01	1.2504E+00	1.7724E+01	2.5646E+01	5.4335E+01	1.6789E+01
	STD	4.6325E-02	2.0562E-01	2.2577E-01	2.7528E-02	1.8332E-02	1.5630E-02	1.9099E-02	2.7289E-02	4.2972E-01	7.6815E-01	9.3713E-01	9.4344E-01
11	AVG	3.0855E-01	7.3145E-01	4.7691E+00	6.9320E-01	4.7033E-01	6.7626E-01	8.1197E-01	1.3006E+00	1.7998E+01	2.5781E+01	5.8960E+01	1.6576E+01
	STD	4.9688E-02	1.0661E-01	1.2558E-01	1.4481E-02	1.3600E-02	1.5626E-02	1.5990E-02	3.9243E-02	8.4674E-01	5.5796E-01	1.4959E+00	7.3743E-01
12	AVG	2.0059E+00	3.9740E+00	1.2411E+01	2.2163E+00	2.0059E+00	3.7565E+00	2.3475E+00	2.8151E+00	1.9333E+01	2.8879E+01	2.1588E+02	1.8099E+01
	STD	2.8338E-01	1.1889E-01	2.8244E-01	3.9900E-02	2.1211E-02	5.9066E-02	7.5961E-02	4.1010E-02	4.9201E-01	8.7795E-01	4.2900E+00	6.5306E-01
13	AVG	1.9770E+00	3.7722E+00	1.2430E+01	2.2158E+00	2.0543E+00	3.8402E+00	2.3415E+00	2.8732E+00	1.9634E+01	2.9020E+01	2.1740E+02	1.8090E+01
	STD	2.7965E-01	5.9836E-02	3.4410E-01	4.2396E-02	1.4573E-01	2.8752E-01	8.5919E-02	1.6768E-01	9.3133E-01	8.8729E-01	2.8759E+00	6.5045E-01

TABLE 15. Results of the computational running time of multimodal benchmark functions with fixed dimensions.

Func.	Metric	DSO	TLBO	GA	DE	PSO	ABC	GWO	SCA	BBO	ACO	RCSA	HS
14	AVG	3.1181E-01	7.1691E-01	1.3601E+00	3.1874E-01	2.6546E-01	6.4102E-01	2.2823E-01	2.6419E-01	4.5375E-01	9.0469E-01	3.9355E+01	6.2578E-01
	STD	5.3591E-02	1.3140E-01	5.2272E-02	9.5423E-03	1.4201E-02	2.2557E-02	3.9048E-02	4.6644E-02	7.6163E-02	5.3740E-02	7.9639E-01	1.9807E-02
15	AVG	7.2984E-02	2.1338E-01	3.0234E-01	1.0512E-01	3.7701E-02	1.5951E-01	1.8265E-02	4.3745E-02	2.7620E-01	5.1175E-01	1.5909E+01	

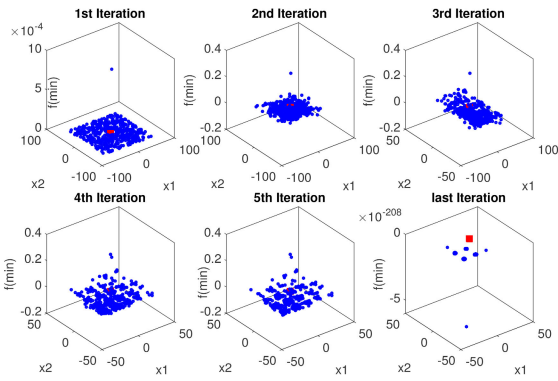


FIGURE 20. Illustration of the DSO search trajectory for F14.

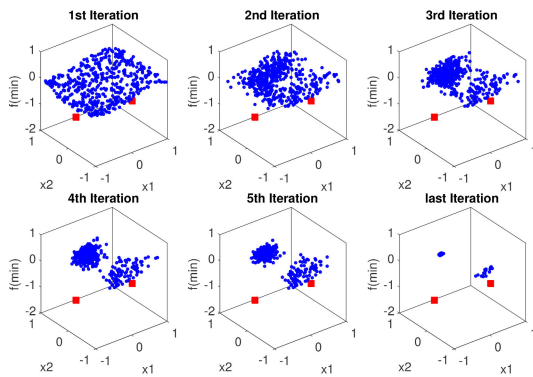


FIGURE 21. Illustration of the DSO search trajectory for F16.

the performance of the DSO improved as the variable dimensional sizes increased for both unimodal and multimodal benchmark functions. In several instances, either DSO outperformed the other metaheuristics, or it was the second-best metaheuristic. Besides, the ranking results of the fixed-dimensional benchmark functions are presented in Table 25. We observe that the Friedman statistic (i.e., -184.05) is far less than the critical value of 19.68. Hence, the null hypothesis is accepted and therefore, the performances of all the metaheuristics are the same. However, from a wholistic view depicted in Table 26, and with a Fieldman statistic value of 40.45 greater than the critical value of 19.68, we observe that both the DSO and ACO outperformed all the other metaheuristics.

B. COMPOSITE BENCHMARK TEST FUNCTIONS

Similar to the multimodal functions, composite functions have several local optima and, consequently, a harsh and challenging search landscape which is highly similar to real search spaces [44]. Figures 22 and 23 illustrate the local optima and a jagged landscape of functions F26 and F27. Composite functions are recursive structurally and an effective way of testing the performance of metaheuristics on local optima avoidance. Hence, composite functions test the exploration and exploitation capabilities of metaheuristics. In this

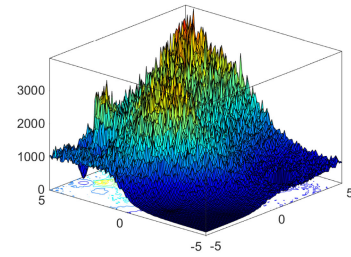


FIGURE 22. Illustration of the rotated hybrid composition function 1 with noise in fitness (i.e., F26).

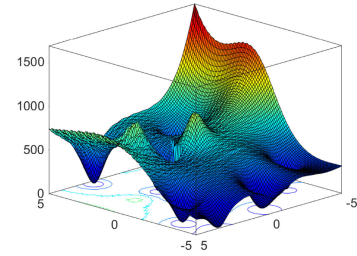


FIGURE 23. Illustration of the rotated hybrid composition function 2 (i.e., F27).

work, we investigate the performance of the DSO in solving composite functions along lines of accuracy, computational running time, and the Wilcoxon rank sum metric. We investigate six composite functions (i.e., F24-F29), namely [118]: (i) hybrid composition function 1, (ii) rotated hybrid composition function 1, (iii) rotated hybrid composition function 1 with noise, (iv) rotated hybrid composition function 2, (v) rotated hybrid composition function with a narrow basin for the global optimum, and (vi) rotated hybrid composition function 2 with the global optimum on bounds. Furthermore, the functional entities, range, and optimal values of the benchmark composite functions in this work are illustrated in Table 27.

1) ACCURACY TEST

In Table 28, we investigate the accuracy of the DSO for the above mentioned composite functions [118] and also comparing with other metaheuristics. We observe that the performance of the DSO is similar to that of the GA, GWO, PSO, SCA, and ABC for functions F24, F25, F27, F28, and F29 respectively, in no particular order.

2) COMPUTATIONAL RUNNING TIME

In Table 29, we observe that the computational running time of the DSO is comparable with other metaheuristics. The DSO’s average computational running time in solving the composite function is 31.75s.

3) WILCOXON RANK SUM TEST AND FRIEDMAN TEST

We investigate the p-values of the DSO and other metaheuristics to see the statistical significance of the results of the metaheuristics. In Table 30, we observe that all the metaheuristics

TABLE 16. Results of the rank sum metric of benchmark functions with 30 dimensions.

Func.	DSO	TLBO	GA	DE	PSO	ABC	GWO	SCA	BBO	ACO	RCSA	HS
1	1.1962E-19	1.1686E-13	1.1962E-19	2.8346E-02	8.1351E-09	4.9723E-13	1.1341E-04	6.1755E-01	2.9754E-01	6.7811E-01	7.8741E-09	1.3070E-04
2	1.1962E-19	1.1686E-13	1.1962E-19	1.5478E-01	1.3985E-13	6.8340E-09	4.9545E-03	2.9134E-03	6.5943E-02	4.4208E-01	1.6732E-07	4.8376E-05
3	1.1962E-19	1.1686E-13	5.2734E-19	1.0987E-01	2.7306E-02	1.3557E-09	4.5099E-02	4.6694E-02	1.5726E-04	5.6131E-13	7.8741E-09	1.0758E-03
4	1.1962E-19	1.1686E-13	6.6457E-12	7.8716E-02	3.5655E-02	1.7768E-10	2.6174E-02	1.0969E-03	4.2646E-05	2.7617E-19	7.8741E-09	4.4208E-01
5	4.0761E-09	5.0650E-14	1.1962E-19	2.3022E-03	4.9417E-06	1.8593E-12	8.7063E-05	7.5277E-03	6.1717E-03	2.4423E-01	1.8633E-18	2.0381E-01
6	5.0302E-01	1.0317E-13	1.1962E-19	3.2919E-01	8.4962E-09	1.7431E-13	1.2603E-02	3.6682E-01	3.5904E-07	1.9870E-03	1.3915E-19	1.6800E-04
7	1.9131E-19	7.9228E-14	1.1962E-19	7.3531E-01	2.7303E-09	4.3442E-13	2.4765E-03	3.5145E-01	1.3168E-04	3.8159E-01	9.3668E-09	2.4497E-01
8	1.0096E-06	4.8705E-03	3.2655E-06	4.4204E-04	9.2918E-01	3.3310E-02	2.0117E-03	1.6456E-19	2.8106E-03	2.0263E-10	1.1686E-13	1.1962E-19
9	4.0968E-07	1.2041E-11	4.5693E-18	1.0347E-01	1.7652E-01	6.2915E-04	1.3919E-06	8.2740E-07	1.7770E-01	5.1795E-15	5.2039E-04	9.3584E-10
10	1.1266E-16	1.4822E-15	5.1524E-08	1.3664E-01	7.9841E-03	2.9915E-03	9.9525E-20	7.2493E-04	5.9814E-05	3.4970E-05	5.2526E-09	9.4802E-01
11	4.8476E-16	9.0033E-17	1.0045E-19	8.7959E-01	3.2368E-09	5.8265E-13	1.1054E-04	6.1940E-01	6.7479E-01	8.2203E-01	5.5714E-09	1.6641E-04
12	8.6403E-05	7.8132E-14	1.1962E-19	1.7300E-04	3.2045E-03	8.1074E-11	1.5425E-01	2.0643E-01	5.6736E-09	1.8573E-05	3.2077E-19	8.3811E-01
13	9.8488E-13	1.5301E-07	1.1962E-19	3.3863E-05	1.8957E-02	3.1391E-12	1.3613E-02	8.7876E-04	8.1436E-07	8.1729E-04	1.1962E-19	7.2154E-01

TABLE 17. Results of the rank sum metric of benchmark functions with 100 dimensions.

Func.	DSO	TLBO	GA	DE	PSO	ABC	GWO	SCA	BBO	ACO	RCSA	HS
1	1.1962E-19	1.1686E-13	2.0115E-19	9.4522E-01	4.3669E-05	8.9697E-09	3.3007E-03	9.2482E-01	2.5747E-04	7.5984E-14	7.8741E-09	1.2345E-02
2	1.1962E-19	1.1686E-13	7.6422E-16	4.2913E-01	1.0896E-08	2.9545E-05	6.5048E-05	2.9149E-02	2.2899E-01	3.4584E-17	7.8741E-09	1.3683E-02
3	1.1962E-19	1.1686E-13	2.2109E-16	3.0010E-01	6.1884E-01	5.9645E-07	7.1743E-01	4.7509E-02	3.7564E-05	2.7367E-16	7.8741E-09	9.0272E-07
4	1.1962E-19	1.1686E-13	3.3462E-02	9.7258E-15	1.5771E-02	1.9353E-05	3.4138E-06	5.3337E-03	3.7564E-05	5.1698E-16	7.8741E-09	3.7762E-01
5	8.4743E-10	1.2069E-14	1.1211E-13	4.1641E-01	3.6140E-02	1.6027E-08	1.3405E-02	8.6403E-05	3.7564E-05	1.3915E-19	4.1077E-17	1.2898E-01
6	7.8740E-09	1.1686E-13	1.5913E-19	9.8611E-01	1.1686E-05	9.9946E-09	3.3400E-03	9.2737E-01	5.201E-04	9.2327E-14	1.1962E-19	1.6416E-02
7	1.3683E-19	1.0461E-13	1.9029E-17	4.1013E-01	1.0214E-03	6.9848E-09	1.3405E-02	1.7012E-03	3.7564E-05	1.5866E-15	7.8741E-09	3.1930E-01
8	1.9870E-03	1.1184E-03	1.4246E-05	9.9050E-01	1.2264E-01	8.1884E-02	6.3136E-07	1.7893E-19	3.7600E-08	1.4094E-12	9.2327E-14	1.5913E-19
9	1.1266E-16	1.9008E-16	4.7842E-14	7.0180E-01	7.7273E-03	2.3053E-08	1.2442E-04	8.6155E-04	3.9263E-01	2.5071E-19	5.5268E-07	1.1841E-02
10	2.4246E-19	1.5126E-13	7.6579E-07	3.0717E-02	1.5295E-01	2.0751E-03	8.9663E-19	3.0390E-03	2.9235E-05	6.1328E-14	5.5612E-09	8.2515E-01
11	1.4085E-16	1.4085E-16	1.3581E-19	8.1485E-01	3.4344E-05	7.8486E-09	3.7858E-03	7.7097E-01	2.2684E-04	7.8735E-14	7.2713E-09	1.6579E-02
12	7.8741E-09	4.5907E-14	1.0905E-13	5.9071E-01	2.2059E-01	1.4715E-08	1.3474E-02	3.1005E-05	3.7564E-05	1.3011E-19	3.6635E-19	6.4872E-02
13	1.1686E-13	7.8741E-09	1.1686E-13	4.2913E-01	5.5161E-02	1.0549E-08	1.3405E-02	2.1986E-04	3.7564E-05	1.2371E-19	1.1962E-19	6.7853E-02

TABLE 18. Results of the rank sum metric of benchmark functions with 250 dimensions.

Func.	DSO	TLBO	GA	DE	PSO	ABC	GWO	SCA	BBO	ACO	RCSA	HS
1	1.1962E-19	1.1686E-13	1.0317E-13	8.5102E-01	3.7564E-05	7.8741E-09	1.3405E-02	8.5245E-01	3.7564E-05	1.3915E-19	7.8741E-09	1.3474E-02
2	1.1962E-19	1.1686E-13	1.1686E-13	4.1117E-01	1.8678E-03	1.4559E-08	1.2666E-08	3.3594E-05	1.1478E-02	1.1962E-19	5.9293E-04	3.2919E-01
3	1.1962E-19	1.1686E-13	2.0918E-17	2.3112E-01	6.1489E-02	6.5048E-05	1.3823E-02	1.2442E-01	4.5784E-05	2.4000E-15	7.8741E-09	5.5807E-07
4	1.1962E-19	1.1686E-13	7.2098E-02	8.1074E-11	1.3405E-02	1.7778E-02	8.4870E-16	6.9727E-05	3.7564E-05	2.7914E-12	7.8741E-09	4.1013E-01
5	1.1526E-13	6.0741E-12	1.4983E-13	3.9063E-01	1.1008E-02	6.4003E-09	1.4769E-02	2.2306E-04	3.7564E-05	1.2165E-19	1.7087E-15	2.3616E-01
6	7.8740E-09	1.1686E-13	1.1057E-13	8.6973E-01	4.9141E-05	7.8740E-09	1.3474E-02	8.6829E-01	3.7563E-05	1.2794E-19	1.1962E-19	1.1241E-02
7	1.2794E-19	1.1057E-13	3.0534E-13	4.0598E-01	1.9619E-02	3.3378E-09	1.3683E-02	4.0967E-04	3.7564E-05	1.3683E-19	7.8741E-09	1.2087E-01
8	4.4708E-02	1.2281E-02	3.2655E-06	6.3835E-01	1.2308E-01	5.1985E-02	7.2747E-07	1.8814E-19	1.2531E-08	1.5873E-12	1.1962E-19	1.1686E-13
9	1.4085E-16	1.4085E-16	1.0259E-13	1.9888E-01	3.6267E-04	7.2713E-09	3.6765E-03	3.5706E-08	1.1570E-01	9.8578E-20	1.1895E-05	6.2191E-01
10	1.8986E-19	1.0258E-12	2.7420E-09	3.2028E-02	2.4847E-01	5.0465E-03	3.2730E-16	4.2738E-03	1.7945E-05	6.0826E-16	2.8675E-09	6.2125E-01
11	1.4085E-16	1.4085E-16	6.6573E-14	9.9927E-01	3.6033E-05	7.2713E-09	1.4539E-02	9.7143E-01	3.6033E-05	1.6616E-19	7.2713E-09	1.3191E-02
12	8.8282E-11	2.3770E-19	1.3234E-13	2.2899E-01	1.3461E-01	6.9848E-09	3.9699E-02	3.8471E-05	3.7564E-05	1.2371E-19	1.1953E-11	7.6864E-02
13	1.1686E-13	7.8741E-09	1.1686E-13	3.6974E-01	4.8544E-02	7.7889E-09	1.6416E-02	8.9072E-05	3.7564E-05	1.2165E-19	1.1962E-19	1.2669E-01

TABLE 19. Results of the rank sum metric of benchmark functions with 500 dimensions.

Func.	DSO	TLBO	GA	DE	PSO	ABC	GWO	SCA	BBO	ACO	RCSA	HS
1	1.1962E-19	1.1686E-13	9.7600E-14	4.9141E-01	1.1257E-04	7.7889E-09	1.3405E-02	4.9141E-01	3.7564E-05	1.5133E-19	7.8741E-09	6.2757E-03
2	1.1962E-19	1.1686E-13	1.1686E-13	3.0439E-01	3.8675E-03	7.8741E-09	8.1351E-09	3.6677E-05	2.3243E-02	1.1962E-19	2.1828E-04	4.0494E-01
3	1.1962E-19	1.1686E-13	1.5551E-16	5.0069E-01	2.6924E-02	3.5640E-04	8.4472E-04	4.0701E-01	3.8166E-05	5.7448E-16	7.8741E-09	2.2058E-07
4	1.1957E-19	1.1683E-13	9.1937E-03	1.7402E-09	1.1538E-02	1.3847E-01	3.2319E-18	2.2413E-06	4.7244E-05	8.2793E-10	7.8726E-09	4.1013E-01
5	6.7732E-18	4.0183E-12	2.4807E-11	9.2613E-04	1.0625E-01	4.9775E-07	1.3965E-02	8.8528E-02	3.7564E-05	2.7063E-18	2.0051E-11	7.4450E-02
6	7.8735E-09	1.1685E-13	1.7915E-13	5.0302E-01	6.7607E-05	5.1390E-09	1.3823E-02	4.9488E-01	3.7862E-05	1.3681E-19	1.1960E-19	9.0475E-03
7	1.3683E-19	1.0461E-13	2.8916E-13	3.8359E-01	9.9585E-03	3.4897E-09	1.5456E-02	3.4197E-03	3.7564E-05	1.3683E-19	7.8741E-09	5.6098E-02
8	1.5425E-01	1.1783E-01	1.8364E-06	2.1648E-01	2.0401E-02	2.1834E-02	1.5582E-06	1.8502E-19	8.4090E-11	6.9586E-13	1.1962E-19	2.1082E-11
9	1.4085E-16	1.4085E-16	1.1465E-13	7.1729E-02	6.8643E-05	6.6621E-09	6.7875E-01	8.8468E-09	3.1286E-01	9.8578E-20	5.1865E-05	1.5142E-02
10	1.1475E-19	9.5968E-13	2.3935E-14	2.7874E-02	3.3904E-01	1.1784E-03	1.7675E-09	1.1557E-02	2.7444E-05	9.7250E-18	2.8674E-09	6.8468E-01
11	1.4085E-16	1.4085E-16	7.9842E-14	4.9970E-01	6.4022E-05	5.2316E-09	1.3465E-02	4.9504E-01	3.6033E-05	2.2094E-19	7.2713E-09	8.9847E-03
12	1.1686E-13	1.1962E-19	3.5681E-09	4.5737E-12	9.9488E-01	9.1158E-06	3.9699E-02	1.0723E-02	3.7564E-05	1.1435E-16	7.8740E-09	7.3945E-01
13	2.4600E-16	5.6736E-09	3.1808E-10	4.8209E-08	6.1755E-01	2.3876E-06	1.7001E-02	1.4620E-02	3.7564E-05	8.1420E-17	1.7579E-16	3.0181E-01

have a p-value of less than 5% and consequently reject the null hypothesis. Moreover, in most instances, the DSO outperforms the other compared metaheuristics except for GA. This shows that the results of the DSO are statistically significant and hence, reliable. Furthermore, we carry out a Friedman test to evaluate the ranking of the metaheuristics. This is similar to the statistical test carried out on the

traditional benchmark function in Section IV-A5. In Table 31, the result of the Friedman test on the composite function is presented. We see that the Friedman statistics value is calculated to be -377.43 and it is less than the value of the critical value (i.e., 19.68). Hence, the null hypothesis that the performances of all the metaheuristics are the same for all the composite benchmark functions is valid.

TABLE 20. Results of the rank sum metric of multimodal benchmark functions with fixed dimensions.

Func.	DSO	TLBO	GA	DE	PSO	ABC	GWO	SCA	BBO	ACO	RCSA	HS
14	1.2450E-08	4.0987E-14	5.5158E-01	5.8664E-03	1.4818E-04	1.6551E-01	5.0210E-18	9.4327E-03	5.2857E-09	7.3282E-13	2.5978E-07	1.6538E-03
15	2.2555E-10	2.2690E-10	1.6272E-05	2.7883E-01	1.9238E-02	5.0365E-04	7.1562E-04	5.8188E-01	2.7073E-06	3.1752E-01	1.5157E-04	1.6499E-02
16	7.4801E-08	3.0971E-11	1.3251E-14	1.4145E-11	6.6945E-11	5.8979E-03	3.3939E-14	2.3492E-08	5.0675E-01	6.3780E-12	1.7710E-02	4.0674E-01
17	1.0972E-05	1.3307E-09	4.7519E-17	1.3307E-09	1.3307E-09	8.4937E-03	5.0371E-12	8.1250E-14	3.1578E-01	1.3307E-09	4.0972E-08	3.4210E-01
18	2.6440E-06	4.8115E-12	1.6623E-10	3.8672E-13	1.4595E-05	1.6698E-07	1.0711E-12	4.3195E-02	1.1977E-01	8.9401E-13	1.5889E-02	2.9667E-01
19	7.7070E-01	7.7070E-01	7.7070E-01	9.4444E-04	7.7070E-01	7.7070E-01	7.7070E-01	7.7070E-01	7.7070E-01	7.7070E-01	7.7070E-01	7.7070E-01
20	1.5307E-02	1.9265E-06	1.6989E-13	4.3852E-02	1.7097E-02	2.2720E-02	2.6853E-01	9.6512E-17	9.7440E-02	1.6762E-08	6.4155E-01	3.4944E-01
21	7.6420E-02	2.7508E-11	3.3382E-08	3.4986E-08	8.5598E-01	1.4573E-02	8.7292E-03	4.4667E-14	6.3210E-03	4.8088E-01	7.6116E-02	5.3007E-01
22	5.0121E-01	2.2832E-09	1.7181E-07	1.7186E-10	3.0986E-02	1.4132E-01	3.2945E-05	1.9070E-08	1.6785E-01	9.4098E-07	1.5070E-02	9.5860E-04
23	1.7344E-01	7.2432E-07	7.0825E-06	1.4454E-08	1.2259E-03	9.7708E-03	1.3304E-02	8.2254E-07	2.5081E-04	2.0348E-07	1.2781E-03	2.7432E-05

TABLE 21. Results of the Fieldman test ranking for the unimodal and multimodal benchmark functions with 30 dimensions.

Func.	DSO	TLBO	GA	DE	PSO	ABC	GWO	SCA	BBO	ACO	RCSA	HS
F1	11.5	10	11.5	4	7	9	6	2	3	1	8	5
F2	11.5	10	11.5	2	9	8	4	5	3	1	7	6
F3	12	10	11	1	4	8	3	2	6	9	7	5
F4	12	10	9	2	3	8	4	5	6	11	7	1
F5	8	10	12	5	7	9	6	3	4	1	11	2
F6	1	10	12	3	8	9	4	2	7	5	11	6
F7	11	10	12	1	8	9	5	3	6	2	7	4
F8	8	3	7	6	1	2	5	11	4	9	10	12
F9	8	10	12	3	2	4	6	7	1	11	5	9
F10	11	10	8	2	3	4	12	5	6	7	9	1
F11	10	11	12	1	8	9	6	4	3	2	7	5
F12	6	10	12	5	4	9	3	2	8	7	11	1
F13	10	8	11.5	6	2	9	3	4	7	5	11.5	1
Total	120	122	141.5	41	66	97	67	55	64	71	111.5	58

TABLE 22. Results of the Fieldman test ranking for the unimodal and multimodal benchmark functions with 100 dimensions.

Func.	DSO	TLBO	GA	DE	PSO	ABC	GWO	SCA	BBO	ACO	RCSA	HS
F1	12	9	11	1	6	7	4	2	5	10	8	3
F2	12	9	10	1	7	6	5	3	2	11	8	4
F3	12	9	11	3	2	7	1	4	5	10	8	6
F4	12	9	2	10	3	6	7	4	5	11	8	1
F5	8	10	9	1	3	7	4	5	6	12	11	2
F6	8	9	11	1	6	7	4	2	5	10	12	3
F7	12	9	11	1	5	8	3	4	6	10	7	2
F8	4	5	6	1	2	3	7	11	8	9	10	12
F9	11	10	9	1	4	8	6	5	2	12	7	3
F10	12	9	7	3	2	5	11	4	6	10	8	1
F11	10.5	10.5	12	1	6	7	4	2	5	9	8	3
F12	8	10	9	1	2	7	4	6	5	12	11	3
F13	9.5	8	9.5	1	3	7	4	5	6	11	12	2
Total	131	116.5	117.5	26	51	85	64	57	66	137	118	45

TABLE 23. Results of the Fieldman test ranking for the unimodal and multimodal benchmark functions with 250 dimensions.

Func.	DSO	TLBO	GA	DE	PSO	ABC	GWO	SCA	BBO	ACO	RCSA	HS
F1	12	9	10	2	5.5	7.5	4	1	5.5	11	7.5	3
F2	11.5	9.5	9.5	1	4	7	8	6	3	11.5	5	2
F3	12	9	11	1	3	5	4	2	6	10	8	7
F4	12	10	2	8	4	3	11	5	6	9	7	1
F5	10	8	9	1	4	7	3	5	6	12	11	2
F6	7.5	9	10	1	5	7.5	3	2	6	11	12	4
F7	12	10	9	1	3	8	4	5	6	11	7	2
F8	4	5	6	1	2	3	7	11	8	9	12	10
F9	10.5	10.5	9	2	5	8	4	7	3	12	6	1
F10	12	9	8	3	2	4	11	5	6	10	7	1
F11	10.5	10.5	9	1	5.5	7.5	3	2	5.5	12	7.5	4
F12	8	11	10	1	2	7	4	5	6	12	9	3
F13	9.5	7	9.5	1	3	8	4	5	6	11	12	2
Total	131.5	117.5	112	24	48	82.5	70	61	73	141.5	111	42

TABLE 24. Results of the Fieldman test ranking for the unimodal and multimodal benchmark functions with 500 dimensions.

Func.	DSO	TLBO	GA	DE	PSO	ABC	GWO	SCA	BBO	ACO	RCSA	HS
F1	12	9	10	1.5	5	8	3	1.5	6	11	7	4
F2	11.5	9.5	9.5	2	4	8	7	6	3	11.5	5	1
F3	12	9	11	1	3	5	4	2	6	10	8	7
F4	12	10	4	8	3	2	11	6	5	9	7	1
F5	11	10	8	5	1	7	4	2	6	12	9	3
F6	7	10	9	1	5	8	3	2	6	11	12	4
F7	11.5	10	9	1	4	8	3	5	6	11.5	7	2
F8	2	3	6	1	5	4	7	11	8	10	12	9
F9	10.5	10.5	9	3	5	8	1	7	2	12	6	4
F10	12	9	10	3	2	5	8	4	6	11	7	1
F11	10.5	10.5	9	1	5	8	3	2	6	12	7	4
F12	10	12	8	9	1	6	3	4	5	11	7	2
F13	10	8	9	7	1	6	3	4	5	12	11	2
Total	132	120.5	111.5	43.5	44	83	60	56.5	70	144	105	44

V. ENGINEERING DESIGN PROBLEMS

Recently, engineering design problems (EDPs) have been solved using optimisation metaheuristics to reduce

TABLE 25. Results of the Fieldman test ranking for the fixed-dimensional multimodal benchmark functions.

Func.	DSO	TLBO	GA	DE	PSO	ABC	GWO	SCA	BBO	ACO	RCSA	HS
F14	8	11	1	4	6	2	12	3	9	10	7	5
F15	12	11	9	3	4	7	6	1	10	2	8	5
F16	5	8	12	9	7	4	11	6	1	10	3	2
F17	4	7.5	12	7.5	7.5	3	10	11	2	7.5	5	1
F18	6	9	8	12	5	7	10	3	2	11	4	1
F19	6	6	6	12	6	6	6	6	6	6	6	6
F20	8	9	11	5	7	6	3	12	4	10	1	2
F21	4	11	10	9	1	6	7	12	8	3	5	2
F22	1	11	9	12	4	3	7	10	2	8	5	6
F23	1	10	8	12	5	3	2	9	6	11	4	7
TOTAL	55	93.5	86	85.5	52.5	47	74	73	50	78.5	48	37

TABLE 26. The overall results of the Fieldman test ranking for the unimodal, multimodal, and fixed-dimensional multimodal benchmark functions.

Func.	DSO	TLBO	GA	DE	PSO	ABC	GWO	SCA	BBO	ACO	RCSA	HS
F1/F13 30 Dim	10	11	12	1	5	8	6	2	4	7	9	3
F1/F13 100 Dim	11	8	9	1	3	7	5	4	6	12	10	2
F1/F13 250 Dim	11	10	9	1	3	7	5	4	6	12	8	2
F1/F13 500 Dim	11	10	9	1	2.5	7	6	4	5	12	8	2.5
Total	43	39	39	4	13.5	29	22	14	21	43	35	9.5

computational cost, testing their accuracy and versatility. In this section, the DSO is applied to solve widely known EDPs, namely: (i) I-beam EDP [119], (ii) Cantilever EDP [120], and (iii) Wind power maximisation and turbulence intensity EDP [121].

A. I-BEAM EDP

The structural representation of the I-beam is illustrated in Fig. 24. This design problem entails the maximisation of the vertical deflection in which the mathematical formulation of the problem is given by

$$\min_{b, h, t_w, t_f} \frac{5000}{\frac{t_w(h-2t_f)^3}{12} + \frac{bt_f^3}{6} + 2bt_f \left(\frac{h-t_f}{2}\right)^2} \tag{6a}$$

subject to:

$$2bt_w + t_w(h - 2t_f) \leq 0 \tag{6b}$$

$$10 \leq b \leq 50 \tag{6c}$$

$$10 \leq h \leq 80 \tag{6d}$$

$$0.9 \leq t_w \leq 5 \tag{6e}$$

$$0.9 \leq t_f \leq 5 \tag{6f}$$

where $b, h, t_w,$ and t_f denote the width, length, thickness of the vertical bar, and thickness of the horizontal bar, respectively. The results of the DSO are presented in Table 33. Similar to the previous tests, we compare the results of the DSO with 11 other metaheuristics. We observe that the DSO provided

TABLE 27. Composite benchmark functions.

Function	Var.	Range	f_{min}
<p>F_{24}: CF1</p> <p>f_1, f_2, \dots, f_{10} = Sphere function.</p> <p>$[\sigma_1, \sigma_2, \dots, \sigma_{10}] = [1, 1, \dots, 1]$</p> <p>$[\lambda_1, \lambda_2, \dots, \lambda_{10}] = [5/100, 5/100, \dots, 5/100]$</p>	10	[-5,5]	0
<p>F_{25}: CF2</p> <p>f_1, f_2, \dots, f_{10} = Griewank's function.</p> <p>$[\sigma_1, \sigma_2, \dots, \sigma_{10}] = [1, 1, \dots, 1]$</p> <p>$[\lambda_1, \lambda_2, \dots, \lambda_{10}] = [5/100, 5/100, \dots, 5/100]$</p>	10	[-5,5]	0
<p>F_{26}: CF3</p> <p>f_1, f_2, \dots, f_{10} = Griewank's function.</p> <p>$[\sigma_1, \sigma_2, \dots, \sigma_{10}] = [1, 1, \dots, 1]$</p> <p>$[\lambda_1, \lambda_2, \dots, \lambda_{10}] = [1, 1, \dots, 1]$</p>	10	[-5,5]	0
<p>F_{27}: CF4</p> <p>f_1, f_2 = Sphere function</p> <p>f_3, f_4 = Rastrigin function</p> <p>f_5, f_6 = Weierstrass function</p> <p>f_7, f_8 = Griewank function</p> <p>f_9, f_{10} = Sphere function</p> <p>$[\sigma_1, \sigma_2, \dots, \sigma_{10}] = [1, 1, \dots, 1]$</p> <p>$[\lambda_1, \lambda_2, \dots, \lambda_{10}] = [5/32, 5/32, 1, 1, 5/0.5, 5/0.5, 5/100, 5/100, 5/100, 5/100]$</p>	10	[-5,5]	0
<p>F_{28}: CF5</p> <p>f_1, f_2 = Rastrigin function</p> <p>f_3, f_4 = Weierstrass function</p> <p>f_5, f_6 = Griewank function</p> <p>f_7, f_8 = Ackley function</p> <p>f_9, f_{10} = Sphere function</p> <p>$[\sigma_1, \sigma_2, \dots, \sigma_{10}] = [1, 1, \dots, 1]$</p> <p>$[\lambda_1, \lambda_2, \dots, \lambda_{10}] = [1/5, 1/5, 5/0.5, 5/0.5, 5/100, 5/100, 5/32, 5/32, 5/100, 5/100]$</p>	10	[-5,5]	0
<p>F_{29}: CF6</p> <p>f_1, f_2 = Rastrigin function</p> <p>f_3, f_4 = Weierstrass function</p> <p>f_5, f_6 = Griewank function</p> <p>f_7, f_8 = Ackley function</p> <p>f_9, f_{10} = Sphere function</p> <p>$[\sigma_1, \sigma_2, \dots, \sigma_{10}] = [0.1, 0.2, 0.3, 0.4, 0.5, 0.6, 0.7, 0.8, 0.9, 1]$</p> <p>$[\lambda_1, \lambda_2, \dots, \lambda_{10}] = [0.1 * 1/5, 0.2 * 1/5, 0.3 * 5/0.5, 0.4 * 5/0.5, 0.5 * 5/100, 0.6 * 5/100, 0.7 * 5/32, 0.8 * 5/32, 0.9 * 5/100, 1 * 5/100]$</p>	10	[-5,5]	0

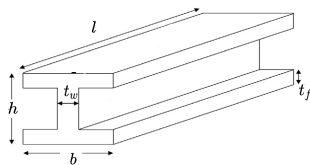


FIGURE 24. Structural parameters of the I-beam.

better results than the GA, GWO, and RCSA, and the same results with the other metaheuristics. This shows the DSO's ability to solve EDP.

B. CANTILEVER EDP

The cantilever structure is made up of five hollow square blocks. Figure 25 shows the structure of the cantilever with each square block denoting an optimisation parameter. The cantilever design problem is premised on minimising the weight of the cantilever beam. The mathematical

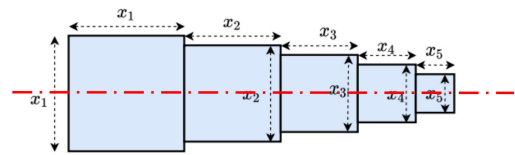


FIGURE 25. Structural parameters of the cantilever.

representation of the EDP is given by

$$\min_{x_1, x_2, x_3, x_4, x_5} 0.6224(x_1 + x_2 + x_3 + x_4 + x_5) \quad (7a)$$

subject to:

$$\frac{61}{x_1^3} + \frac{27}{x_2^3} + \frac{19}{x_3^3} + \frac{7}{x_4^3} + \frac{1}{x_5^3} - 1 \leq 0 \quad (7b)$$

$$0.01 \leq x_1, x_2, x_3, x_4, x_5 \leq 100 \quad (7c)$$

where $x_1, x_2, x_3, x_4,$ and x_5 denote the dimension of each of the five hollow square blocks. Table 33 shows the results of the DSO and other metaheuristics when applied to solve the Cantilever EDP. In Table 33, we observe that the DSO performed better than GA, PSO, ABC, GWO, and SCA.

C. WIND POWER MAXIMISATION AND TURBULENCE INTENSITY EDP

Green energy has received enormous attention in recent times, owing to global warming. Wind power is one major way of generating clean and green energy [122]. Optimal wind turbine placement is critical in wind power maximisation in wind plants. To do this, in this section, we engage the work in [121] to optimise the placement of wind turbines in maximising wind power generation and turbulence intensity. The mathematical formulation of the problem is by [121]

$$\max_{U_{m,i}, P_{m,i}} \sum_{b=1}^{\mathcal{B}} \sum_{m=1}^{\mathcal{M}} \sum_{i=1}^{\mathcal{T}} \beta_{b,m,i} U_{b,m,i}^3 \quad (8a)$$

subject to:

$$a_{m,i} \leq a^{max} \quad (8b)$$

$$0 \leq \beta_{b,m,i} U_{b,m,i}^3 \leq P^{max} \quad (8c)$$

$$T \leq T^{max} \quad (8d)$$

$$\sum_{i=1}^{\mathcal{T}} \beta_{b,m,i}^{ideal} U_{b,m,i}^3 < \sum_{i=1}^{\mathcal{T}} \beta_{b,m,i}^* U_{b,m,i}^3 \quad (8e)$$

where P^{max} is the maximum power of the turbine at free stream wind speed. T denotes the turbulence intensity. U represents the wind speed m/s at turbine hub height. The notation a is the turbine axial induction factor. \mathcal{B} and \mathcal{M} denote the set of bins and wake zones, respectively.

Figures 26(a)-26(d) show the base case of a hexagonally placed wind turbine farm with 30 rotor diameter at 4D, 5D, 6D, and 7D turbine spacing respectively, being compared to the PSO [121], and the DSO optimised cases for each wind inflow, power production, and turbulence intensity (TI) experienced at each turbine in a major wake zone (MWZ),

TABLE 28. Results of composite benchmark functions with 30 dimensions.

Func.	Metric	DSO	TLBO	GA	DE	PSO	ABC	GWO	SCA	BBO	ACO	RCSA	HS
24	AVG	6.0170E+01	2.3831E-01	2.0277E+02	1.8729E-01	6.6609E-01	3.4007E-01	4.5361E+01	4.9358E+00	2.1528E-01	1.7777E-01	1.7777E-01	1.8365E-01
	STD	1.1729E+02	2.4598E-01	1.1217E+02	1.4924E-01	7.4961E-01	2.3365E-01	1.9639E+01	3.2391E+00	1.4303E-01	1.4045E-01	1.4045E-01	1.3032E-01
25	AVG	1.2256E+01	5.5912E-01	8.2212E+01	2.6005E-01	8.0771E-01	5.2847E-01	1.8962E+01	2.2806E+00	2.5651E-01	1.3250E-01	1.3250E-01	1.8561E-01
	STD	1.0969E+01	1.0106E+00	3.9172E+01	3.7411E-01	1.3856E+00	2.4313E-01	1.7113E+01	1.0263E+00	2.8889E-01	4.3465E-02	4.3465E-02	2.4287E-01
26	AVG	3.9746E+01	8.8268E-01	9.6861E+01	5.3755E-01	8.3133E+00	3.7273E+00	3.3828E+01	7.5063E+00	1.5609E+00	7.5626E-01	7.5626E-01	8.8122E-01
	STD	3.5247E+01	7.8187E-01	5.9368E+01	6.2459E-01	8.3262E+00	1.9084E+00	1.2232E+01	3.9070E+00	1.3582E+00	6.8196E-01	6.8196E-01	8.9604E-01
27	AVG	5.8011E+02	2.3687E+02	8.2889E+02	1.8750E+02	4.6027E+02	5.1309E+02	5.7633E+02	5.6224E+02	8.6432E-01	8.9318E-02	8.9318E-02	1.2383E+02
	STD	1.7727E+01	2.1752E+02	6.7577E+01	1.8219E+02	1.1037E+02	6.8025E+01	1.4467E+01	1.7229E+01	4.1318E-01	1.6554E-01	1.6554E-01	1.7124E+02
28	AVG	6.5429E+02	9.2635E+01	8.9199E+02	1.0423E+02	4.3361E+02	5.3499E+02	6.1982E+02	5.8984E+02	6.6099E-01	3.1672E+02	3.1672E+02	8.2450E+02
	STD	2.0353E+01	1.5212E+02	6.6686E+01	1.0969E+02	1.4841E+02	7.4854E+01	3.3111E+01	3.8322E+01	2.2419E-01	5.9805E+01	5.9805E+01	1.1121E+02
29	AVG	5.6092E+02	5.0856E+01	7.7485E+02	1.4447E+02	3.9997E+02	4.9259E+02	5.5900E+02	5.3761E+02	7.1943E-01	9.2173E-02	9.2173E-02	1.4010E+02
	STD	1.5010E+01	1.0926E+02	5.2757E+01	1.4337E+02	1.2577E+02	5.4187E+01	1.2674E+01	1.2236E+01	1.8231E-01	6.9715E-02	6.9715E-02	1.3568E+02

TABLE 29. Results of computational time of composite benchmark functions with 30 dimensions.

Func.	Metric	DSO	TLBO	GA	DE	PSO	ABC	GWO	SCA	BBO	ACO	RCSA	HS
24	AVG	3.1244E+01	5.8938E+01	2.9439E+01	2.9423E+01	2.9791E+01	5.9681E+01	2.9074E+01	2.9078E+01	3.0574E+01	5.9247E+01	5.9247E+01	3.0375E+01
	STD	3.4957E+00	5.5841E+00	2.8937E+00	3.3007E+00	4.3372E+00	6.2840E+00	2.7167E+00	2.3602E+00	3.7412E+00	4.9717E+00	4.9717E+00	2.9613E+00
25	AVG	3.0232E+01	5.5753E+01	2.7948E+01	2.8647E+01	5.7004E+01	5.7004E+01	2.8062E+01	2.7871E+01	2.9252E+01	5.7191E+01	5.7191E+01	2.9133E+01
	STD	1.6718E+00	1.5105E+00	8.6941E-01	2.2389E+00	7.0043E-01	2.4737E+00	1.5757E+00	9.2946E-01	1.6801E+00	1.7073E+00	1.7073E+00	1.3593E+00
26	AVG	3.2089E+01	6.0141E+01	3.0312E+01	2.9945E+01	3.0182E+01	6.1128E+01	2.9438E+01	2.9575E+01	3.0547E+01	6.1250E+01	6.1250E+01	3.0755E+01
	STD	2.7830E+00	4.2354E+00	2.8506E+00	2.6089E+00	2.5375E+00	3.9540E+00	2.1346E+00	2.0766E+00	1.8516E+00	4.1985E+00	4.1985E+00	1.9830E+00
27	AVG	3.0695E+01	5.7391E+01	2.8605E+01	2.9403E+01	2.8790E+01	5.9173E+01	2.9096E+01	2.9026E+01	3.0445E+01	5.9871E+01	5.9871E+01	3.0619E+01
	STD	1.6740E+00	2.6737E+00	1.4063E+00	3.0484E+00	3.3899E+00	4.4117E+00	2.1322E+00	2.4180E+00	2.9732E+00	5.3730E+00	5.3730E+00	3.2175E+00
28	AVG	3.1600E+01	6.0350E+01	2.9585E+01	2.9166E+01	2.9528E+01	5.9801E+01	2.9104E+01	2.9709E+01	3.0458E+01	6.0239E+01	6.0239E+01	3.0079E+01
	STD	3.4222E+00	5.9308E+00	3.4883E+00	2.0333E+00	2.9713E+00	4.2453E+00	2.1803E+00	2.9951E+00	4.6704E+00	4.6704E+00	4.6704E+00	2.0482E+00
29	AVG	3.4663E+01	6.4118E+01	3.1159E+01	3.1412E+01	3.1277E+01	6.2994E+01	3.1470E+01	3.0849E+01	3.2189E+01	6.3583E+01	6.3583E+01	3.2460E+01
	STD	4.4237E+00	8.6447E+00	4.1633E+00	4.2292E+00	3.2321E+00	6.1715E+00	4.8346E+00	2.8426E+00	3.7099E+00	6.0462E+00	6.0462E+00	3.2518E+00

TABLE 30. Results of the rank sum metric of composite benchmark functions with 30 dimensions.

Func.	DSO	TLBO	GA	DE	PSO	ABC	GWO	SCA	BBO	ACO	RCSA	HS
1	2.0505E-10	4.6068E-04	3.8498E-19	6.9724E-05	9.2336E-01	8.0287E-02	9.0341E-12	3.2016E-05	1.3642E-03	2.2275E-07	2.2275E-07	3.3934E-04
2	2.2059E-09	6.7852E-02	2.6708E-19	9.1817E-05	8.1954E-01	2.5249E-01	3.7170E-12	6.5046E-05	2.7439E-03	5.3567E-14	5.3567E-14	4.6706E-04
3	6.2722E-10	1.7243E-05	3.5045E-18	1.6077E-09	1.8771E-02	3.0526E-01	2.5117E-11	9.3831E-04	6.8571E-03	3.8788E-08	3.8788E-08	2.5962E-05
4	3.2951E-10	4.2606E-02	1.1960E-19	4.6290E-02	4.5303E-01	3.8653E-02	1.5539E-09	2.0663E-06	6.7593E-09	2.3858E-16	2.3858E-16	6.1716E-03
5	2.3962E-12	1.3799E-09	1.1534E-19	1.7846E-06	6.1353E-01	1.4283E-02	1.0971E-07	6.3087E-05	1.6239E-17	6.2399E-02	6.2399E-02	1.3677E-07
6	1.2095E-10	1.3565E-04	1.1960E-19	5.0888E-02	4.6302E-01	2.9149E-02	2.0505E-10	8.3706E-06	4.3026E-08	2.6543E-16	2.6543E-16	1.0665E-01

TABLE 31. Results of the Fieldman test ranking for the composite benchmark functions.

Func.	DSO	TLBO	GA	DE	PSO	ABC	GWO	SCA	BBO	ACO	RCSA	HS
F24	10	4	12	6	1	2	11	7	3	8.5	8.5	5
F25	8	3	12	6	1	2	9	7	4	10.5	10.5	5
F26	10	6	12	9	2	1	11	4	3	7.5	7.5	5
F27	9	3	12	2	1	4	8	6	7	10.5	10.5	5
F28	10	9	12	6	1	4	8	5	11	2.5	2.5	7
F29	9	5	12	3	1	4	8	6	7	10.5	10.5	2
TOTAL	56	30	72	32	7	17	55	35	35	50	50	29

TABLE 32. Results of the I-beam design problem.

Meta-h	Optimal values of variables					Opt. Vert. Defl.
	b	h	t _w	t _f		
DSO	50	80	5	5	0.005903	
TLBO	50	80	5	5	0.005903	
GA	41.11519	75.40916	2.898461	3.8565	0.010942	
DE	50	80	5	5	0.005903	
PSO	50	80	5	5	0.005903	
ABC	50	80	5	5	0.005903	
GWO	49.88889	79.85318	4.990413	4.989573	0.006008	
SCA	50	80	5	5	0.005903	
BBO	50	80	5	5	0.005903	
ACO	50	80	5	5	0.005903	
RC-SA	42.07324	73.31952	3.624627	3.957323	0.010788	
HS	50	80	5	5	0.005903	

using three mean inflow wind conditions (7, 8, and 10 m/s). The wind rose and wind speed distribution for the considered site are given in Appendix A section in [121]. By optimising the axial induction factor (a parameter which is controlled by

TABLE 33. Results of the cantilever beam design problem.

Meta-h	x ₁	x ₂	x ₃	x ₄	x ₅	f _{min}
DSO	6.07E+00	4.64E+00	4.42E+00	3.56E+00	2.33E+00	1.31E+01
TLBO	5.98E+00	4.87E+00	4.47E+00	3.48E+00	2.14E+00	1.30E+01
GA	2.26E+01	5.34E+00	1.43E+01	5.65E+00	2.93E+00	3.37E+01
DE	5.97E+00	4.87E+00	4.47E+00	3.48E+00	2.14E+00	1.30E+01
PSO	5.81E+00	5.11E+00	4.77E+00	3.41E+00	2.08E+00	1.32E+01
ABC	5.67E+00	5.21E+00	5.66E+00	3.60E+00	2.32E+00	1.40E+01
GWO	5.82E+00	5.02E+00	4.43E+00	3.57E+00	2.11E+00	1.38E+01
SCA	6.21E+00	5.31E+00	4.25E+00	4.20E+00	2.42E+00	1.39E+01
BBO	5.97E+00	4.79E+00	4.48E+00	3.60E+00	2.14E+00	1.31E+01
ACO	5.97E+00	4.87E+00	4.47E+00	3.48E+00	2.14E+00	1.30E+01
RCSA	5.98E+00	4.88E+00	4.47E+00	3.48E+00	2.14E+00	1.30E+01
HS	5.84E+00	4.98E+00	4.57E+00	3.47E+00	2.12E+00	1.31E+01

pitching turbine blades or adjusting generator torque to affect the tip speed ratio), the power production of each turbine in the MWZ as well as the turbulence intensity at each turbine is affected. The result here shows an improved performance in power production in DSO optimised cases when compared to the base and PSO optimised cases, for all inflow wind conditions and turbine spacing.

Although the DSO algorithm is lightweight and performs better than most metaheuristic algorithms used in this study, they were a few limitations observed in its performance, especially when dealing with lower or fixed dimension multimodal problems, which lead to premature convergence and local optima. The advantage of DSO, however, is in its computation efficiency and accuracy when dealing with

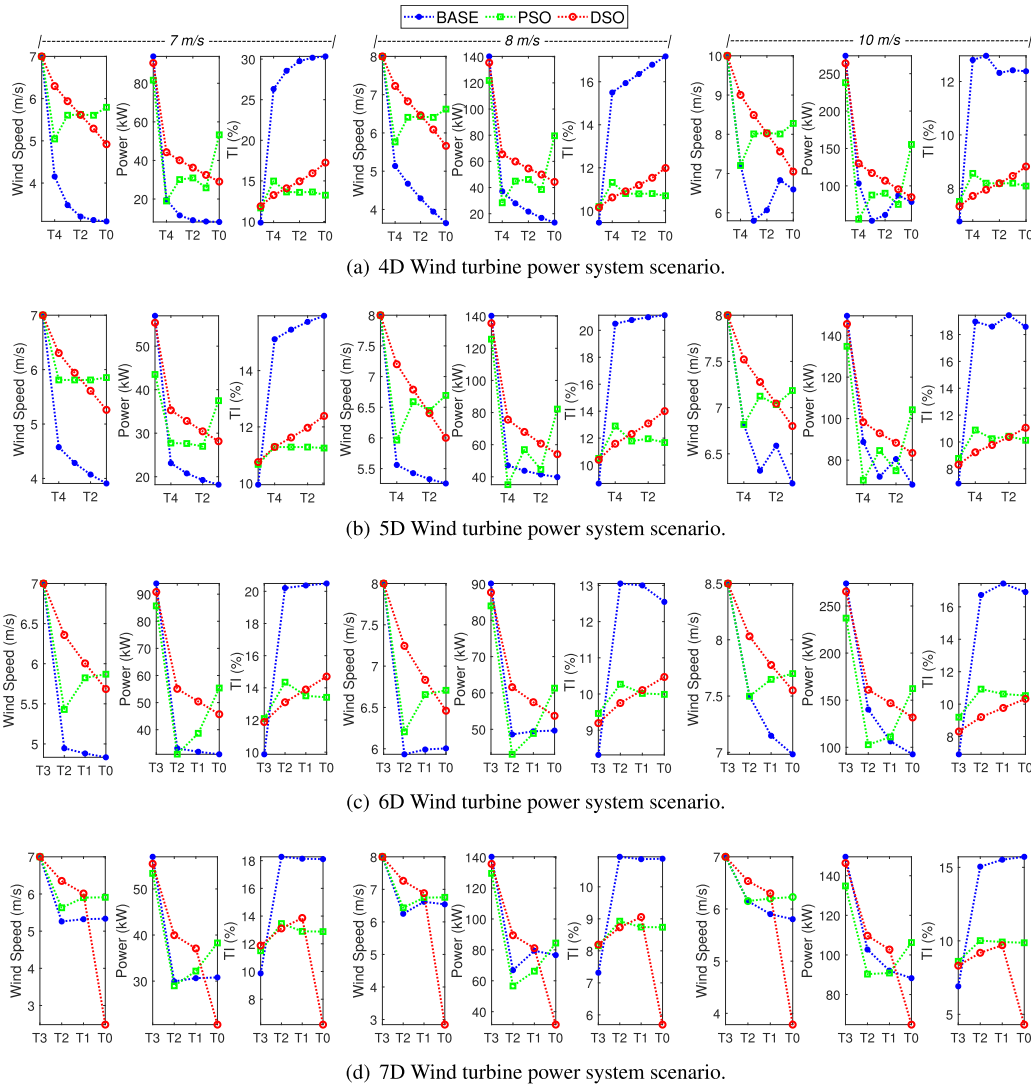


FIGURE 26. Comparison of the performance of the DSO with the BASE, and PSO cases for a 4D, 5D, 6D, and 7D wind turbine power system.

real-world engineering design problems. Additionally, the DSO, performs excellently well with high dimensional problems as in the results discussed in Sections IV and V.

VI. NP-HARD PROBLEMS

In this section, we show the capability and proof that the DSO can be employed to solve NP-hard problems. NP-hard problems are computationally intractable in finding exact solutions. Most combinatorial optimisation problems are NP-hard, and we see from the literature that there are no deterministic polynomial exact algorithms, except when $P=NP$, or else they are computationally intractable [123]. Approximate algorithms such as metaheuristics can find near-optimal solutions. Most combinatorial optimisation problems are in the form given by [124], [125]

$$\sum_{e \in I^*} G(e) = \max \left\{ \sum_{e \in I} G(e) \mid I \in \mathcal{J} \right\}, \quad (9)$$

where F is a finite set and \mathcal{J} is a set of subsets of F and is otherwise called a set of feasible solutions. Moreover, $G : F \rightarrow \mathbb{R}$ is a linear objective function. The obtained feasible solution(s) I^* , is such that $I^* \in \mathcal{J}$. Examples of NP-Hard problems are the Travelling Salesman’s Problem (TSP [126], [127], the knapsack problem [128], and the subset sum problem [129]. Herein, we solve knapsack problems and TSPs.

A. KNAPSACK PROBLEMS

Knapsack problems entail the optimal selection of items, with each having a unique weight and value such that the total collection value is at its possible largest while the collections’ weight is less than or equal to a constraint limit. To this end, DSO’s performance is examined via two types of knapsack problems, namely: (i) 0 – 1 knapsack problems [130] and (ii) bounded knapsack problems [131]. The mathematical

TABLE 34. Comparing DSO and DP optimised value, weight, and computational run time (in seconds) performances for a 0-1 knapsack problem.

Dim	v_{DSO}	v_{DP}	W_{DSO}	W_{DP}	t_{DSO}	t_{DP}
30	18946	18946	1004	1004	0.1284713	0.0053158
100	51339	51339	3557	3557	0.1704211	0.0871618
500	239441	240878	16666	16832	0.4366101	5.8017735
1000	510978	516024	34901	35283	0.729872	43.2838574

TABLE 35. Comparing best, worst, average, standard deviation, and standard error of DSO best cost value for the various dimensions in a 0-1 knapsack problem.

Dim	Best	Worst	Avg.	Std.	Err.
30	18946	17745	18827.83333	294.8652624	1.74706655
100	51339	47601	49957.76667	904.7002812	3.324663055
500	239441	227290	233343.5667	3047.101366	9.057879804
1000	510978	486485	499351.8667	5291.074493	13.74763718

expressions of these models are expressed respectively,

$$\max \sum_{i=1}^n v_i x_i \tag{10a}$$

subject to:

$$\sum_{i=1}^n w_i x_i \leq W, \tag{10b}$$

$$x_i \in \{0, 1\}, \tag{10c}$$

and,

$$\max \sum_{i=1}^n v_i x_i \tag{11a}$$

subject to:

$$\sum_{i=1}^n w_i x_i \leq W, \tag{11b}$$

$$x_i \in \{0, 1, 2, 3, \dots, c\}, \tag{11c}$$

where a set of n items indexed from 1 up to n , each having a weight w_i , and a value v_i along with a maximum weight capacity W . Besides, x_i denotes the number of instances of an item i to include in the knapsack. In Tables 34-37, we illustrate the performance of DSO for several dimensions of knapsack problems. In Table 34, we compare DSO's performance with dynamic programming (DP) for the same problem. DP in this case serves as an exact solution baseline. In Table 34, the number of instances an item is selected is set to 1, while the dimensionality of the problem is varied from 30 to 1000.

It is observed that the performance of DSO is optimal for dimensions 30 and 100 and near-optimal for dimensions 500 and 1000 but with a far better optimised running time. In Tables 35 and 36, we give detailed results of the optimised value and running time obtained via DSO in Table 34. Additionally, in Table 37, we present the performances of DSO for a bounded knapsack problem when ranges from 1 to 3.

B. TRAVELING SALESMAN'S PROBLEM

Herein, DSO is employed to solve the widely known TSP. TSP entails finding the shortest possible route in a set of

TABLE 36. Comparing best, worst, average, and standard deviation of the computational run-time performance in seconds of DSO in a 0-1 knapsack problem.

Dim	Best	Worst	Avg.	Std.
30	0.1284713	0.3548117	0.166291763	0.046583335
100	0.1704211	0.3898098	0.219719773	0.045168853
500	0.4366101	0.8875365	0.58448194	0.096466835
1000	0.729872	0.8507135	0.777692267	0.030670322

cities, such that a city is visited exactly once and returns to the starting city. The TSP is expressed as,

$$\min \sum_{i=1}^n \sum_{j \neq i, j=1}^n c_{ij} x_{ij} \tag{12a}$$

subject to:

$$\sum_{i=1, i \neq j}^n x_{ij} = 1, \tag{12b}$$

$$\sum_{j=1, j \neq i}^n x_{ij} = 1, \tag{12c}$$

$$\sum_{i \in Q} \sum_{j \neq i, j \in Q} x_{ij} \leq |Q| - 1, \tag{12d}$$

$$\forall Q \subsetneq \{1, \dots, n\}, |Q| \geq 2 \tag{12d}$$

$$x_{ij} \in \{0, 1\}, \tag{12e}$$

where c_{ij} denotes the cost, that is, distance from city i to city j and x_{ij} represents the decision variable of traveling from city i to city j . In this work, DSO is applied to solve six TSPs and four of which are from the traveling salesman problem library set [132], [133]. The TSPs examined herein are namely: (i) a 5-city problem; (ii) a 13-city problem [134]; (iii) gr17, a 17-city problem [132]; (iv) fri26, a 26-city problem [132]; (v) dantzig42, a 42-city problem [132], and (vi) att48, a 48-city problem [132]. In Tables 38 and 39, we present the performance evaluation of DSO in solving the above-named TSPs. The optimal cost values of the TSPs are 19; 7293; 2085; 937; 699, and 33523, respectively.

In Table 38, the accuracy of DSO is presented for the examined TSPs. We observe that DSO arrived at the optimal cost for four out of the six TSPs; and near-optimal results for the other two TSPs. Additionally, it is seen that the performance of DSO improves as the number of agent size increases. Furthermore, in Table 39, the computational run time of DSO for results shown in Table 38 is presented. We observe that the run time of DSO is fast and less than 10 seconds for an agent size of 1000 and less than 100 seconds for an extreme agent size of 5000.

VII. GENERALIZABILITY, CHALLENGES, FUTURE IMPROVEMENTS, AND REAL-WORLD APPLICATION OF DSO

A. GENERALIZABILITY

The applicability and generalizability of metaheuristics, such as DSO, for solving optimisation problems hinge on two primary factors: (i) the characteristics of the optimisation

TABLE 37. Comparing DSO and DP optimised values and weights on a bounded knapsack problem with $i = 1, 2, 3$.

Dim	v_{DP}			v_{DSO}			W_{DP}			W_{DSO}		
	$i = 1$	$i = 2$	$i = 3$	$i = 1$	$i = 2$	$i = 3$	$i = 1$	$i = 2$	$i = 3$	$i = 1$	$i = 2$	$i = 3$
30	18946	11805	16219	18946	16758	25543	1004	1051	1088	1004	1051	1088
100	51339	46290	50819	51339	58372	64015	3557	3802	3549	3557	3802	3549
500	240878	253660	249759	239441	284732	274455	16832	17037	17972	16666	17096.65	17972
1000	516024	508420	503545	510978	558951	540914	35283	35592	36303	34901	35592	36303

TABLE 38. Performance evaluation of DSO's accuracy with varying agent size when applied to six TSPs respectively.

TSP	Accuracy	DSO Agent Size						
		30	100	250	500	750	1000	5000
5-City	Best	19	19	19	19	19	19	19
	Worst	19	19	19	19	19	19	19
	Mode	19	19	19	19	19	19	19
13-City	Best	7293	7293	7293	7293	7293	7293	7293
	Worst	8766	8549	8357	8060	8056	8028	7815
	Mode	7293	7293	7293	7293	7293	7293	7293
gr17	Best	2088	2095	2085	2085	2085	2085	2085
	Worst	2898	2761	2682	2605	2618	2593	2520
	Mode	2374	2267	2306	2338	2095	2095	2085
fri26	Best	1031	1031	1031	1031	1031	1003	1031
	Worst	1750	1589	1503	1539	1177	1402	1539
	Mode	1100	1031	1031	1031	1031	1031	1031
dantzig42	Best	699	699	699	699	699	699	699
	Worst	2230	2023	2091	1775	699	1851	699
	Mode	699	699	699	699	699	699	699
att48	Best	80474	70286	67129	67986	60461	64486	62768
	Worst	115709	111761	108719	105872	103873	104802	100577
	Mode	86903	86085	86904	78390	89001	78522	82754

TABLE 39. Performance evaluation of DSO's computational run time (i.e., in seconds) with varying agent size when applied to six TSPs respectively.

TSP	Run Time	DSO Agent Size						
		30	100	250	500	750	1000	5000
5-City	mean	0.4872	1.4015	3.1326	4.8282	6.7434	8.5851	47.7111
	std	0.0777	0.0587	0.1132	0.0856	0.1086	0.2081	1.8895
	mode	0.4503	1.3232	2.9789	4.7499	6.6267	8.6043	46.1868
13-City	mean	0.1912	0.6287	1.5941	3.2694	4.9840	6.7549	43.3195
	std	0.0127	0.0426	0.0998	0.2673	0.2261	0.2698	0.5416
	mode	0.1846	0.6166	1.5439	3.1872	4.8447	6.6227	42.3579
gr17	mean	0.4698	1.3867	3.0369	4.8863	6.7735	8.7007	47.8180
	std	0.0488	0.1042	0.1912	0.2685	0.3168	0.3308	0.9725
	mode	0.4245	1.3740	2.9047	4.7287	6.5811	8.5459	46.6257
fri26	mean	0.5960	1.6670	3.2892	5.4558	7.0929	9.1530	51.2916
	std	0.1477	0.2741	0.3676	0.5407	0.3374	0.3438	3.0595
	mode	0.3808	1.3367	2.9338	4.6987	6.8633	8.8851	48.9098
dantzig42	mean	0.5741	1.6616	3.4551	6.0382	8.0433	10.1624	64.5657
	std	0.0608	0.1123	0.2105	0.5561	0.4495	0.4073	98.3560
	mode	0.5302	1.5844	3.3357	5.4913	7.6846	9.7083	52.8344
att48	mean	0.6197	1.8593	3.5184	5.8032	8.1449	10.5583	62.5703
	std	0.0939	0.2660	0.2704	0.3165	0.3688	0.4237	120.4369
	mode	0.5671	1.6928	3.4218	5.6539	7.9533	10.2015	55.7084

problem and (ii) the ability of the metaheuristic. The characteristics of the problem may include the complexity of the search space, nonlinearity, the size of the decision variables, the number of optimal solutions, i.e., multi-modality, the number of objective functions, and the continuous versus discrete nature of the variables. The ability of metaheuristics to adapt to the characteristics of the optimisation problem and provide near-optima or optima solutions has been demonstrated. DSO's capability is due to its aptness to explore and exploit the search landscape by fine-tuning its parameters. In DSO, control parameters such as minimum initial homeostatic, maximum initial homeostatic, sleep power index, wake power index, and maximum sleep duration enabled search

agents to adapt to the search landscape of the different optimisation problems. Generally, fine-tuning these control parameters increases the likelihood that DSO will yield favorable results. Critical to generalizability is the adaptability of DSO to new problems. Consequently, we investigate the applicability of DSO to traditional and composite benchmarks; real-world engineering design problems such as I-beam design problems, cantilever design problems, wind power maximization, and turbulence intensity design problems; TSPs; and knapsack problems. In our future work, we will investigate the applicability of DSO to other real-world optimisation problems, such as the optimal hyper-parameter tuning of MLs (i.e., SVM, DL), optimal resource allocation problems in next-generation wireless and mobile networks, and medical image enhancement.

B. CHALLENGES

DSO, in rare cases, can sometimes converge prematurely, meaning that it may converge to a suboptimal solution before finding the global optimum. This can happen when the search agents converge to a local optimum and fail to explore other regions of the search space. This limitation has been addressed using perturbation strategies such as randomization to promote exploration and prevent premature convergence. Additionally, the inclusion of agent switch asymptote helps to fine-tune the exploration and exploitation dynamics. To guarantee DSOs find the near-optima or optima solutions, we have embedded the laws of large numbers and Monte-Carlo simulations by running extensive multiple iterations of DSO.

C. FUTURE IMPROVEMENTS

DSO, just like many other metaheuristics, could be improved primarily by three methods [135]: (i) hybridisation, (ii) improved learning and search strategies, and (iii) new variants. The performance of DSO could be improved by hybridising DSO with other metaheuristics. Hybridisation of metaheuristics leverages the strengths of the respective metaheuristics. In this case, DSO's performance could be enhanced by hybridising or combining with metaheuristics such as ACO, GWO, and WOA. Secondly, DSO's learning and search strategies could be further enhanced if strategies such as mutation [136], Levy flight [137], or opposition-based learning [138] employed in other metaheuristics could be incorporated or embedded. Moreover, the parallelisation technique could be incorporated into DSO to enhance search strategies. Lastly, the DSO algorithm could be modified leading to variants that can be applied to solve, for instance, multi-objective optimisation problems [139].

D. REAL-WORLD APPLICATIONS OF DSO

DSO, owing to its flexibility and adaptability to highly complex problems akin to real-world challenges, could be applied to the vehicle-routing problems in fleet and trains routing; facility location problems such as warehouse and distribution centers location problems; complex job scheduling in industries and manufacturing; maximizing returns on investment while managing risks in finance portfolio management; image reconstruction, segmentation, and enhance problems in image and signal processing; hyper-parameter optimisation problems in machine learning; disease diagnosis and classification, resource scheduling and allocation in health-related problems; optimal power generation and transmission problem in the face of several sources of power; resource allocation and scheduling in wireless mobile communications; computational fluid dynamics analysis and optimum design for a centrifugal pump; and optimising magnification ratio for the flexible hinge displacement amplifier mechanism design.

VIII. CONCLUSION

In this work, a novel metaheuristic algorithm, Deep Sleep Optimisation (DSO), has been proposed. The sleeping patterns of humans (i.e., agents) are explored in the DSO. The homeostatic pressure which determines the sleep state of the agents is mathematically modelled according to the literature. We demonstrate that the DSO has been tested on widely acceptable test functions in the literature, including unimodal, multi-modal, fixed-multimodal, and composite functions. Moreover, we test the performance of the DSO in real-life engineering design problems. Additionally, DSO's capability was also demonstrated by solving NP-hard problems. To establish the performance of the DSO, we carry out extensive Monte Carlo simulations in determining the accuracy, computational running time, and Wilcoxon rank sum and Friedman ranking tests to establish the statistical significance of the DSO's results.

From Friedman's ranking test, we see that DSO outperformed the other 11 metaheuristics in several instances for the traditional benchmark functions (i.e., unimodal, multimodal, and fixed-dimensional functions). However, according to Friedman's ranking test, there was no statistical difference in the performances of all the metaheuristics, including DSO, with regard to the composite functions benchmarking. Moreover, DSO produced optimal and near-optimal results when applied to real-world EDPs. Besides, DSO's performance in solving TSPs such as 5, 13, 17, 26, 42, and 48 problems was satisfying with optimal results in most instances. DSO showed its ability to handle large dimensional problems by producing optimal results with considerable computational run time when employed to solve the 0 – 1 and bounded knapsack problems with dimensionality as large as 1000. For instance, it took DSO about 1 second to solve a 1000-dimensional bounded knapsack problem, whereas DP solved the same in about 43 seconds. We have demonstrated that DSO can solve several types of optimisation prob-

lems and it performs excellently well with high dimensional problems.

DSO could solve continuous-based optimisation problems as we demonstrated in evaluating its performance regarding the traditional and composite benchmark functions. These benchmark functions are continuous-based problems. Moreover, we further proved that DSO could solve real-world continuous-based problems by benchmarking with the three engineering design problems. Besides, we have also demonstrated that DSO could solve discrete-based problems by applying DSO to solve the traveling salesman's problems and knapsack optimisation problems as indicated in the modified manuscript. Lastly and to conclude, we observe that the DSO performed better than other metaheuristics examined in this work such as PSO and GA.

APPENDIX A

Herein, we give a brief description of the benchmark functions used in this work with a pictorial view of the functions in Figures 27(a)-27(w). Simply put, unimodal benchmark functions evaluate the exploitative capabilities of metaheuristics. In Table 2, we benchmark DSO on 7 unimodal functions. Function F1 is characteristically a continuous, convex function with 3-dimensional parabola with a spherical constant-cost contours. F1 is widely known as the sphere function. Owing to its simplicity and symmetry, it is often the first test in most instances. F2 is the Schwefel's Problem 2.22 [140]. It is a non-differentiable, non-random, and non-parametric function. Search agents in finding the optimal solution may get stuck in F2' sharp pointed corners and hence converges abruptly. F3 is a rotated hyper-ellipsoid and non-separable function. It is otherwise referred to as Schwefel's Problem 1.2 and it is a minimum quadratic problem [140]. In simple words, F4 which is Schwefel's Problem 2.21 in [140], has an inverted pyramidal shape. F5 is the Rosenbrock function [141] and otherwise called Banana function or the Valley function. It is a continuous, non-convex, and low-dimensional quartic function. The function is well-suited for the testing the performance of gradient-based optimisation algorithms. The minimisation might be difficult to solve owing to the deep parabolic valley along the curve where $\mathcal{X}_2 = \mathcal{X}_1^2$ [142]. F6 is similar to F1. Moreover, it is a shifted sphere function. F7 is a continuous, convex, and high-dimensional quartic function with Gaussian noise [142], [143]. The Gaussian noise makes it difficult for metaheuristics to find the optimal solution. F8, otherwise referred as Schwefel's Problem 2.26 [115], [144], is a scalable and separable test function. Its variable size can be scaled to any number. Besides, separability is a measure of the difficulty in finding the optimal solution of a test function. Separable functions are easy to solve compared to non-separable functions because the variables are independent of each other [115]. The Rastrigin function, F9, is a non-convex, non-linear, separable, and multi-modal benchmark function [143]. F10 is widely known Ackley function [145]. The addition of the term $20 + e$ transforms the function by shifting the global minimum to the origin, that is

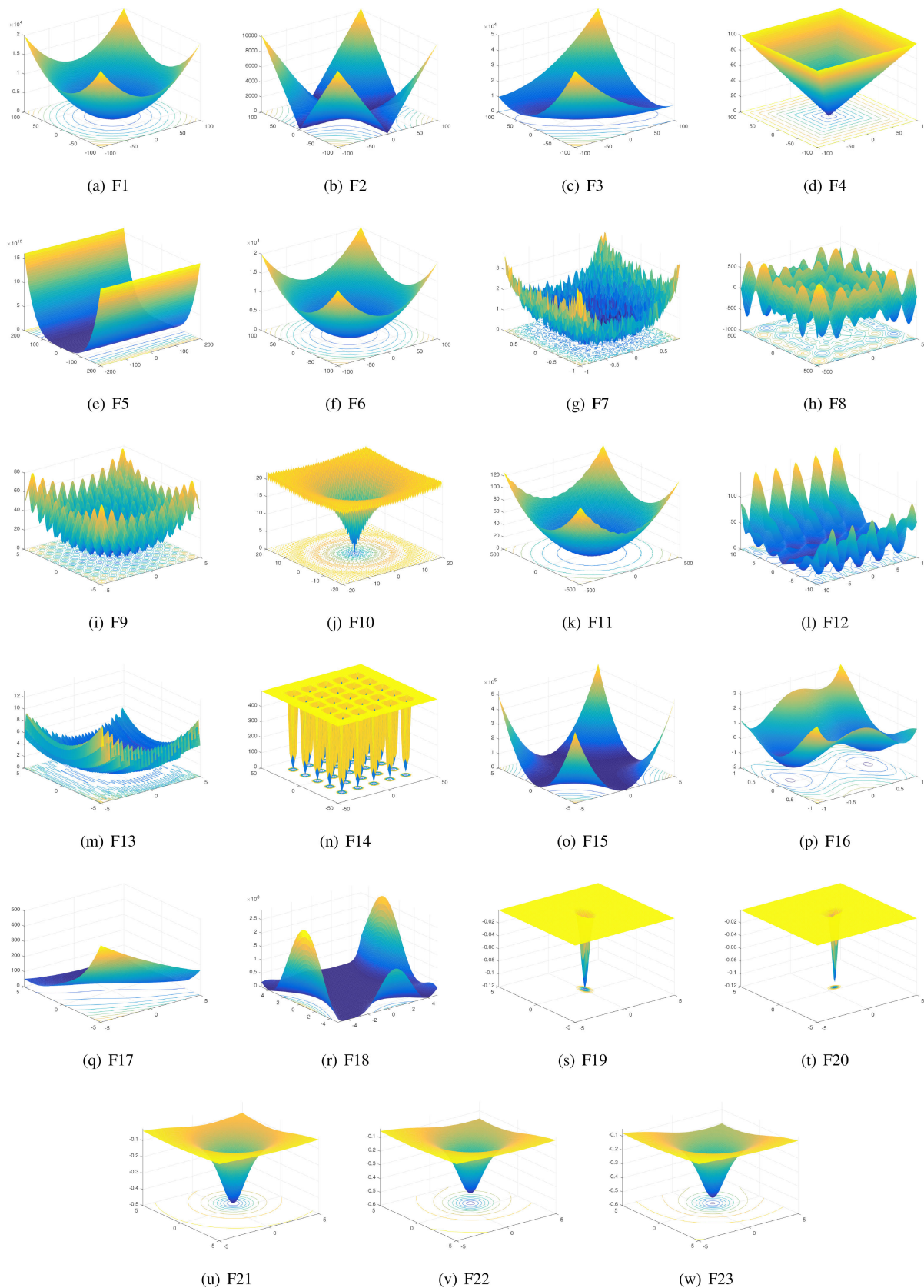


FIGURE 27. Schematic diagram of the unimodal, multimodal, and fixed-dimension multimodal benchmark functions.

at zero. F11 is otherwise referred to as Griewangk’s function is a non-linear optimisation problem and characteristically non-separable. The first term which contains the spherical function help create a parabolic shape and the cosine function in the second term imposes a wave-like on the parabolic terrain surface generated by the first term. The wave-like terrain caused by the cosine function creates multiple local optima. However, as the dimensionality of the problem increases the evaluation of the second term reduces owing to product operator, thereby making its wave-like terrain become less obvious and the problem easy to solve [143], [146]. F16 is also known as the Camel function [115], [147], F17 is the Branin RCOS function [115], and F18 is the Goldstein price function [115], [148]. F16, F17, and F18 are a continuous, non-separable, and differentiable functions. Additionally, they are a non-scalable and multi-modal functions.

APPENDIX B

Friedman’s test is a non-parametric test for the comparison among groups. Non-parametric tests are employed when the data is normally distributed. Consider an observed dataset, \mathcal{A} , having k columns, otherwise known as blocks, and n rows (i.e., observations) given by:

Observations	Block			
	1	2	...	k
1	x_{11}	x_{12}	...	x_{1k}
2	x_{21}	x_{22}	...	x_{2k}
...
n	x_{n1}	x_{n2}	...	x_{nk}

In this work, the blocks denote the metaheuristics (e.g. GA, PSO) considered in the evaluation including DSO, whereas the observations are the functions described in Tables 2-4, and 27. In Friedman test, \mathcal{A} is transformed into \mathcal{B} , by ordering the values in \mathcal{A} according by the observations. For the ordering, the best value in an observation across the block as the highest value. We denote \mathcal{B} as:

Observations	Block			
	1	2	...	k
1	r_{11}	r_{12}	...	r_{1k}
2	r_{21}	r_{22}	...	r_{2k}
...
n	r_{n1}	r_{n2}	...	r_{nk}
Sum	R_1	R_2	...	R_k

where the rank sum for each block across the observations is given by

$$R_i = \sum_{j=1}^n r_{ji}. \tag{13}$$

According to Friedman test, the null hypothesis states that all the blocks have the same performance (i.e., no significant

difference between the blocks), while the alternative hypothesis portends that there is a significant difference between the groups.

The alternative hypothesis is true such that

$$X_r^2 \gg x^2(\alpha, \nu), \tag{14}$$

where X_r^2 is the Friedman statistics and $x^2(\alpha, \nu)$ is the critical chi-square value. The mathematical expression for X_r^2 is given by

$$X_r^2 = \left[\frac{12}{nk(k+1)} \sum_{i=1}^k R_i \right] - 3n(k+1), \tag{15}$$

and $x^2(\alpha, \nu)$, which is the critical chi-square value is dependent on a statistical significance level, α ($\alpha = 0.05$ in this case) and ν is the degree of freedom (i.e., $\nu = k - 1$).

REFERENCES

- [1] S. Mirjalili, S. M. Mirjalili, and A. Lewis, “Grey wolf optimizer,” *Adv. Eng. Softw.*, vol. 69, pp. 46–61, Mar. 2014.
- [2] S. Mirjalili and A. Lewis, “The whale optimization algorithm,” *Adv. Eng. Softw.*, vol. 95, pp. 51–67, May 2016.
- [3] S. Mirjalili, A. H. Gandomi, S. Z. Mirjalili, S. Saremi, H. Faris, and S. M. Mirjalili, “Salp swarm algorithm: A bio-inspired optimizer for engineering design problems,” *Adv. Eng. Softw.*, vol. 114, pp. 163–191, Dec. 2017.
- [4] E.-G. Talbi, *Metaheuristics: From Design to Implementation*, vol. 74. Hoboken, NJ, USA: Wiley, 2009.
- [5] S. O. Oladejo and O. E. Falowo, “Latency-aware dynamic resource allocation scheme for multi-tier 5G network: A network slicing-multitenancy scenario,” *IEEE Access*, vol. 8, pp. 74834–74852, 2020.
- [6] S. O. Oladejo and O. E. Falowo, “Latency-aware dynamic resource allocation scheme for 5G heterogeneous network: A network slicing-multitenancy scenario,” in *Proc. Int. Conf. Wireless Mobile Comput., Netw. Commun. (WiMob)*, Oct. 2019, pp. 1–7.
- [7] S. O. Oladejo and O. E. Falowo, “Profit-aware resource allocation for 5G sliced networks,” in *Proc. Eur. Conf. Netw. Commun. (EuCNC)*, Jun. 2018, p. 43.
- [8] S. O. Ekwe, S. O. Oladejo, L. A. Akinyemi, and N. Ventura, “A socially-inspired energy-efficient resource allocation algorithm for future wireless network,” in *Proc. 16th Int. Comput. Eng. Conf. (ICENCO)*, Dec. 2020, pp. 168–173.
- [9] S. O. Ekwe, L. A. Akinyemi, S. O. Oladejo, and N. Ventura, “Social-aware joint uplink and downlink resource allocation scheme using genetic algorithm,” in *Proc. IEEE AFRICON*, Sep. 2021, pp. 1–6.
- [10] F. Glover, “Future paths for integer programming and links to artificial intelligence,” *Comput. Oper. Res.*, vol. 13, no. 5, pp. 533–549, Jan. 1986.
- [11] K. Sørensen and F. Glover, “Metaheuristics,” *Encyclopedia Oper. Res. Manag. Sci.*, vol. 62, pp. 960–970, Jan. 2013.
- [12] M. Birattari, L. Paquete, T. Stützle, and K. Varentrapp, “Classification of metaheuristics and design of experiments for the analysis of components,” Darmstadt Univ. Technol., Darmstadt, Germany, Tech. Rep., Nov. 2001.
- [13] H. Stegherr, M. Heider, and J. Hähner, “Classifying metaheuristics: Towards a unified multi-level classification system,” *Natural Comput.*, vol. 21, no. 2, pp. 155–171, 2020.
- [14] N. Abd-alsabour and S. Ramakrishnan, “Hybrid metaheuristics for classification problems,” *Pattern Recognition-Analysis Appl.*, vol. 10, p. 65253, Dec. 2016.
- [15] I. Boussaïd, J. Lepagnot, and P. Siarry, “A survey on optimization metaheuristics,” *Inf. Sci.*, vol. 237, pp. 82–117, Jul. 2013. [Online]. Available: <https://www.sciencedirect.com/science/article/pii/S0020025513001588>
- [16] S. Kirkpatrick, C. D. Gelatt Jr., and M. P. Vecchi, “Optimization by simulated annealing,” in *Readings in Computer Vision*. Amsterdam, The Netherlands: Elsevier, 1987, pp. 606–615.
- [17] H. R. Lourenco, O. C. Martin, and T. Stützle, “Iterated local search,” in *Handbook of Metaheuristics*. Berlin, Germany: Springer, 2003, pp. 320–353.

- [18] E. Aarts, E. H. Aarts, and J. K. Lenstra, *Local Search in Combinatorial Optimization*. Princeton, NJ, USA: Princeton Univ. Press, 2003.
- [19] F. Glover and M. Laguna, "Tabu search," in *Handbook of Combinatorial Optimization*. Berlin, Germany: Springer, 1998, pp. 2093–2229.
- [20] T. A. Feo and M. G. C. Resende, "A probabilistic heuristic for a computationally difficult set covering problem," *Oper. Res. Lett.*, vol. 8, no. 2, pp. 67–71, Apr. 1989.
- [21] X.-S. Yang, *Nature-Inspired Metaheuristic Algorithms*. Frome, U.K.: Luniver Press, 2010.
- [22] J. D. Mello-Román and A. Hernández, "KPLS optimization with nature-inspired metaheuristic algorithms," *IEEE Access*, vol. 8, pp. 157482–157492, 2020.
- [23] J. H. Holland, *Adaptation in Natural and Artificial Systems: An Introductory Analysis With Applications to Biology, Control, and Artificial Intelligence*. Cambridge, MA, USA: MIT Press, 1992.
- [24] J. H. Holland, "Genetic algorithms," *Sci. Amer.*, vol. 267, no. 1, pp. 66–73, 1992.
- [25] J. Kennedy, "Particle swarm optimization," in *Proc. IEEE Int. Conf. Neural Netw.*, vol. 4, Dec. 2011, pp. 1942–1948.
- [26] R. Storn and K. Price, "Differential evolution—A simple and efficient heuristic for global optimization over continuous spaces," *J. Global Optim.*, vol. 11, no. 4, pp. 341–359, 1997.
- [27] M. Dorigo, "Optimization, learning and natural algorithms," Ph.D. thesis, Dept. Electron., Politecnico di Mila, Milan, Italy, 1992.
- [28] M. Dorigo and C. Blum, "Ant colony optimization theory: A survey," *Theor. Comput. Sci.*, vol. 344, nos. 2–3, pp. 243–278, Nov. 2005.
- [29] D. Karaboga, "An idea based on honey bee swarm for numerical optimization," Eng. Fac., Compute, Erciyes Univ., Kayseri, Turkey, Tech. Rep., tr06, 2005.
- [30] D. Karaboga and B. Basturk, "A powerful and efficient algorithm for numerical function optimization: Artificial bee colony (ABC) algorithm," *J. Global Optim.*, vol. 39, no. 3, pp. 459–471, Oct. 2007.
- [31] A. A. Heidari, S. Mirjalili, H. Farris, I. Aljarah, M. Mafarja, and H. Chen, "Harris hawks optimization: Algorithm and applications," *Future Gener. Comput. Syst.*, vol. 97, pp. 849–872, Aug. 2019.
- [32] J. Koza, "Genetic programming as a means for programming computers by natural selection," *Statist. Comput.*, vol. 4, no. 2, pp. 87–112, Jun. 1994.
- [33] D. Simon, "Biogeography-based optimization," *IEEE Trans. Evol. Comput.*, vol. 12, no. 6, pp. 702–713, Dec. 2008.
- [34] I. Rechenberg, "Evolution strategy: Nature's way of optimization," in *Optimization: Methods and Applications, Possibilities and Limitations*. Berlin, Germany: Springer, 1989, pp. 106–126.
- [35] D. B. Fogel, *Artificial Intelligence Through Simulated Evolution*. Hoboken, NJ, USA: Wiley, 1998, pp. 227–296.
- [36] D. B. Fogel, *System Identification Through Simulated Evolution: A Machine Learning Approach to Modeling*. Needham, MA, USA: Ginn Press, 1991.
- [37] D. B. Fogel, *Artificial Intelligence Through Simulated Evolution*. Hoboken, NJ, USA: Wiley, 1998.
- [38] N. Hansen, "The CMA evolution strategy: A comparing review," in *Towards a New Evolutionary Computation (Studies in Fuzziness and Soft Computing)*, vol. 192, L. Lozano P. Larranaga, I. Inza, and E. Bengoetxea, Eds. Berlin, Germany: Springer, 2006, pp. 75–102, doi: [10.1007/3-540-32494-1_4](https://doi.org/10.1007/3-540-32494-1_4).
- [39] H. Talbi and A. Draa, "A new real-coded quantum-inspired evolutionary algorithm for continuous optimization," *Appl. Soft Comput.*, vol. 61, pp. 765–791, Dec. 2017.
- [40] A. P. Engelbrecht, *Computational Intelligence: An Introduction*. Hoboken, NJ, USA: Wiley, 2007.
- [41] A. P. Engelbrecht, *Fundamentals of Computational Swarm Intelligence*. Hoboken, NJ, USA: Wiley, 2006.
- [42] X.-S. Yang, "Firefly algorithm, stochastic test functions and design optimisation," *Int. J. Bio-Inspired Comput.*, vol. 2, no. 2, pp. 78–84, 2010.
- [43] X. Yang and A. H. Gandomi, "Bat algorithm: A novel approach for global engineering optimization," *Eng. Comput.*, vol. 29, no. 5, pp. 464–483, Jul. 2012.
- [44] S. Saremi, S. Mirjalili, and A. Lewis, "Grasshopper optimisation algorithm: Theory and application," *Adv. Eng. Softw.*, vol. 105, pp. 30–47, Mar. 2017.
- [45] X.-S. Yang and S. Deb, "Cuckoo search via Lévy flights," in *Proc. World Congr. Nature Biologically Inspired Comput. (NaBIC)*, 2009, pp. 210–214.
- [46] A. Kaveh and N. Farhoudi, "A new optimization method: Dolphin echolocation," *Adv. Eng. Softw.*, vol. 59, pp. 53–70, May 2013.
- [47] A. Kaveh and N. Farhoudi, "Dolphin monitoring for enhancing metaheuristic algorithms: Layout optimization of braced frames," *Comput. Struct.*, vol. 165, pp. 1–9, Mar. 2016.
- [48] S. Mirjalili, "The ant lion optimizer," *Adv. Eng. Softw.*, vol. 83, pp. 80–98, May 2015.
- [49] S. Salcedo-Sanz, "Modern meta-heuristics based on nonlinear physics processes: A review of models and design procedures," *Phys. Rep.*, vol. 655, pp. 1–70, Oct. 2016.
- [50] S. Mirjalili, "SCA: A sine cosine algorithm for solving optimization problems," *Knowl.-Based Syst.*, vol. 96, pp. 120–133, Mar. 2016.
- [51] O. K. Erol and I. Eksin, "A new optimization method: Big Bang–Big crunch," *Adv. Eng. Softw.*, vol. 37, no. 2, pp. 106–111, 2006.
- [52] E. Rashedi, H. Nezamabadi-pour, and S. Saryzadi, "GSA: A gravitational search algorithm," *Inf. Sci.*, vol. 179, no. 13, pp. 2232–2248, Jun. 2009.
- [53] R. A. Formato, "Central force optimization," *Prog. Electromagn. Res.*, vol. 77, pp. 425–491, 2007.
- [54] F. Zitouni, S. Harous, and R. Maamri, "The solar system algorithm: A novel metaheuristic method for global optimization," *IEEE Access*, vol. 9, pp. 4542–4565, 2021.
- [55] S. Talatahari, M. Azizi, M. Tolouei, B. Talatahari, and P. Sareh, "Crystal structure algorithm (CryStAl): A metaheuristic optimization method," *IEEE Access*, vol. 9, pp. 71244–71261, 2021.
- [56] S. He, Q. H. Wu, and J. R. Saunders, "A novel group search optimizer inspired by animal behavioural ecology," in *Proc. IEEE Int. Conf. Evol. Comput.*, Jul. 2006, pp. 1272–1278.
- [57] S. He, Q. H. Wu, and J. R. Saunders, "Group search optimizer: An optimization algorithm inspired by animal searching behavior," *IEEE Trans. Evol. Comput.*, vol. 13, no. 5, pp. 973–990, Oct. 2009.
- [58] R. V. Rao, V. J. Savsani, and D. P. Vakharia, "Teaching-learning-based optimization: An optimization method for continuous non-linear large scale problems," *Inf. Sci.*, vol. 183, no. 1, pp. 1–15, Jan. 2012.
- [59] R. V. Rao, V. J. Savsani, and D. P. Vakharia, "Teaching-learning-based optimization: A novel method for constrained mechanical design optimization problems," *Comput.-Aided Des.*, vol. 43, no. 3, pp. 303–315, Mar. 2011.
- [60] S. Talatahari, H. Bayzidi, and M. Sarace, "Social network search for global optimization," *IEEE Access*, vol. 9, pp. 92815–92863, 2021.
- [61] Z. Woo Geem, J. Hoon Kim, and G. V. Loganathan, "A new heuristic optimization algorithm: Harmony search," *Simulation*, vol. 76, no. 2, pp. 60–68, Feb. 2001.
- [62] Y. Tan and Y. Zhu, "Fireworks algorithm for optimization," in *Advances in Swarm Intelligence*, Y. Tan, Y. Shi, and K. C. Tan, Eds. Berlin, Germany: Springer, 2010, pp. 355–364.
- [63] Y. Et al., "Taxonomy of memory usage in swarm intelligence-based metaheuristics," *Baghdad Sci. J.*, vol. 16, p. 0445, Jun. 2019.
- [64] É. D. Taillard, L. M. Gambardella, M. Gendreau, and J.-Y. Potvin, "Adaptive memory programming: A unified view of metaheuristics," *Eur. J. Oper. Res.*, vol. 135, no. 1, pp. 1–16, Nov. 2001.
- [65] J. Montgomery, M. Randall, and T. Hendtlass, "Search bias in constructive metaheuristics and implications for ant colony optimisation," in *Proc. Int. Workshop Ant Colony Optim. Swarm Intell.* Cham, Switzerland: Springer, 2004, pp. 390–397.
- [66] M. Randall, "A general framework for constructive meta-heuristics," in *Operations Research/Management Science at Work*. Berlin, Germany: Springer, 2002, pp. 111–128.
- [67] B. Meyer, "Hybrids of constructive metaheuristics and constraint programming: A case study with ACO," in *Hybrid Metaheuristics*. Berlin, Germany: Springer, 2008, pp. 151–183.
- [68] T. A. Feo and M. G. Resende, "Greedy randomized adaptive search procedures," *J. Global Optim.*, vol. 6, no. 2, pp. 109–133, 1995.
- [69] F. Glover, M. Laguna, and R. Martí, "Fundamentals of scatter search and path relinking," *Control Cybern.*, vol. 29, no. 3, pp. 653–684, 2000.
- [70] J. Pearl, *Heuristics: Intelligent Search Strategies for Computer Problem Solving*. Reading, MA, USA: Addison-Wesley, 1984.
- [71] H. Shah-Hosseini, "Intelligent water drops algorithm: A new optimization method for solving the multiple knapsack problem," *Int. J. Intell. Comput. Cybern.*, vol. 1, no. 2, pp. 193–212, Jun. 2008.
- [72] B. Crawford, R. Soto, G. Astorga, and J. García, "Constructive metaheuristics for the set covering problem," in *Proc. Int. Conf. Bioinspired Methods Their Appl.* Cham, Switzerland: Springer, 2018, pp. 88–99.

- [73] H. R. Lourenco, O. C. Martin, and T. Stützle, "Iterated local search: Framework and applications," in *Handbook of Metaheuristics*. Berlin, Germany: Springer, 2019, pp. 129–168.
- [74] H. H. Hoos and T. Stützle, *Stochastic Local Search: Foundations and Applications*. Amsterdam, The Netherlands: Elsevier, 2004.
- [75] N. Mladenović and P. Hansen, "Variable neighborhood search," *Comput. Oper. Res.*, vol. 24, no. 11, pp. 1097–1100, Nov. 1997.
- [76] C. Voudouris and E. Tsang, "Guided local search and its application to the traveling salesman problem," *Eur. J. Oper. Res.*, vol. 113, no. 2, pp. 469–499, Mar. 1999.
- [77] D. H. Wolpert and W. G. Macready, "No free lunch theorems for optimization," *IEEE Trans. Evol. Comput.*, vol. 1, no. 1, pp. 67–82, Apr. 1997.
- [78] W. Lyu and Z.-A. Wang, "Global classical solutions for a class of reaction-diffusion system with density-suppressed motility," *Electron. Res. Arch.*, vol. 30, no. 3, pp. 995–1015, 2022.
- [79] H.-Y. Jin and Z.-A. Wang, "Asymptotic dynamics of the one-dimensional attraction-repulsion Keller–Segel model," *Math. Methods Appl. Sci.*, vol. 38, no. 3, pp. 444–457, Feb. 2015.
- [80] H.-Y. Jin and Z.-A. Wang, "Global stabilization of the full attraction-repulsion Keller–Segel system," *Discrete Continuous Dyn. Syst.*, vol. 40, no. 6, pp. 3509–3527, 2020.
- [81] Y. Wang, N. Xu, A.-A. Liu, W. Li, and Y. Zhang, "High-order interaction learning for image captioning," *IEEE Trans. Circuits Syst. Video Technol.*, vol. 32, no. 7, pp. 4417–4430, Jul. 2022.
- [82] A.-A. Liu, Y. Zhai, N. Xu, W. Nie, W. Li, and Y. Zhang, "Region-aware image captioning via interaction learning," *IEEE Trans. Circuits Syst. Video Technol.*, vol. 32, no. 6, pp. 3685–3696, Jun. 2022.
- [83] G. Zhou, R. Zhang, and S. Huang, "Generalized buffering algorithm," *IEEE Access*, vol. 9, pp. 27140–27157, 2021.
- [84] Q. Ni, J. Guo, W. Wu, H. Wang, and J. Wu, "Continuous influence-based community partition for social networks," *IEEE Trans. Neww. Sci. Eng.*, vol. 9, no. 3, pp. 1187–1197, May 2022.
- [85] Z. Xiong, X. Li, X. Zhang, M. Deng, F. Xu, B. Zhou, and M. Zeng, "A comprehensive confirmation-based selfish node detection algorithm for socially aware networks," *J. Signal Process. Syst.*, pp. 1–19, Apr. 2023, doi: 10.1007/s11265-023-01868-6.
- [86] X. Zenggang, Z. Mingyang, Z. Xuemin, Z. Sanyuan, X. Fang, Z. Xiaochao, W. Yunyun, and L. Xiang, "Social similarity routing algorithm based on socially aware networks in the big data environment," *J. Signal Process. Syst.*, vol. 94, no. 11, pp. 1253–1267, Nov. 2022.
- [87] Y. Duan, Y. Zhao, and J. Hu, "An initialization-free distributed algorithm for dynamic economic dispatch problems in microgrid: Modeling, optimization and analysis," *Sustain. Energy, Grids Netw.*, vol. 34, Jun. 2023, Art. no. 101004.
- [88] Y. Mao, Y. Zhu, Z. Tang, and Z. Chen, "A novel airspace planning algorithm for cooperative target localization," *Electronics*, vol. 11, no. 18, p. 2950, Sep. 2022.
- [89] G. Liu, "Data collection in MI-assisted wireless powered underground sensor networks: Directions, recent advances, and challenges," *IEEE Commun. Mag.*, vol. 59, no. 4, pp. 132–138, Apr. 2021.
- [90] X. Li and Y. Sun, "Application of RBF neural network optimal segmentation algorithm in credit rating," *Neural Comput. Appl.*, vol. 33, no. 14, pp. 8227–8235, Jul. 2021.
- [91] X. Li and Y. Sun, "Stock intelligent investment strategy based on support vector machine parameter optimization algorithm," *Neural Comput. Appl.*, vol. 32, no. 6, pp. 1765–1775, Mar. 2020.
- [92] S. Wang, X. Hu, J. Sun, and J. Liu, "Hyperspectral anomaly detection using ensemble and robust collaborative representation," *Inf. Sci.*, vol. 624, pp. 748–760, May 2023.
- [93] J. M. Gregory, "Mathematical nature of sleep components for adults," *Int. J. Sleep Disorders*, vol. 1, no. 1, pp. 13–17, 2017.
- [94] O. Faust, H. Razaghi, R. Barika, E. J. Ciccio, and U. R. Acharya, "A review of automated sleep stage scoring based on physiological signals for the new millennia," *Comput. Methods Programs Biomed.*, vol. 176, pp. 81–91, Jul. 2019.
- [95] F. P. Cappuccio, D. Cooper, L. D'Elia, P. Strazzullo, and M. A. Miller, "Sleep duration predicts cardiovascular outcomes: A systematic review and meta-analysis of prospective studies," *Eur. Heart J.*, vol. 32, no. 12, pp. 1484–1492, Jun. 2011.
- [96] F. P. Cappuccio, L. D'Elia, P. Strazzullo, and M. A. Miller, "Sleep duration and all-cause mortality: A systematic review and meta-analysis of prospective studies," *Sleep*, vol. 33, no. 5, pp. 585–592, May 2010.
- [97] J. A. Hobson, "Sleep is of the brain, by the brain and for the brain," *Nature*, vol. 437, no. 7063, pp. 1254–1256, 2005.
- [98] J. A. Hobson, *The Dreaming Brain*. 1988.
- [99] V. Drago, P. S. Foster, K. M. Heilman, D. Arico, J. Williamson, P. Montagna, and R. Ferri, "Cyclic alternating pattern in sleep and its relationship to creativity," *Sleep Med.*, vol. 12, no. 4, pp. 361–366, Apr. 2011.
- [100] A. K. Patel, V. Reddy, and J. F. Araujo, "Physiology, sleep stages," StatPearls Publishing, Treasure Island, FL, USA, Tech. Rep., 2020.
- [101] P. Maquet, "Sleep on it!" *Nature Neurosci.*, vol. 3, no. 12, pp. 1235–1236, 2000.
- [102] J. Peever, P.-H. Luppi, and J. Montplaisir, "Breakdown in REM sleep circuitry underlies REM sleep behavior disorder," *Trends Neurosciences*, vol. 37, no. 5, pp. 279–288, May 2014.
- [103] P. Alhola and P. Polo-Kantola, "Sleep deprivation: Impact on cognitive performance," *Neuropsychiatric Disease Treat.*, vol. 3, no. 5, pp. 553–567, 2007.
- [104] J. J. Pilcher and A. I. Huffcutt, "Effects of sleep deprivation on performance: A meta-analysis," *Sleep*, vol. 19, no. 4, pp. 318–326, Jun. 1996.
- [105] A. A. Borbély, "A two process model of sleep regulation," *Hum. Neurobiol.*, vol. 1, no. 3, pp. 195–204, 1982.
- [106] S. Daan, D. G. Beersma, and A. A. Borbély, "Timing of human sleep: Recovery process gated by a circadian pacemaker," *Amer. J. Physiol.-Regulatory, Integrative Comparative Physiol.*, vol. 246, no. 2, pp. 161–183, Feb. 1984.
- [107] P. Achermann and A. A. Borbély, "Mathematical models of sleep regulation," *Front Biosci*, vol. 8, no. 6, p. 1064, 2003.
- [108] D. G. M. Beersma, "Models of human sleep regulation," *Sleep Med. Rev.*, vol. 2, no. 1, pp. 31–43, Feb. 1998.
- [109] A. A. Borbély and P. Achermann, "Concepts and models of sleep regulation: An overview," *J. Sleep Res.*, vol. 1, no. 2, pp. 63–79, Jun. 1992.
- [110] A. C. Skeldon, D.-J. Dijk, and G. Derks, "Mathematical models for sleep-wake dynamics: Comparison of the two-process model and a mutual inhibition neuronal model," *PLoS ONE*, vol. 9, no. 8, Aug. 2014, Art. no. e103877.
- [111] D. E. Knuth, "Big omicron and big Omega and big theta," *ACM SIGACT News*, vol. 8, no. 2, pp. 18–24, Apr. 1976.
- [112] P. E. Black, Ed., "big-O notation," in *Dictionary of Algorithms and Data Structures*, Sep. 2019. Accessed: Aug. 5, 2023. [Online]. Available: <https://www.nist.gov/dads/HTML/bigOnotation.html>
- [113] M. Molga and C. Smutnicki, "Test functions for optimization needs," *Test Functions Optim. Needs*, vol. 101, p. 48, Apr. 2005.
- [114] K. Hussain, M. N. M. Salleh, S. Cheng, and R. Naseem, "Common benchmark functions for metaheuristic evaluation: A review," *Int. J. Informat. Visualizat.*, vol. 1, nos. 2–4, pp. 218–223, 2017.
- [115] M. Jamil and X.-S. Yang, "A literature survey of benchmark functions for global optimisation problems," *Int. J. Math. Modeling Numer. Optim.*, vol. 4, no. 2, pp. 150–194, 2013.
- [116] J. G. Dugalakis and K. G. Margaritis, "On benchmarking functions for genetic algorithms," *Int. J. Comput. Math.*, vol. 77, no. 4, pp. 481–506, Jan. 2001.
- [117] S. A. McLeod. (2019). *What a p-value tells you about statistical significance. Simply Psychology*. [Online]. Available: <https://www.simplypsychology.org/p-value.html>
- [118] P. N. Suganthan, N. Hansen, J. J. Liang, K. Deb, Y.-P. Chen, A. Auger, and S. Tiwari, "Problem definitions and evaluation criteria for the CEC 2005 special session on real-parameter optimization," Nanyang Technol. Univ., Singapore, Tech. Rep., May 2005.
- [119] S. Mirjalili, "Evolutionary algorithms and neural networks," in *Studies in Computational Intelligence*, vol. 780. Berlin, Germany: Springer, 2019.
- [120] H. Chickermane and H. C. Gea, "Structural optimization using a new local approximation method," *Int. J. Numer. Methods Eng.*, vol. 39, no. 5, pp. 829–846, Mar. 1996.
- [121] M. Charles, D. T. O. Oyedokun, and M. Dlodlo, "Power maximization and turbulence intensity management through axial induction-based optimization and efficient static turbine deployment," *Energies*, vol. 14, no. 16, p. 4943, Aug. 2021.
- [122] D. Y. C. Leung and Y. Yang, "Wind energy development and its environmental impact: A review," *Renew. Sustain. Energy Rev.*, vol. 16, no. 1, pp. 1031–1039, Jan. 2012.
- [123] M. R. Garey, "A guide to the theory of NP-completeness," in *Computers and Intractability*. 1979.

- [124] B. H. Korte, *Modern Applied Mathematics : Optimization and Operations Research: Collection of State-of-the-Art Surveys Based on Lectures Presented at the Summer School 'Optimization and Operations Research' Held at the University of Bonn, September 14–22, 1979*, 1982.
- [125] D. T. Hoang, "Metaheuristics for NP-hard combinatorial optimization problems," Ph.D. dissertation, Dept. Elect. Comput. Eng., Nat. Univ. Singapore, Singapore, 2008.
- [126] P. Larrañaga, C. M. H. Kuijpers, R. H. Murga, I. Inza, and S. Dizdarevic, "Genetic algorithms for the travelling salesman problem: A review of representations and operators," *Artif. Intell. Rev.*, vol. 13, no. 2, pp. 129–170, Apr. 1999.
- [127] E. L. Lawler, J. K. Lenstra, A. H. G. Rinnooy Kan, and D. B. Shmoys, "Erratum: The traveling salesman problem: A guided tour of combinatorial optimization," *J. Oper. Res. Soc.*, vol. 37, no. 6, p. 655, Jun. 1986.
- [128] S. Martello and P. Toth, *Knapsack Problems: Algorithms and Computer Implementations*. Hoboken, NJ, USA: Wiley, 1990.
- [129] T. H. Cormen, C. E. Leiserson, R. L. Rivest, and C. Stein, *Introduction to Algorithms*. Cambridge, MA, USA: MIT Press, 2022.
- [130] M. Abdel-Basset, D. El-Shahat, and A. K. Sangaiah, "A modified nature inspired meta-heuristic whale optimization algorithm for solving 0–1 knapsack problem," *Int. J. Mach. Learn. Cybern.*, vol. 10, no. 3, pp. 495–514, Mar. 2019.
- [131] H. Kellerer, U. Pferschy, D. Pisinger, H. Kellerer, U. Pferschy, and D. Pisinger, "The bounded knapsack problem," in *Knapsack Problems*. Berlin, Germany: Springer, 2004, pp. 185–209.
- [132] G. Reinelt, "TSPLIB—A traveling salesman problem library," *ORSA J. Comput.*, vol. 3, no. 4, pp. 376–384, 1991.
- [133] D. L. Applegate, R. E. Bixby, V. Chvátal, and W. J. Cook, "The traveling salesman problem," in *The Traveling Salesman Problem*. Princeton, NJ, USA: Princeton Univ. Press, 2011.
- [134] *Traveling Salesperson Problem*. Accessed: Mar. 25, 2023. [Online]. Available: <https://developers.google.com/optimization/routing/tsp>
- [135] A. G. Gad, "Particle swarm optimization algorithm and its applications: A systematic review," *Arch. Comput. Methods Eng.*, vol. 29, no. 5, pp. 2531–2561, Aug. 2022.
- [136] B. Jana, S. Mitra, and S. Acharyya, "Repository and mutation based particle swarm optimization (RMPSO): A new PSO variant applied to reconstruction of gene regulatory network," *Appl. Soft Comput.*, vol. 74, pp. 330–355, Jan. 2019.
- [137] E. Emary, H. M. Zawbaa, and M. Sharawi, "Impact of Lévy flight on modern meta-heuristic optimizers," *Appl. Soft Comput.*, vol. 75, pp. 775–789, Feb. 2019.
- [138] H. R. Tizhoosh, "Opposition-based learning: A new scheme for machine intelligence," in *Proc. Int. Conf. Comput. Intell. for Model., Control Autom. Int. Conf. Intell. Agents, Web Technol. Internet Commerce*, 2005, pp. 695–701.
- [139] Q. Lin, Y. Ma, J. Chen, Q. Zhu, C. A. C. Coelho, K.-C. Wong, and F. Chen, "An adaptive immune-inspired multi-objective algorithm with multiple differential evolution strategies," *Inf. Sci.*, vols. 430–431, pp. 46–64, Mar. 2018.
- [140] H. Schwefel, *Evolution and Optimum Seeking*, 3rd ed. New York, NY, USA: Wiley, 1995.
- [141] H. H. Rosenbrock, "An automatic method for finding the greatest or least value of a function," *Comput. J.*, vol. 3, no. 3, pp. 175–184, Mar. 1960.
- [142] K. A. De Jong, "An analysis of the behavior of a class of genetic adaptive systems," Ph.D. dissertation, Dept. Comput. Commun. Sci., Univ. Michigan, Ann Arbor, MI, USA, 1975.
- [143] D. Whitley, S. Rana, J. Dzuberka, and K. E. Mathias, "Evaluating evolutionary algorithms," *Artif. Intell.*, vol. 85, nos. 1–2, pp. 245–276, Aug. 1996.
- [144] H.-P. Schwefel, *Numerical Optimization of Computer Models*. Hoboken, NJ, USA: Wiley, 1981.
- [145] T. Bäck and H.-P. Schwefel, "An overview of evolutionary algorithms for parameter optimization," *Evol. Comput.*, vol. 1, no. 1, pp. 1–23, Mar. 1993.
- [146] K. E. Mathias and L. D. Whitley, "Transforming the search space with gray coding," in *Proc. Ist IEEE Conf. Evol. Comput. IEEE World Congr. Comput. Intell.*, Jun. 1994, pp. 513–518.
- [147] F. H. Branin, "Widely convergent method for finding multiple solutions of simultaneous nonlinear equations," *IBM J. Res. Develop.*, vol. 16, no. 5, pp. 504–522, Sep. 1972.
- [148] A. A. Goldstein and J. F. Price, "On descent from local minima," *Math. Comput.*, vol. 25, no. 115, pp. 569–574, 1971.



SUNDAY O. OLADEJO received the B.Eng. degree in electrical and electronic engineering from the Federal University of Technology Akure, Nigeria, the M.Eng. degree in communication engineering from the Federal University of Technology, Minna, Nigeria, the M.B.A. degree in strategic and project management from Ecole Supérieure de Gestion, Paris, France, and the Ph.D. degree in electrical and electronic engineering from the University of Cape Town, South Africa.

From 2007 to 2017, he was a Senior Core Network Engineer with Glo-Mobile, Nigeria. He is currently a Lecturer with the School for Data Science and Computational Thinking, Stellenbosch University, Stellenbosch, South Africa. His research interests include radio resource management in wireless networks, artificial intelligence, swarm intelligence, machine learning, optimization, computational thinking, data science, and analytics.



STEPHEN O. EKWE received the bachelor's degree in electrical and electronic engineering from the Cross River University of Technology, Calabar, Nigeria, and the master's degree in personal mobile and satellite communication from the University of Bradford, West Yorkshire, U.K. He is currently pursuing the Ph.D. degree in electrical engineering with the University of Cape Town, South Africa. He is currently a Lecturer with the Department of Electrical, Electronic, and Computer Engineering, Cape Peninsula University of Technology, South Africa. His research interests include radio resource management in wireless networks, socially aware device-to-device communication, network optimization, meta-heuristics, and artificial intelligence.



LATEEF A. AKINYEMI received the B.Sc. degree (Hons.) in electronic and computer engineering (computational electronics) and the M.Sc. degree in electronic and computer engineering from Lagos State University, Lagos, Nigeria, the M.Sc. degree in electrical and electronics engineering (communication engineering option) from the University of Lagos, Akoka, Nigeria, and the Ph.D. degree in electrical engineering from the Department of Electrical Engineering, Faculty of

Engineering and the Built Environment, University of Cape Town, Western Cape, South Africa. He is a Lecturer, a Researcher, and a Scholar with the Department of Electronic and Computer Engineering, Faculty of Engineering, Lagos State University, Epe campus, Lagos. His research areas are wireless communications, computational electronics, modeling and simulations of quantum-inspired nano-particles and devices, microwave engineering and antennas, artificial intelligence-inspired algorithms, and machine learning.



SEYEDALI A. MIRJALILI (Senior Member, IEEE) is currently a Professor and the Director of the Torrens University Center for Artificial Intelligence Research and Optimization and is internationally recognized for his advances in nature-inspired artificial intelligence (AI) techniques. He is the author of more than 150 publications, including five books, 100 journal articles, 20 conference papers, and 30 book chapters. With over 77,000 citations and an H-index of 92, he is one of the most influential AI researchers in the world. From Google Scholar metrics, he is globally the most cited researcher in optimization using AI techniques, which is his main area of expertise. He has been a keynote speaker at several international conferences. He is serving as an Associate Editor for top AI journals, including *Neurocomputing*, *Applied Soft Computing*, *Advances in Engineering Software*, *Applied Intelligence*, *IEEE Access*, and the *Journal of Algorithms*.